

สารออกฤทธิ์ทางชีวภาพจากเถาไม้กระที่บโรง *Ficus foveolata* Wall.

นายเชียวดนัย เสริมบุญไพศาล

วิทยานิพนธ์นี้เป็นส่วนหนึ่งของการศึกษาตามหลักสูตรปริญญาวิทยาศาสตรมหาบัณฑิต

สาขาวิชาเคมี ภาควิชาเคมี

คณะวิทยาศาสตร์ จุฬาลงกรณ์มหาวิทยาลัย

ปีการศึกษา 2553

ลิขสิทธิ์ของจุฬาลงกรณ์มหาวิทยาลัย

BIOACTIVE COMPOUNDS FROM THE VINE OF *Ficus foveolata* Wall.

Mr. Thiendanai Sermboonpaisarn

A Thesis Submitted in Partial Fulfillment of the Requirements  
for the Degree of Master of Science Program in Chemistry

Department of Chemistry

Faculty of Science

Chulalongkorn University

Academic Year 2010

Copyright of Chulalongkorn University

Thesis Title                      BIOACTIVE COMPOUNDS FROM THE VINE OF  
*Ficus foveolata* Wall.  
By                                      Mr. Thiendanai Sermboonpaisarn  
Field of Study                      Chemistry  
Thesis Advisor                      Assistant Professor Pattara Sawasdee, Ph.D.

---

Accepted by the Faculty of Science, Chulalongkorn University in Partial  
Fulfillment of the Requirements for the Master's Degree

..... Dean of the Faculty of Science  
(Professor Supot Hannongbua, Dr.rer.nat.)

#### THESIS COMMITTEE

..... Chairman  
(Assistant Professor Warinthorn Chavasiri, Ph.D.)

..... Thesis Advisor  
(Assistant Professor Pattara Sawasdee, Ph.D.)

..... Examiner  
(Assistant Professor Preecha Phuwapraisirisan, Ph.D.)

..... External Examiner  
(Associate Professor Kornkanok Ingkaninan, Ph.D.)

เถียรดนัย เสริมบุญไพศาล : สารออกฤทธิ์ทางชีวภาพจากเถาไม้กระที่บโรง *Ficus foveolata* Wall. (BIOACTIVE COMPOUNDS FROM THE VINE OF *Ficus foveolata* Wall.) อ.ที่ปรึกษาวิทยานิพนธ์หลัก : ผศ. ดร.พัชพร สวัสดิ์, 97 หน้า.

รายงานฉบับนี้เป็นครั้งแรกของการศึกษาองค์ประกอบทางเคมีจากเถาไม้กระที่บโรงสามารถแยกสารบริสุทธิ์ได้ 10 ชนิดจากสิ่งสกัดไดคลอโรมีเทนและบิวทานอลโดยวิธีทางโครมาโทกราฟี อาศัยสมบัติทางกายภาพและข้อมูลทางสเปกโทรสโกปี สามารถระบุโครงสร้างของสารที่แยกได้ ดังนี้ เรสเวอราทรอล (1), ไอโซราฟอนิเจนิน (2), โฟโนซิลวิน (3), นีทอล (4), 24'-ไฮดรอกซี-เตตระโคซิล เฟอรูเลต (5), สารผสมระหว่าง 1,22-ไดโคเซนไดออล ไดเฟอรูเลต และ 1,24-เตตระโคเซนไดออล ไดเฟอรูเลต (6), กาแลนกิน 3-เมทิล อีเทอร์ (7), เทคโทโครซิน (8), 5-ไฮดรอกซี-3,7-ไดเมทอกซีฟลาโวน (9), เควอซิทิน (10) จากสารที่แยกได้ทั้งหมดพบว่า 1,22-ไดโคเซนไดออล ไดเฟอรูเลต เป็นสารชนิดใหม่ในธรรมชาติ ซึ่งยังไม่เคยมีรายงานมาก่อน นอกจากนี้นำสารบริสุทธิ์ที่แยกได้ไปทดสอบฤทธิ์ทางชีวภาพต่างๆ ได้แก่ ฤทธิ์ยับยั้งเอนไซม์โคลินเอสเทอเรส, เอนไซม์แอลฟา-กลูโคซิเดส และฤทธิ์ต้านการอักเสบ พบว่า นีทอล (4) แสดงฤทธิ์เอนไซม์บิวทิลโคลินเอสเทอเรสได้ดีกว่าเอนไซม์แอซีทิลโคลินเอสเทอเรส มีค่าการยับยั้งเอนไซม์ที่ร้อยละ 50 เท่ากับ 1.27 ไมโครโมลาร์ ซึ่งมากกว่าสารมาตรฐานกาแลนทามีน 20 เท่า นอกจากนี้เควอซิทิน (10) และ นีทอล (4) ยังแสดงฤทธิ์ยับยั้งเอนไซม์แอลฟา-กลูโคซิเดสได้ดี มีค่าการยับยั้งเอนไซม์ที่ร้อยละ 50 เท่ากับ 5.62 และ 17.21 ไมโครโมลาร์ ซึ่งสารทั้งสองแสดงฤทธิ์ยับยั้งได้ดีกว่าสารมาตรฐานอะคาโบส 120 และ 40 เท่า ตามลำดับ และ เควอซิทิน (10) ยังแสดงฤทธิ์ต้านการอักเสบอย่างมีนัยสำคัญผ่านกลไกยับยั้งการสร้างไนตริกออกไซด์จากเซลล์เม็ดเลือดขาวที่ความเข้มข้น 5 ไมโครกรัมต่อมิลลิลิตร

ภาควิชา.....เคมี.....  
สาขาวิชา.....เคมี.....  
ปีการศึกษา.....2553.....

ลายมือชื่อนิสิต.....  
ลายมือชื่ออ.ที่ปรึกษาวิทยานิพนธ์หลัก.....

# # 5272351723 : MAJOR CHEMISTRY

KEYWORDS: *Ficus foveolata* Wall. / MORACEAE / ANTICHOLINESTERASE / ANTI- $\alpha$ -GLUCOSIDASE / ANTI-INFLAMMATORY

THIENDANAI SERMBOONPAISARN: BIOACTIVES COMPOUNDS FROM THE VINE OF *Ficus foveolata* Wall. ADVISOR: ASST. PROF. PATTARA SAWASDEE, Ph.D., 97 pp.

This is the first report in the chemical constituent investigation from the vine of *Ficus foveolata* Wall. Ten compounds were isolated from the dichloromethane and butanolic extracts using chromatographic methods. Physical properties and spectroscopic evidences led to the structural elucidation of all isolated compounds as resveratrol (**1**), isorhapongetin (**2**), pinosylvin (**3**), gnetol (**4**), 24'-hydroxy-tetracosyl ferulate (**5**), a mixture of 1,22-docosanediol diferluate and 1,24-tetracosanediol diferulate (**6**), galangin 3-methyl ether (**7**), tectochrysin (**8**), 5-hydroxy-3,7-dimethoxyflavone (**9**), quercetin (**10**). Among them, 1,22-docosanediol diferluate was characterized as a new naturally occurring compound. Moreover, all isolated compounds were further evaluated their biological activities; anticholinesterase, anti- $\alpha$ -glucosidase and anti-inflammatory activities. The results found that gnetol (**4**) exhibited the high selectivity on butyrylcholinesterase (BChE) over acetylcholinesterase (AChE). The IC<sub>50</sub> value of compound **4** toward BChE was 1.27  $\mu$ M which 20 folds higher than standard galanthamine. In addition, quercetin (**10**) and gnetol (**4**) showed strong  $\alpha$ -glucosidase inhibitory effects with IC<sub>50</sub> values of 5.62 and 17.21  $\mu$ M, respectively. Both showed 40 and 120 folds higher than those of standard acarbose, respectively. Of isolated compounds, quercetin (**10**) was significantly potential inhibition on the nitric oxide production in macrophages at concentration of 5  $\mu$ g/mL.

Department:.....Chemistry.....

Student's Signature: .....

Field of Study:.....Chemistry.....

Advisor's Signature: .....

Academic Year: .....2010.....

## ACKNOWLEDGEMENTS

First of all, I would like to convey my sincere gratitude to Assistant Professor Pattara Sawasdee, Ph.D., my advisor, for her advice, assistance, and encouragement as well as any supports provided during the course of this research and my master degree student life. My grateful thank also extends to the members of thesis committee consisting of Assistant Professor Warinthorn Chavasiri, Ph.D., Assistant Professor Preecha Phuwapraisirisan, Ph.D., and Associate Professor Kornkanok Ingkaninan, Ph.D., the external examiner from Department of Pharmaceutical Chemistry and Pharmacognosy, Faculty of Pharmaceutical, Naresuan University, Phitsanulok, for their valuable comments arising from the discussion. I would like to acknowledge Associate Professor Nijsiri Ruangrunsi, Ph.D., Department of Pharmacognosy and Pharmaceutical Botany, Faculty of Pharmaceutical Sciences, Chulalongkorn University, for his kind assistance in relation to the plant identification of *Ficus foveolata* Wall. I would also like to thank Assistant Professor Preecha Phuwapraisirisan, Ph.D., and Miss Wisuttaya Worawalai for support the  $\alpha$ -glucosidase inhibitory assay and Assistant Professor Tanapat Palaga, Ph.D., for kindly evaluating the nitric oxide inhibitory assay of isolated compounds. My appreciation is also extended to Natural Products Research Unit, Department of Chemistry, Faculty of Science, Chulalongkorn University for the support of chemical and laboratory facilities and all members in the research unit for their friendship and help during the graduate study. Furthermore, I would not be successful without the financial support from the National Research University Project of CHE, the Ratchadaphiseksomphot Endowment Fund (FW654A) and Center of Petroleum, Petrochemicals and Advanced Materials. Finally, I would like to express my thankfulness to my parents and family members for their inspiration, understanding, great support and encouragement throughout the entire education.

# CONTENTS

	<b>Page</b>
Abstract in Thai.....	iv
Abstract in English.....	v
Acknowledgements.....	vi
Contents .....	vii
List of Tables .....	ix
List of Figures .....	x
List of Schemes.....	xiii
List of Abbreviations .....	xiv
Chapter	
<b>I Introduction</b> .....	1
1.1 Botanical Aspects and Distribution of <i>Ficus foveolata</i> Wall. ....	2
1.2 The Literature Reviews of <i>F. foveolata</i> .....	2
1.3 Cholinesterase Inhibitory Activities.....	3
1.4 $\alpha$ -Glucosidase Inhibitory Activity.....	6
1.5 Nitric Oxide Inhibitory Activity .....	9
1.6 The Goals of This Research .....	11
<b>II Experimental</b> .....	12
2.1 Plant Materials .....	12
2.2 Instruments and Equipments.....	12
2.3 Extraction Procedure of the <i>F. foveolata</i> Vine .....	12
2.4 Bioassay Procedures .....	13
2.4.1 Cholinesterase Inhibitory Assay .....	13
2.4.1.1 Chemical Reagents.....	13
2.4.1.2 Chemical Preparation.....	14
2.4.1.3 Assay Method .....	15
2.4.2 $\alpha$ -Glucosidase Inhibition Assay .....	15
2.4.2.1 Chemical Reagents.....	16
2.4.2.2 Chemical Preparation.....	16
2.4.2.3 Assay Method .....	16
2.4.3 Nitric Oxide Inhibitory Activity .....	17
2.4.3.1 Chemical Reagents .....	18

Chapter	Page
2.4.3.2 Cell Culture and Treatment .....	18
2.4.3.3 Assay Method .....	20
<b>III Results and Discussion</b> .....	<b>21</b>
3.1 Primary Bioassay Screening Results of Crude Extracts .....	21
3.2 Chemical Constituents from the vine of <i>F. foveolata</i> .....	21
3.2.1 Separation of the BuOH Extract .....	21
3.2.2 Separation of the CH <sub>2</sub> Cl <sub>2</sub> Extract.....	26
3.2.3 Structural Elucidation of the Isolated Compounds .....	30
3.2.3.1 Structural Elucidation of Compounds <b>1-4</b> .....	30
3.2.3.1.1 Structural Elucidation of Compound <b>1</b> .....	30
3.2.3.1.2 Structural Elucidation of Compound <b>2</b> .....	32
3.2.3.1.3 Structural Elucidation of Compound <b>3</b> .....	34
3.2.3.1.4 Structural Elucidation of Compound <b>4</b> .....	36
3.2.3.2 Structural Elucidation of Compounds <b>5-6</b> .....	38
3.2.3.2.1 Structural Elucidation of Compound <b>5</b> .....	38
3.2.3.2.2 Structural Elucidation of Mixture <b>6</b> .....	40
3.2.3.4 Structural Elucidation of Compounds <b>7-10</b> .....	43
3.2.3.4.1 Structural Elucidation of Compound <b>7</b> .....	43
3.2.3.4.2 Structural Elucidation of Compound <b>8</b> .....	45
3.2.3.4.3 Structural Elucidation of Compound <b>9</b> .....	47
3.2.3.4.4 Structural Elucidation of Compound <b>10</b> .....	49
3.3 Biological Activity Study of the Isolated Compounds from the Vine of <i>F. foveolata</i> .....	51
3.3.1 The Results of Cholinesterase Inhibitory Activity Test.....	51
3.3.2 The Results of $\alpha$ -Glucosidase Inhibitory Activity Test .....	55
3.3.3 The Results of Nitric Oxide Inhibitory Activity Test .....	57
<b>IV Conclusion</b> .....	<b>60</b>
References.....	64
Appendix.....	69
Vita.....	97



## LIST OF TABLES

Table	Page
3.1 Anticholinesterase activities of <i>F. foveolata</i> extracts .....	21
3.2 The separation of the BuOH extract from the vine of <i>F. foveolata</i> .....	22
3.3 The separation and anticholinesterase activity results of fraction B1-6 .....	22
3.4 The separation of the CH <sub>2</sub> Cl <sub>2</sub> extract from the vine of <i>F. foveolata</i> .....	26
3.5 The <sup>1</sup> H and <sup>13</sup> C-NMR chemical shift assignments of compound <b>1</b> compared with those of resveratrol.....	31
3.6 The <sup>1</sup> H and <sup>13</sup> C-NMR chemical shift assignments of compound <b>2</b> compared with those of isorhapontigenin.....	33
3.7 The <sup>1</sup> H and <sup>13</sup> C-NMR chemical shift assignments of compound <b>3</b> compared with those of pinosylvin.....	35
3.8 The <sup>1</sup> H and <sup>13</sup> C-NMR and HMBC assignments of compound <b>4</b> .....	37
3.9 The <sup>1</sup> H and <sup>13</sup> C-NMR chemical shift assignments of compound <b>5</b> compared with those of 24'-hydroxy-tetracosyl ferulate. ....	39
3.10 The <sup>1</sup> H, <sup>13</sup> C-NMR, HMBC and <sup>1</sup> H- <sup>1</sup> H COSY assignments of compound <b>6a</b> ..	41
3.11 The <sup>1</sup> H and <sup>13</sup> C-NMR chemical shift assignments of compound <b>6b</b> compared with those of 1,24-tetracosanediol diferulate. ....	42
3.12 The <sup>1</sup> H and <sup>13</sup> C-NMR chemical shift assignments of compound <b>7</b> compared with those of galangin 3-methyl ether.....	44
3.13 The <sup>1</sup> H and <sup>13</sup> C-NMR chemical shift assignments of compound <b>8</b> compared with those of tectochrysin. ....	46
3.14 The <sup>1</sup> H and <sup>13</sup> C-NMR chemical shift assignments of compound <b>9</b> compared with those of 5-hydroxy-3,7-dimethoxyflavone. ....	48
3.15 The <sup>1</sup> H and <sup>13</sup> C-NMR chemical shift assignments of compound <b>10</b> compared with those of quercetin.....	50
3.16 Cholinesterase inhibitory activity of the isolated compounds at final concentration 0.1 mg/mL .....	52
3.17 The IC <sub>50</sub> values of cholinesterase inhibitory activity of isolated stilbenes....	54
3.18 The IC <sub>50</sub> values of α-glucosidase inhibitory effect of the isolated compounds .....	55
4.1 Isolated compounds from <i>F. foveolata</i> and their bioactivities.....	61

## LIST OF FIGURES

Figure	Page
1.1 Tree and leaves, heartwood and fruit of <i>F. foveolata</i> .....	2
1.2 The action mechanism of acetylcholinesterase.....	4
1.3 The chemical structure of AD treatment drugs.....	5
1.4 Regulation of glucose enters bloodstream in type 1 and 2 diabetes .....	6
1.5 Transition state in reaction of D-glucose with $\alpha$ -glucosidase and inhibitors 1-deoxynojirimycin (DNJ).....	8
1.6 Structure of $\alpha$ -glucosidase inhibitors .....	9
1.7 The NO biosynthesis in the cellular system.....	10
1.8 Structure of parthenolide, a potent anti-inflammatory agent.....	11
2.1 A plot of log concentration value versus percentage inhibition of inhibitor .	15
2.2 A plot of concentration versus percentage inhibition of inhibitor .....	17
3.1 A <i>trans</i> -stilbene skeleton .....	30
3.2 Compound <b>1</b> : resveratrol.....	31
3.3 Compound <b>2</b> : isorhapontigenin .....	32
3.4 Selected HMBC correlations of compound <b>2</b> .....	33
3.5 Compound <b>3</b> : pinosylvin.....	34
3.6 Compound <b>4</b> : gnetol.....	36
3.7 Selected HMBC correlations of compound <b>4</b> .....	37
3.8 A structure of ferulate moiety .....	38
3.9 Compound <b>5</b> : 24'-hydroxy-tetracosyl ferulate .....	39
3.10 Mixture <b>6</b> : A mixture of 1,22-docosanediol diferulate and 1,24-tetracosanediol diferulate .....	40
3.11 HMBC and COSY correlation of mixture <b>6</b> .....	41
3.12 A flavone skeleton .....	43
3.13 Compound <b>7</b> : galangin 3-methyl ether.....	44
3.14 Compound <b>8</b> : tectochrysin .....	45
3.15 Compound <b>9</b> : 5-hydroxy-3,7-dimethoxyflavone .....	47
3.16 Compound <b>10</b> : quercetin.....	49
3.17 Structure of stilbene-oligomer, (+)- $\alpha$ -viniferin, neohopeaphenol.....	53
3.18 Anti-inflammatory activity and cytotoxicity of compounds <b>1, 2, 3, 4</b> and parthenolide standard. ....	58

<b>Figure</b>	<b>Page</b>
3.19 Cytotoxicity and anti-inflammatory activity of compounds <b>8-10</b> and parthenolide standard. ....	59
A-1 The <sup>1</sup> H-NMR spectrum of compound <b>1</b> .....	70
A-2 The <sup>13</sup> C-NMR spectrum of compound <b>1</b> .....	70
A-3 The HSQC spectrum of compound <b>1</b> .....	71
A-4 The HMBC spectrum of compound <b>1</b> .....	71
A-5 The COSY spectrum of compound <b>1</b> .....	72
A-6 The <sup>1</sup> H-NMR spectrum of compound <b>2</b> .....	72
A-7 The <sup>13</sup> C-NMR spectrum of compound <b>2</b> .....	73
A-8 The HSQC spectrum of compound <b>2</b> .....	73
A-9 The HMBC spectrum of compound <b>2</b> .....	74
A-10 The COSY spectrum of compound <b>2</b> .....	74
A-11 The <sup>1</sup> H-NMR spectrum of compound <b>3</b> .....	75
A-12 The <sup>13</sup> C-NMR spectrum of compound <b>3</b> .....	75
A-13 The HSQC spectrum of compound <b>3</b> .....	76
A-14 The HMBC spectrum of compound <b>3</b> .....	76
A-15 The COSY spectrum of compound <b>3</b> .....	77
A-16 The <sup>1</sup> H-NMR spectrum of compound <b>4</b> .....	77
A-17 The <sup>13</sup> C-NMR spectrum of compound <b>4</b> .....	78
A-18 The HSQC spectrum of compound <b>4</b> .....	78
A-19 The HMBC spectrum of compound <b>4</b> .....	79
A-20 The COSY spectrum of compound <b>4</b> .....	79
A-21 The <sup>1</sup> H-NMR spectrum of compound <b>5</b> .....	80
A-22 The <sup>13</sup> C-NMR spectrum of compound <b>5</b> .....	80
A-23 The HSQC spectrum of compound <b>5</b> .....	81
A-24 The HMBC spectrum of compound <b>5</b> .....	81
A-25 The COSY spectrum of compound <b>5</b> .....	82
A-26 The positive mass spectrum of compound <b>5</b> .....	82
A-27 The <sup>1</sup> H-NMR spectrum of mixture <b>6</b> .....	83
A-28 The <sup>13</sup> C-NMR spectrum of mixture <b>6</b> .....	83
A-29 The HSQC spectrum of mixture <b>6</b> .....	84
A-30 The HMBC spectrum of mixture <b>6</b> .....	84
A-31 The COSY spectrum of mixture <b>6</b> .....	85

<b>Figure</b>	<b>Page</b>
A-32 The positive mass spectrum of mixture <b>6</b> .....	85
A-33 The negative mass spectrum of mixture <b>6</b> .....	86
A-34 The <sup>1</sup> H-NMR spectrum of compound <b>7</b> .....	86
A-35 The <sup>13</sup> C-NMR spectrum of compound <b>7</b> .....	87
A-36 The HSQC spectrum of compound <b>7</b> .....	87
A-37 The HMBC spectrum of compound <b>7</b> .....	88
A-38 The COSY spectrum of compound <b>7</b> .....	88
A-39 The <sup>1</sup> H-NMR spectrum of compound <b>8</b> .....	89
A-40 The <sup>13</sup> C-NMR spectrum of compound <b>8</b> .....	89
A-41 The HSQC spectrum of compound <b>8</b> .....	90
A-42 The HMBC spectrum of compound <b>8</b> .....	90
A-43 The COSY spectrum of compound <b>8</b> .....	91
A-44 The <sup>1</sup> H-NMR spectrum of compound <b>9</b> .....	91
A-45 The <sup>13</sup> C-NMR spectrum of compound <b>9</b> .....	92
A-46 The HSQC spectrum of compound <b>9</b> .....	92
A-47 The HMBC spectrum of compound <b>9</b> .....	93
A-48 The COSY spectrum of compound <b>9</b> .....	93
A-49 The <sup>1</sup> H-NMR spectrum of compound <b>10</b> .....	94
A-50 The <sup>13</sup> C-NMR spectrum of compound <b>10</b> .....	94
A-51 The HSQC spectrum of compound <b>10</b> .....	95
A-52 The HMBC spectrum of compound <b>10</b> .....	95
A-53 The COSY spectrum of compound <b>10</b> .....	96

**LIST OF SCHEMES**

<b>Scheme</b>	<b>Page</b>
1.1 The reaction during hydrolysis of acetylcholine.....	4
2.1 Extraction procedure of the <i>F. foveolata</i> .....	13
2.2 Cholinesterase catalyzed hydrolysis of acetylthiocholine .....	14
2.3 Hydrolysis of <i>p</i> -nitrophenyl- $\alpha$ -D-glucopyranoside by $\alpha$ -glucosidase .....	16
2.4 Chemical reactions involved the measurement of nitrite using the Griess reagents system. ....	18
3.1 Isolated diagram of the BuOH extract from the vine of <i>F. foveolata</i> .....	24
3.2 Separation diagram of fraction B1B2B1C2 from BuOH extract.....	25
3.3 Isolated diagram of the CH <sub>2</sub> Cl <sub>2</sub> extract from the vine of <i>F. foveolata</i> .....	28
3.4 Separation diagram of fraction H from the CH <sub>2</sub> Cl <sub>2</sub> extract.....	29

**LIST OF ABBREVIATIONS**

<i>br</i>	=	broad (NMR)
C	=	carbon
<sup>13</sup> C-NMR	=	carbon-13 nuclear magnetic resonance
cm	=	centimeter (s)
COSY	=	correlation spectroscopy
<i>J</i>	=	coupling constant
°C	=	degree Celsius
C <sub>6</sub> D <sub>6</sub>	=	deuterated benzene
DMSO- <i>d</i> <sub>6</sub>	=	deuterated dimethylsulfoxide
<i>d</i>	=	doublet (NMR)
<i>dd</i>	=	doublet of doublet (NMR)
ESI-MS	=	electrospray ionization mass spectroscopy
U	=	enzyme unit
<i>F. foveolata</i>	=	<i>Ficus foveolata</i> Wall.
g	=	gram (s)
Hz	=	hertz (NMR)
HMBC	=	heteronuclear multiple bond correlation
HSQC	=	heteronuclear single quantum coherence
H	=	hydrogen
kg	=	kilogram (s)
<i>in vitro</i>	=	literally in glass
MHz	=	megahertz (NMR)
m.p.	=	melting point
M	=	meter (s)
OMe	=	methoxy group
μg	=	microgram (s)
μL	=	microliter (s)
μM	=	micromolar
mg	=	milligram (s)
mL	=	milliliter (s)
mM	=	millimolar

min	=	minute (s)
M	=	molarity
<i>m</i>	=	multiplet (NMR)
nm	=	nanometer (s)
N	=	normal
ppm	=	part per million
<i>p</i>	=	pentet (NMR)
%	=	percentage
<sup>1</sup> H-NMR	=	proton-1 nuclear magnetic resonance
q-TOF	=	quadrupole time-of-flight tandem
R <sub>f</sub>	=	retarding factor in chromatography
<i>n</i>	=	sample size (statistic)
<i>s</i>	=	singlet (NMR)
S.D.	=	standard deviation (statistic)
S.E.M.	=	standard error of the mean (statistic)
<i>t</i>	=	triplet (NMR)
δ	=	unit of chemical shift
<i>vs</i>	=	versus
<i>v</i>	=	volume
H <sub>2</sub> O	=	water
<i>w</i>	=	weight
<i>in vivo</i>	=	within a living organism

## CHAPTER I

### INTRODUCTION

It has been long known that natural products serve as a major source of drugs. Nowadays, about half of use drugs are derived from natural sources. Chemodiversity in nature from plants, microorganisms and marine organisms, still offer a valuable source for novel lead discovery and potent biological activity compounds used for human or animal therapy. Though the useful of bioactive nature products as herbal drug preparations dates back hundreds of years ago, their application as isolated and characterized compounds to modern drug discovery and development only started in the 19<sup>th</sup> century, the dawn of the chemotherapy era. It has been well documented that natural products played important roles in modern drug development, especially for antibacterial and antitumor agents. More importantly, natural products presented scientists with unique chemical structures, which are beyond human imagination most of the time, and inspired scientist to pursue new chemical entities with completely different structures from known drugs (Tringali, 2001).

Propitiously, Thailand locates in the tropical region of the world and has abundant kinds of plants, especially herbs which are used as a great source of drugs. The usage of folklore medicines demonstrates the potential of plants for aging-associated diseases such as neurodegenerative disorder, diabetes and inflammation. To study the knowledge in this area, the screening test of some Thai medicinal herbs was investigated by cholinesterase inhibitory activity. The results showed that the extract from *Ficus foveolata* Wall. or Ma Kra Theup Rong (in the family Moraceae) exhibited significant anticholinesterase activity. Interestingly, it was found that the phytochemistry including bioactivities of this plant was rare. Thus, this research aims to isolate and determine the components of this plant together with study their bioactivities such as anti-cholinesterase,  $\alpha$ -glucosidase inhibitory and anti-inflammatory activities. These will be fully represented either phytochemical information or benefit to the development of Thai medicinal knowledge.



**1.1 Botanical Aspects and Distribution of *Ficus foveolata* Wall.** (Madidol University, Department of Pharmaceutical Botany, 1995)

In Thailand *F. foveolata* has been known as Ma Kra Theup Rong. Other names are Duea khrueta, Ma Kok Taek and others. This plant is an indigenous tree and abundantly distributed in many parts of Thailand. The plant was traditionally medicinal plant as a rejuvenating as well as maintain sexual performance or tonic, blood tonic agents and for treatment of body pain (Wutthamawech, 1997). The botanical characteristics can be described as follows:

**Tree:** Scandent shrub to 25 m long; laticiferous, young branches, petioles, lower surfaces of the leaves and young receptacles pubescent.

**Flowers:** Inflorescence in axillary, single syconium; flowers unisexual, monoecious, in the same syconium; receptacle globular.

**Leaves:** Leaf simple, alternate, lanceolate, oblong-lanceolate, ovate or oblong-elliptic, 7-9 cm wide, 12-18 cm long oblong, 7 to 15 cm long, 3 to 5 cm wide and smooth

**Fruit:** Fruit fleshy, globose, reddish inside.



(a)

(b)

(c)

**Figure 1.1** Tree and leaves (a), heartwood (b) and fruit (c) of *F. foveolata*

([http://herbstohealth.blogspot.com/2009\\_05\\_01\\_archive.html](http://herbstohealth.blogspot.com/2009_05_01_archive.html))

**1.2 The Literature Reviews of *F. foveolata***

From the literature reviews, only few publications studied on *F. foveolata* which can be summarized as follows:

Attakorn Palasuwan *et al.* (2005) investigated the antioxidant activity of the water extracts from several Thai medicinal plants by using decolorized ABTS (2,2'-azinobis-(3-ethylbenzothiazoline-6-sulphonic acid diamonium salt) radical cation assay. Among of tested extracts, the stem extract of *Ficus pubigera* (synonym as *F. foveolata*) showed high antioxidant activity.

Prapapan Temkitthawon *et al.* (2006) reported that the ethanolic extract of *F. foveolata* at concentration 1.0 mg/mL inhibited phosphodiesterase (PDEs) more than

80%. PDEs inhibitory agent was known as an agent for treatment in many indications such as cardiovascular disease, chronic obstructive pulmonary disease and erectile dysfunction.

### 1.3 Cholinesterase Inhibitory Activities

Alzheimer's disease (AD) is the well-known disease of progressive neurodegenerative disorder. The symptom is involved a decline in impaired memory and cognitive function. In the later stages of the disease, language deficits, depression, agitation, mood disturbances and psychosis are often seen (Meek *et al.*, 1998). Although a definitive cause has not been discovered but several hypotheses have been proposed. The important hypotheses include: 1.) Cholinergic hypothesis - neurotransmitter deficiencies and dysfunction in brain cell communication, 2.) Amyloid hypothesis -  $\beta$ -amyloid protein and senile plaques and their role in the disease process, 3.) Tau hypothesis - tau protein and neurofibrillary tangles and their role in the disease process. Recently, the cholinergic hypothesis has been several studies for treatment of AD. It was related with the loss of cholinergic neurotransmission in the brain.

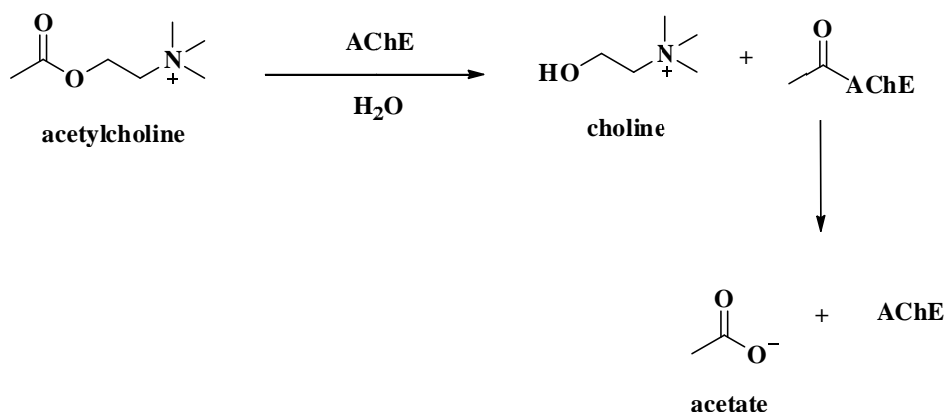
In a cellular brain system, the neurotransmission process begins with the releasing of acetylcholine (ACh) to travel across the synaptic cleft (Figure 1.2). ACh binds at an acetylcholine receptor on the post-synaptic terminal: the other side of the synapse to transmit nerve signal, follow with rapidly broken down by an enzyme, acetylcholinesterase (AChE), and liberating choline. This is followed by a rapid hydrolysis of the acylated enzyme yielding acetate (Scheme 1.1), and the restoration of the esteratic cells.

The ACh deficiency seen in AD led to the formulation of the cholinergic hypothesis, which states that the inability to transmit neurologic impulses across brain synapses is the cause of cognitive. Thus the primary approach in treating AD has aimed at augmenting the cholinergic system in brain (Mukherjee *et al.*, 2007).

To date, cholinesterase inhibition is most effective, widely studied, and developed approach for treating the symptoms. However, several cholinesterase inhibitors were sometimes limited mainly due to their some adverse effects. Therefore, novel more effective therapy, including inhibitors of AChE from plants, needs to be alternative developed for improving the cholinergic deficit (Menichini *et al.*, 2009).

AChE inhibitors represent a well-established class of drugs for the symptomatic treatment of AD, recent findings also point to butyrylcholinesterase (BChE) inhibition as

an additional tool to increase the cholinergic activity in AD patients affected by severe symptoms. Interestingly, levels of AChE decline by up to 85% and BChE represents the predominant cholinesterase in the brain. It is suggested that BChE can partly compensate for AChE action in severe AD (Gemma *et al.*, 2006). Such studies have targeted BChE as a new approach to intercede in the progression of AD.



**Scheme 1.1** The reaction during hydrolysis of acetylcholine

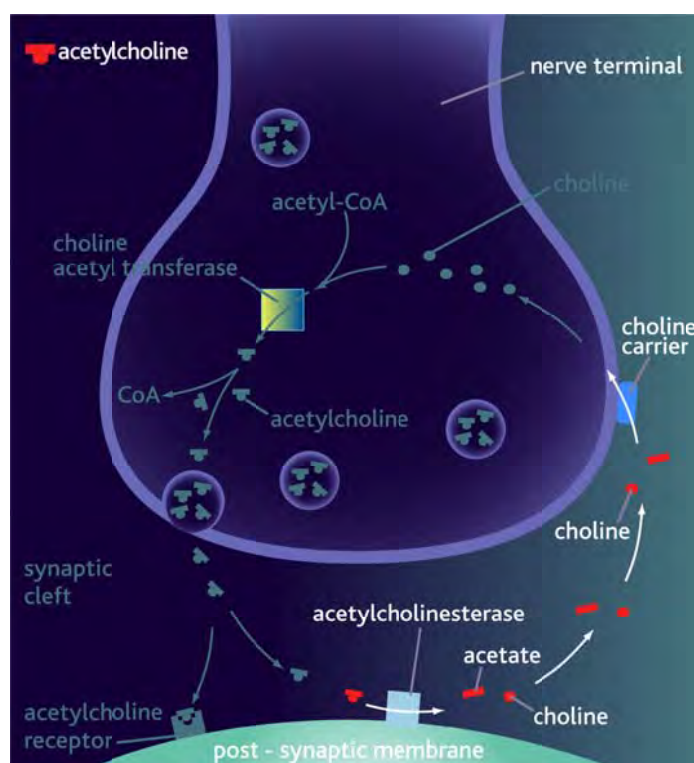


**Figure 1.2** The action mechanism of acetylcholinesterase

([http://www.cnsforum.com/content/pictures/imagebank/hirespng/rcpt\\_sys\\_ACH\\_esterase.png](http://www.cnsforum.com/content/pictures/imagebank/hirespng/rcpt_sys_ACH_esterase.png))

Currently, four available cholinesterase inhibitory drugs; tacrine, donepezil, rivastigmine, and galantamine, are the only therapy drugs which showed consistent

positive results in the AD treatment (Holden and Kelly, 2002). Tacrine (THA, Cognex<sup>®</sup>) was the first synthetic drug approved by United States Food and Drug Administration (FDA) for prescription use (Viegas *et al*, 2005), and belong to the drug category of cholinesterase inhibitors that showed moderate effect in relieving AD symptoms with severe to medium intensity. However, its applications became limited due to serious side effects, like hepatotoxicity that forced patients to discontinue treatment. Besides tacrine, there are three other cholinesterase inhibitor drugs available in United States and Europe for treating AD. Pertaining to donepezil (Aricept<sup>®</sup>), it was a selective inhibitor of AChE and, to date, individuals with AD often respond well to donepezil, showing improvement in cognition, general function, and behavior, with generally few serious side effects. Its common side effect is diarrhea. Regarding rivastigmine (Exelon<sup>®</sup>), it was co-inhibited both AChE and BChE. Rivastigmine was not subject to hepatic metabolism, and hence lacking the potential of adverse drug interactions with a number of agents that were commonly prescribed to the elderly. The most common side effects were nausea and vomiting, with a corresponding loss of appetite, fatigue, and weight loss. Finally, there is galantamine (Reminyl<sup>®</sup>), it was a low selectivity for AChE versus BChE and its most common side effects are nausea. Of these, tacrine, donepezil and galantamine are reversible inhibitors, while rivastigmine acts pseudo-irreversibly. These compounds also differ with regard to selectivity for AChE versus BChE and central versus peripheral activities. Galantamine is a natural product that has the additional effect of allosterically potentiating nicotinic acetylcholine receptors, and it has been used as a prototype in anti-cholinesterase drug development.

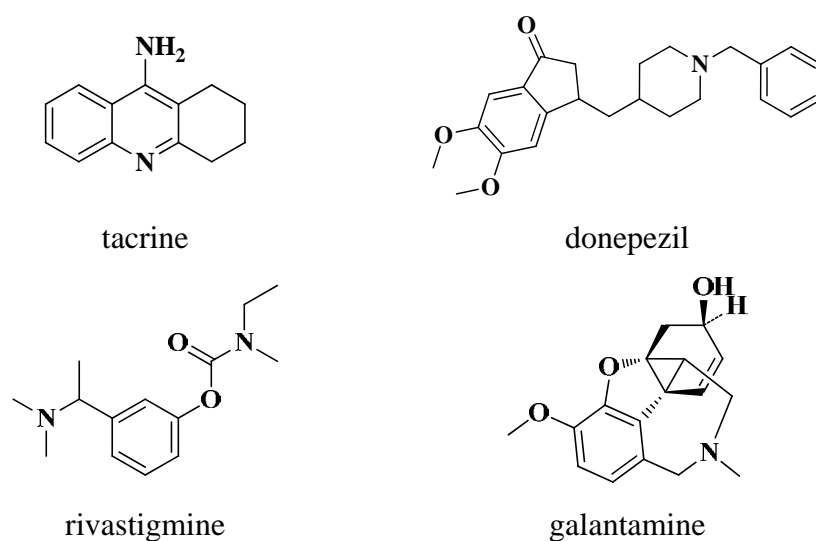


**Figure 1.3** The chemical structures of AD treatment drugs

However, four drugs for AD (galantamine, tacrine, rivastigmine and donepezil) with AChE inhibitory activity possess some side effects and are effective only against the mild type of AD and there has been no drug available with BChE inhibitory activity to present yet. Consequently, it is compulsory to develop new drugs in order to combat AD.

#### 1.4 $\alpha$ -Glucosidase Inhibitory Activity

Diabetes mellitus (DM) is a common metabolic disease characterized by elevated blood glucose levels, resulting from absent or inadequate pancreatic insulin secretion with or without concurrent impairment of insulin action (Hermel and Mathur, 2004).

Insulin is a hormone, which is released from the pancreas and controls the amount of glucose in the blood. When the person consumes foods or drinks, they are digested to glucose, which is absorbed by the bloodstream and stimulates the pancreas to produce insulin. Therefore, glucose is transported into the cells when insulin binds to insulin receptor, which bestrides the cell membrane of many cells (Leroith *et al.*, 2004).

Lacking of productive insulin action results in carbohydrate, fat revision, and protein metabolism. The chronic hyperglycemia of DM is collaborated with long-term dysfunction and damage of organs particularly the kidneys, eyes, nerves, heart, and blood vessels. There are two main types of DM: type 1 diabetes or insulin-dependent diabetes mellitus (IDDM) and type 2 diabetes or non-insulin-dependent diabetes mellitus (NIDDM), as illustrated in Figure 1.4 (Hermel and Mathur, 2004).

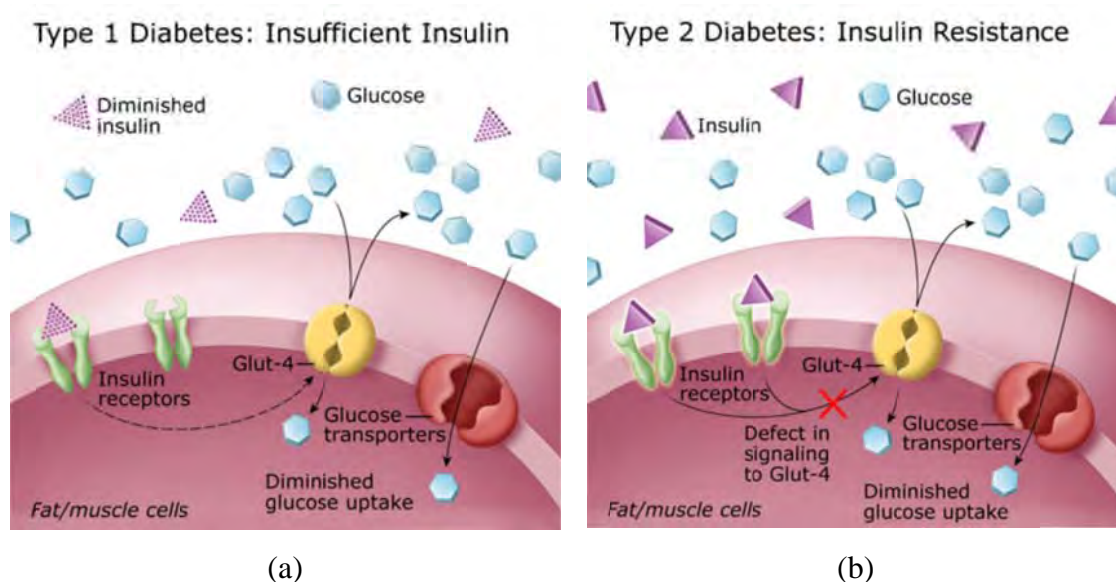


**Figure 1.4** Regulation of glucose enters bloodstream in type 1 (a) and 2 (b) diabetes

([www.ucsf.mightyminnow.com/images/charts](http://www.ucsf.mightyminnow.com/images/charts))

Type 1 diabetes develops by the loss of the insulin producing pancreatic  $\beta$ -cell islets, leading to a deficiency of insulin. Type 1 diabetes usually appears before the age of 40. This type of DM contains approximately 5% to 15% of all people with DM. Type 1 diabetes have been postulated that environmental factors such as certain viral infections and possibly chemical or nutritional agents may worsen these genetic factors (Leroith *et al.*, 2004).

Type 2 diabetes develops by insulin resistance or reduced insulin responsiveness, mixed with relatively reduced insulin secretion. Insulin secretion from the pancreas normally reduces glucose output by the liver, enhances glucose uptake by skeletal muscle, and suppresses fatty acid release from fat tissue. The various factors showed that contribute to the pathogenesis of type 2 diabetes affect both insulin secretion and insulin action. Decreased insulin secretion will reduce insulin signaling in its target tissues. Insulin resistance pathways affect the action of insulin in each of the major target tissues, leading to increased circulating fatty acids and the hyperglycaemia of diabetes. In turn, the raised concentrations of glucose and fatty acids in the bloodstream will feed back to worsen both insulin secretion and insulin resistance. This type of DM consists of approximately 90% to 95% of all diabetes. It usually exists in adults, as well as young people. In all probability, the causes of type 2 diabetes are believed that they come from environmental and lifestyle factors. The most essential factor is obesity, and approximately 50% to 90% of all patients with type 2 diabetes are obese. Intra-abdominal fat deposition is the important site conveying enhanced risk for type 2 diabetes. Furthermore, other factors are increasing age, high caloric intake, stationary lifestyle, and low weight (Leroith *et al.*, 2004; Gravier-Pelletier *et al.*, 2003).

There are many approaches for type 2 diabetes treatment that differs at different stages of the condition. In the early stages, many people with type 2 diabetes can control their blood glucose levels by diet, exercise, and weight loss (Nolan, 2000). Besides, a proficient therapeutic approach for treatment of type 2 diabetes is to delay the postprandial hyperglycemia by retarding the rate of carbohydrate digestion through the inhibition of  $\alpha$ -glucosidase enzyme (Krentz and Bailey, 2005).

In the small intestine, starch is digested to oligosaccharide by amylase, and further digested by membrane-bound  $\alpha$ -glucosidase (isomaltase, maltase, and sucrase) to glucose via the hydrolytic separating of  $\alpha$ -1,4-glycosidic bond. The mechanism of glycoside separating have been examined several times recently (Zechel, 2000), involving a covalent glycosyl-enzyme intermediate.

The  $\alpha$ -glucosidase inhibitors show their structures as mimic of the oligosaccharide substrate. They competitively bind to the active site of the  $\alpha$ -glucosidase, thus preventing the binding and enzymatic hydrolysis of the oligosaccharide substrate (Figure 1.5). In this way,  $\alpha$ -glucosidase inhibition represents a pharmacologic approach for modifying the digestion and absorption of dietary carbohydrates as an adjunct to dietary changes. On account of their competitive mechanism of action,  $\alpha$ -glucosidase inhibitors need to be taken at the start of a meal. After inhibiting the breakdown of carbohydrate by  $\alpha$ -glucosidase inhibitors, in turn causing a reduction in the rate of glucose absorption and also blunting the postprandial plasma glucose level (Rhabasa-Lhoret and Chiasson, 2004).

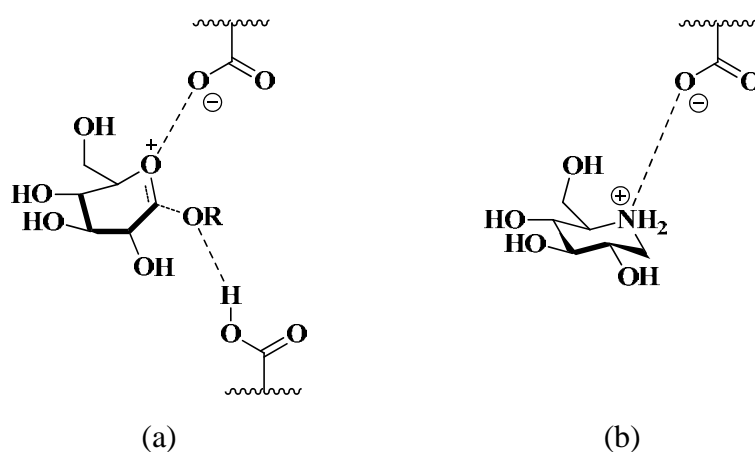


**Figure 1.5** Transition state in reaction of D-glucose with  $\alpha$ -glucosidase (a), and inhibitors 1-deoxynojirimycin (DNJ) (b)

The  $\alpha$ -glucosidase inhibitors are utilized as the oral antidiabetic drugs for example acarbose (Precose<sup>®</sup> or Glucobay<sup>®</sup>), voglibose (Basen<sup>®</sup>) and miglitol (Glyset<sup>®</sup>) which are recently introduced onto the drug market (Borges de Melo *et al.*, 2006).

Acarbose, a prominent  $\alpha$ -glucosidase inhibitor, was first isolated from soil bacteria *Actinoplanes* sp. (Chen *et al.*, 2005). Catalytic hydrogenation of acarbose afforded fragments consisting of trisaccharide derivatives. It was effective in carbohydrate loading tests in rats and healthy volunteer, reducing postprandial blood glucose and increasing insulin secretion (Bischoff, 2004).

DNJ was isolated from *Morus alba* (Singab *et al.*, 2005), It was found to have inhibitory effect against  $\alpha$ -glucosidase. However, the activity of DNJ *in vivo* against intestinal sucrase was lower than that seen *in vitro*. Thus, a large number of DNJ

derivatives, miglitol, were prepared. It was found as the most favorable inhibitor of *in vivo* active agents which showed reducing postprandial blood glucose level.

Voglibose, can be regarded as derivative of DNJ, which has a high inhibitory activity against sucrase and maltase. It has been employed in Japan for the treatment of diabetes since 1994. It was shown to be 20 to 30 fold more potent than acarbose based on  $\alpha$ -glucosidase inhibitory activity (Borges de Melo *et al.*, 2006).

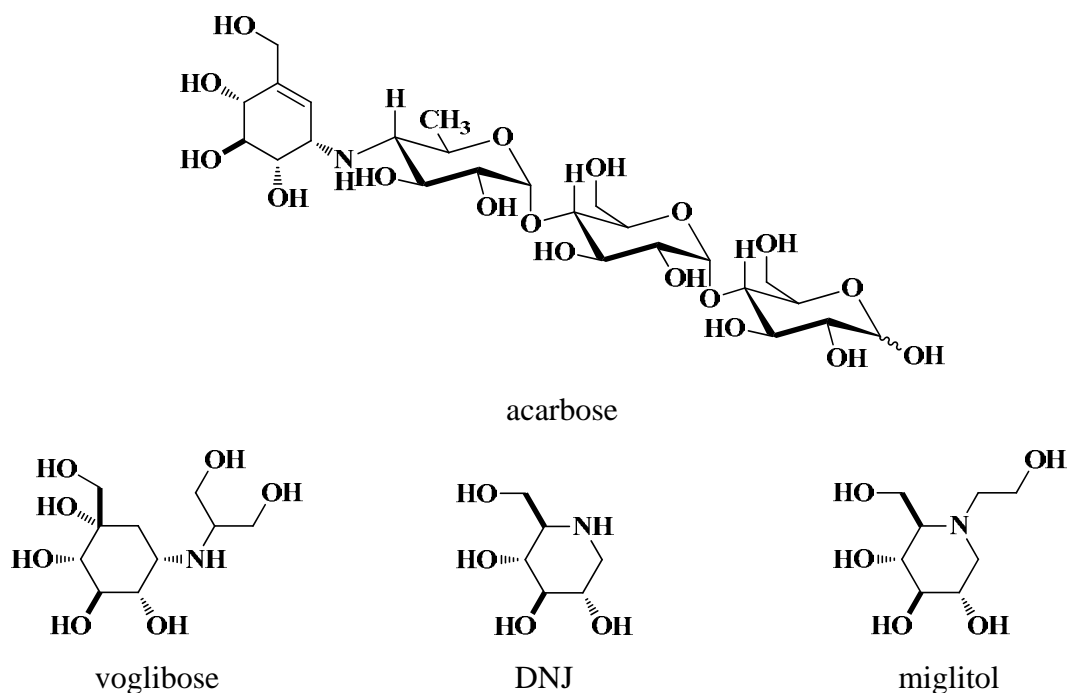


**Figure 1.6** Structure of  $\alpha$ -glucosidase inhibitors

### 1.5 Nitric Oxide Inhibitory Activity

Inflammation is part of the complex biological response of vascular tissues to harmful stimuli, such as pathogens, damaged cells, or irritants (Ferrero-Miliani *et al.*, 2007). Inflammation is a protective attempt by the organism to remove the injurious stimuli and to initiate the healing process. Inflammation can be classified as several pathways. There are many mediators of intercellular and intracellular communications to regulating inflammation or immune functions. Some inflammatory diseases are commonly associated with prostaglandins and nitric oxide (NO) (Minghetti *et al.*, 1996; Goodwin *et al.*, 1999; Yun *et al.*, 2003).

NO is a free radical capable of reacting with a variety of molecules in biological fluids and tissues. These interactions produce not only the oxidation products, nitrite and



nitrate, but also lead to formation of nitrosyl species and modification of thiols and amines to produce S- and N-nitroso products (Bryan *et al.*, 2004).

NO was produced from the oxidation of L-arginine, a reaction catalyzed by the enzyme nitric oxide synthase (NOS) (Song *et al.*, 2002). NOS exists in two major isoforms: the constitutive form (cNOS) and the inducible form (iNOS). cNOS, which is an important regulator of homeostasis, is responsible for the release of physiological levels of NO (Minghetti *et al.*, 1996; Mac Micking *et al.*, 1997) while iNOS is expressed by many types of stimuli, including bacterial lipopolysaccharide (LPS) and pro-inflammatory cytokines such as interleukin-1 (IL-1), tumor necrosis factor (TNF- $\alpha$ ) and gamma interferon (IFN- $\gamma$ ) in various cell types such as macrophages, neutrophils, mesangial cells, hepatocytes, and chondrocytes. Excessive NO production by iNOS has been closely associated with pathogenesis in several inflammatory diseases including septic shock, rheumatoid arthritis, graft rejection and DM (Song *et al.*, 2002).

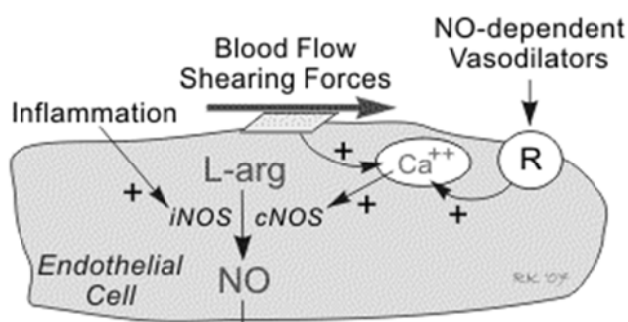


**Figure 1.7** The NO biosynthesis in the cellular system

(<http://www.cvphysiology.com/Blood%20Flow/BF011.htm>)

Since its discovery as a biological messenger molecule more than 10 years ago, the gaseous molecule NO is now well recognized for its involvement in diverse biological processes, including vasodilation, bronchodilation, neurotransmission, tumor surveillance, antimicrobial defense and regulation of inflammatory-immune processes (Weinberger *et al.*, 1999).

In that way, new anti-inflammatory agents derived from natural leads can be used for treatment of inflammatory processes to inhibit NO production. Parthenolide is well known in natural medicine. It is a sesquiterpene lactone which occurs naturally in the plant feverfew (*Tanacetum parthenium*). It is found in highest concentration in the flowers and fruit. Tablets and tinctures are used for the relief of migraine, inflammation and pain (López-Franco *et al.*, 2006).

Since the recent report of anti-inflammatory agents from plant origin, several inhibitors have attracted the attention of NO production through the suppression of iNOS protein and messenger ribonucleic acid (mRNA) expression. Recent data focus on the other natural inhibitory compounds and disclose the involvement of inflammation that highly enhances knowledge for treatment.

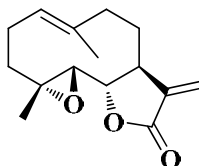


**Figure 1.8** Structure of parthenolide, a potent anti-inflammatory agent

### 1.6 The Goals of This Research

According to the high cholinesterase activity of *F. foveolata* extract together with no reports on constituents and their bioactivities, this research aims to:

- 1.6.1 extract and isolate the chemical constituents from the vine of *F. foveolata*.
- 1.6.2 elucidate the structures of compounds isolated from the vine of *F. foveolata*.
- 1.6.3 investigate the bioactivities; anticholinesterase, anti- $\alpha$ -glucosidase and anti-inflammatory activities of compounds isolated from the vine of *F. foveolata*.

## **CHAPTER II**

### **EXPERIMENTAL**

#### **2.1 Plant Materials**

The vine of *F. foveolata* was collected in September 2009 from Surin province, Thailand and identified by Associate Professor Nijisiri Ruangrunsi, Ph.D., Department of Pharmacognosy and Pharmaceutical Botany, Faculty of Pharmaceutical Sciences, Chulalongkorn University. A voucher specimen was No. NPRU 0001 is deposited at Natural Products Research Unit, Department of Chemistry, Faculty of Science, Chulalongkorn University, Thailand.

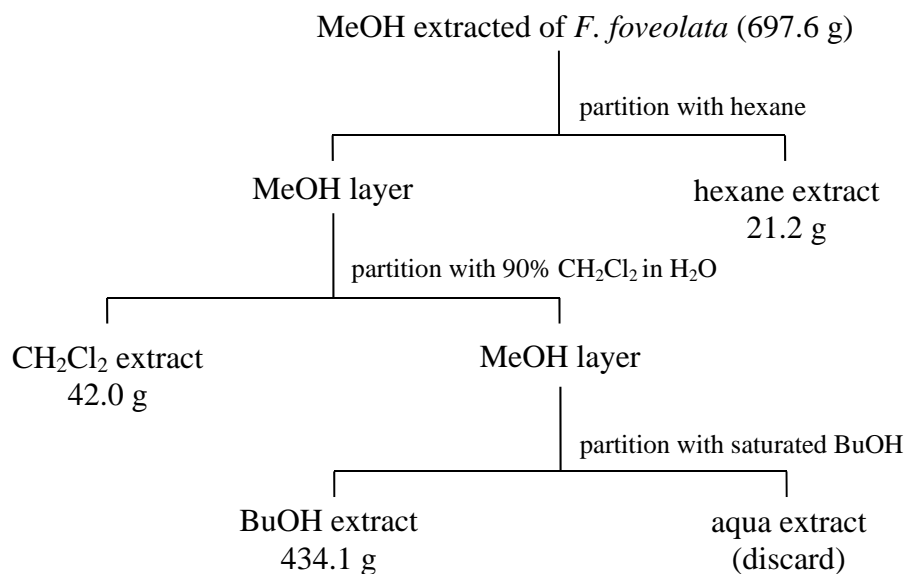
#### **2.2 Instruments and Equipments**

The  $^1\text{H}$  and  $^{13}\text{C}$ -NMR spectra in chloroform- $d_1$  ( $\text{CDCl}_3$ ), methanol- $d_4$  ( $\text{CD}_3\text{OD}$ ) and acetone- $d_6$  were determined with a nuclear magnetic resonance spectrometer of Varian model Mercury+ 400 and Bruker (Both are 400 MHz and using tetramethylsilane as internal standard). ESIMS and HRESIMS were obtained from mass spectrometer model VG TRIO 2000 and Bruker micrOTOF<sup>TM</sup>-Q II mass spectrometer, respectively. Ultra Violet (UV) spectra were measured on Shimadzu UV-160A photodiode array spectrophotometer. Melting points were recorded with Fisher-John melting point apparatus. Adsorbents used for separation were silica gel 60 Merck, No. 7734 and 7731 for column chromatography and quick column chromatography, respectively. Thin layer chromatography (TLC) was performed on aluminium sheets precoated with silica gel (Merck Kieselgel 60 PF254). The spots on plate were detected under UV or visualized. Gel filtration chromatography was performed on sephadex LH-20. Radial chromatography on silica gel was performed on a Harrison Research 7924T Chromatotron<sup>®</sup>.

#### **2.3 Extraction Procedure of the *F. foveolata* Vine**

The dried vine (5 kg) of *F. foveolata* was extracted with methanol (MeOH) by using Soxhlet's extractor. The extract was further partitioned with hexane,

dichloromethane ( $\text{CH}_2\text{Cl}_2$ ) and butanol (BuOH), yielding after evaporation hexane (21.2 g),  $\text{CH}_2\text{Cl}_2$  (42.0 g), and BuOH (434.1 g) extracts, respectively. The extraction procedure was summarized as shown in Scheme 2.1.



**Scheme 2.1** Extraction procedure of the *F. foveolata*

## 2.4 Bioassay Procedures

### 2.4.1 Cholinesterase Inhibitory Assay

The microplate assay was modified from Ellman's method (Ellman *et al.*, 1961). The test relies on the hydrolysis of acetylthiocholine by cholinesterase to form thiocholine which in turn reacts with 5,5-dithiobis-2-nitrobenzoic acid (DTNB) to give a yellow colored of 5-thio-2-nitrobenzoate (Scheme 2.2). Inhibitors are naturally occurring or synthetic molecules that decrease enzyme activity or prevents any substrate molecules from reacting with the enzyme.

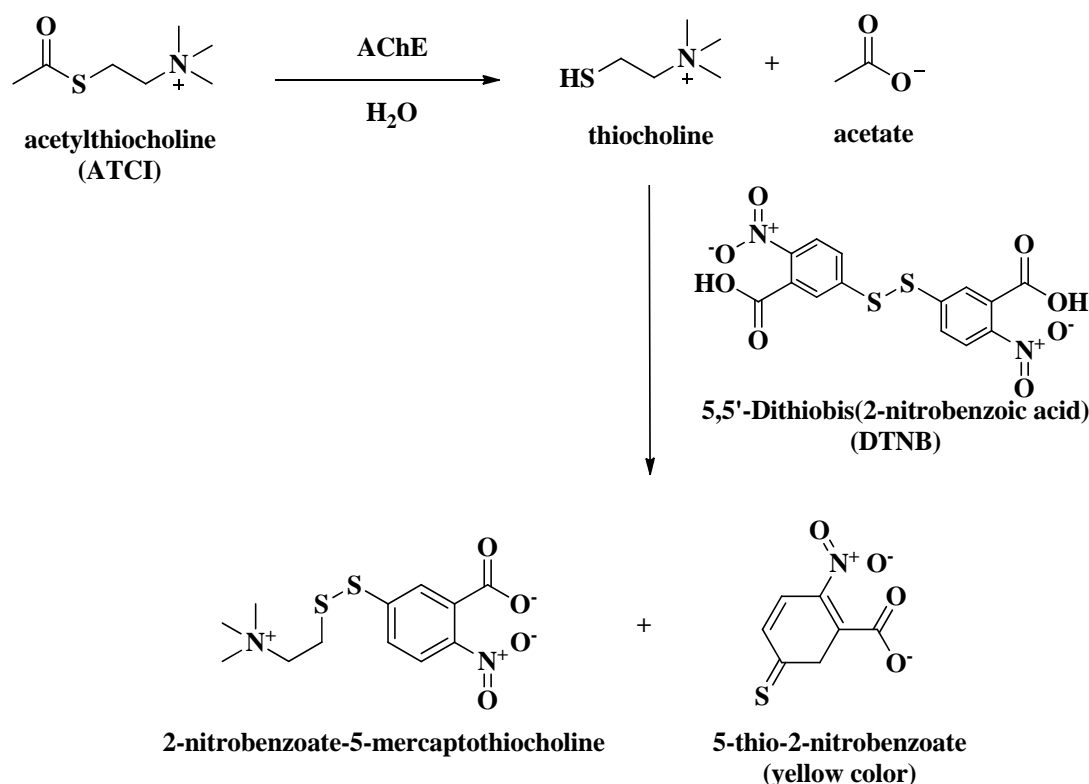
#### 2.4.1.1 Chemical Reagents

All commercial solvents used in this research were distilled prior to use except for those which were reagent grades.

AChE from electric eels (Type-VI-S lyophilized powder, EC 3.1.1.7), BChE from equine serum (lyophilized powder EC 3.1.1.8), acetylthiocholine iodide (ATCI), butyrylthiocholine iodide (BTCI), 5,5-dithiobis-2-nitrobenzoic acid (DTNB), galantamine and eserine were purchased from Sigma (St. Louis, MO, USA).

Albumin from bovine serum (BSA) was purchased from Fluka chemical company.

*Tris*-(hydroxymethyl)-aminomethane (*Tris*-HCl) was purchased from Merck (Darmstadt, Germany).



**Scheme 2.2** Cholinesterase catalyzed hydrolysis of acetylthiocholine

#### 2.4.1.2 Chemical Preparation

**Buffers** The following buffers were used;

Buffer A: 50 mM *Tris*-HCl, pH 8

Buffer B: 50 mM *Tris*-HCl, pH 8 containing 0.1% bovine serum albumin (BSA)

Buffer C: 50 mM *Tris*-HCl, pH 8 containing 1 M sodium chloride (NaCl) and 0.2 mM magnesium chloride hexahydrate ( $\text{MgCl}_2 \cdot 6\text{H}_2\text{O}$ )

#### Enzymes

Cholinesterase enzymes (AChE and BChE) were dissolved in buffer A to make 1130 U/mL stock solution, and further diluted with buffer B to get 0.3 U/mL enzymes for the microplate assay.

#### Substrate

ATCI and BTCl were dissolved in MilliQ water to make 15 mM substrate for the microplate assay.

#### Ellman Reagent

3 mM DTNB in buffer C was used for the microplate assay.

### Sample and Standard Compound

The samples were dissolved in buffer A containing not more than 10 % MeOH.

#### 2.4.1.3 Assay Method

AChE and BChE inhibitory activities were measured by slightly modifying the spectrophotometric based on Ellman's method and Ingkaninan *et al.* (2003). In the 96-well plates, 25  $\mu$ L of substrate, 125  $\mu$ L of DTNB, 50  $\mu$ L of buffer A, 25  $\mu$ L of sample and 25  $\mu$ L of enzyme were added and the absorbance was measured at 405 nm over 2 mins with a 5-s interval by Sunrise™ microplate reader. The resulting velocity was calculated and used for the determination of the enzyme and percentage inhibition as the equation was shown below.

$$\% \text{ inhibition} = \left( \frac{v_{\text{blank}} - v_{\text{sample}}}{v_{\text{blank}}} \right) \times 100 \quad (1)$$

When  $v_{\text{blank}}$  represents velocity of reaction of blank obtained from the assay.  $v_{\text{sample}}$  represents velocity of reaction of sample obtained from the assay

Each concentration was analyzed in triplicate. The concentration of sample required to inhibit 50% of the maximum observed enzymatic activity ( $IC_{50}$ ) were determined graphically from a plot of percentage inhibition versus log sample concentration value (Figure 2.1) using the GraphPad Prism 5.01 software of GraphPad Software Inc.

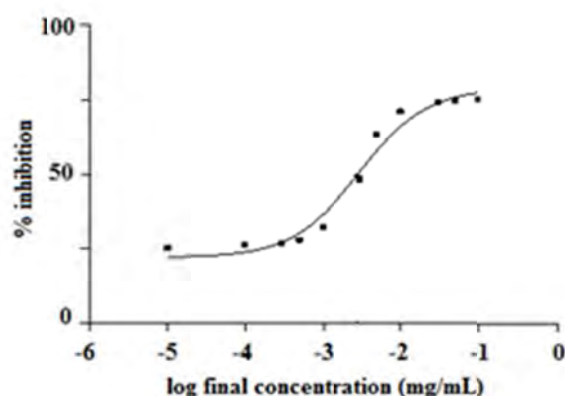
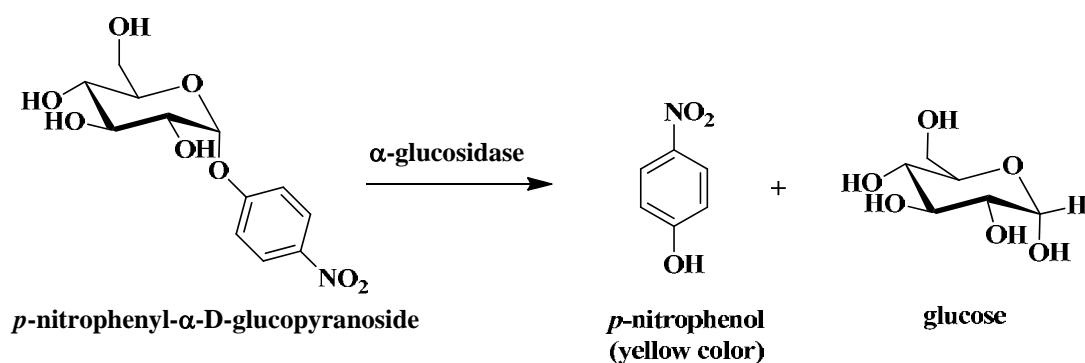


**Figure 2.1** A plot of log concentration value versus percentage inhibition of inhibitor

#### 2.4.2 $\alpha$ -Glucosidase Inhibition Assay

The  $\alpha$ -glucosidase inhibitory activity was performed using colorimetric method (Adisakwattana *et al.*, 2004) with a slight modification. The  $\alpha$ -glucosidase activity was

determined by measuring the product *p*-nitrophenol release from *p*-nitrophenyl- $\alpha$ -D-glucopyranoside (pNPG) at UV 405 nm using microplate reader (Scheme 2.3).



**Scheme 2.3** Hydrolysis of *p*-nitrophenyl- $\alpha$ -D-glucopyranoside by  $\alpha$ -glucosidase

#### 2.4.2.1 Chemical Reagents

Phosphate buffer,  $\alpha$ -glucosidase (EC 3.2.1.20) from Baker's yeast was purchased from Sigma-Aldrich (St.Louis, MO, USA). pNPG which was purchased from Sigma-Aldrich (St. Louis, MO, USA), was used as a substrate. Acarbose (Glucobay<sup>®</sup> 50 N 1; Bayer Vital, Leverkusen, Germany) as an inhibitor of  $\alpha$ -glucosidase was obtained from a local pharmacy.

#### 2.4.2.2 Chemical Preparation

##### Buffers

0.1 M phosphate buffer containing 2.84 g of disodium hydrogen orthophosphate ( $\text{Na}_2\text{HPO}_4$ ) and 2.72 g of potassium dihydrogen phosphate ( $\text{KH}_2\text{PO}_4$ ) were dissolved in 200 mL of distilled water, adjusted to pH 6.9.

##### Enzymes

$\alpha$ -Glucosidase was dissolved in phosphate buffer to make 0.1 U/mL stock solution, and further diluted with buffer to get 1 U/mL used for this test.

##### Substrate

pNPG dissolved in phosphate buffer to make concentration of 1 mM.

##### Sample and Standard Compound

The samples were dissolved in DMSO.

#### 2.4.2.3 Assay Method

In the 96-well plate, 50  $\mu\text{L}$  of buffer, 10  $\mu\text{L}$  of sample and 40  $\mu\text{L}$  of  $\alpha$ -glucosidase were added and incubated at 37  $^\circ\text{C}$  for 10 mins. Then, 50  $\mu\text{L}$  of pNPG was added and mixed. The enzyme reaction was carried out at 37  $^\circ\text{C}$  for 20 mins and then 100  $\mu\text{L}$  of 1 M sodium carbonate ( $\text{Na}_2\text{CO}_3$ ) was added to terminate the reaction. Enzymatic activity was

quantified by measuring the absorbance at 405 nm by Sunrise™ microplate reader. Percentage inhibition was calculated according to the equation shown below (Ogawa *et al.*, 2005).

$$\% \text{ inhibition} = \left( \frac{A_{\text{blank}} - A_{\text{sample}}}{A_{\text{blank}}} \right) \times 100 \quad (2)$$

$A_{\text{blank}}$  is the absorbance of control without test solution.  $A_{\text{sample}}$  is the absorbance of sample with test solution.

The concentration of tested compounds required to inhibit 50% of the  $\alpha$ -glucosidase activity under the assay conditions was determined from dose–response curves and defined as the half maximal inhibitory concentration or  $IC_{50}$  value by a plot of percentage inhibition versus sample concentration. Statistical significance was evaluated using the SigmaPlot 11.0 Graph software of GraphPad Software Inc. Acarbose was used as standard controls and the experiment was performed in duplicate.

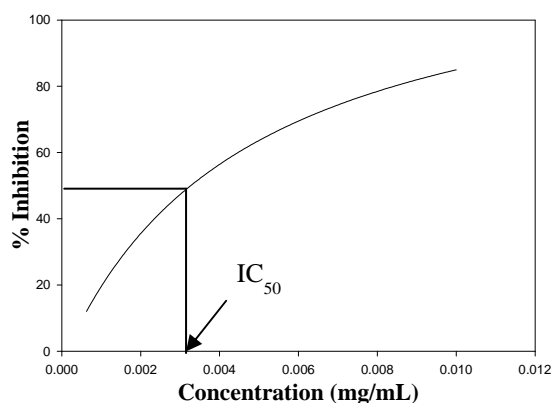
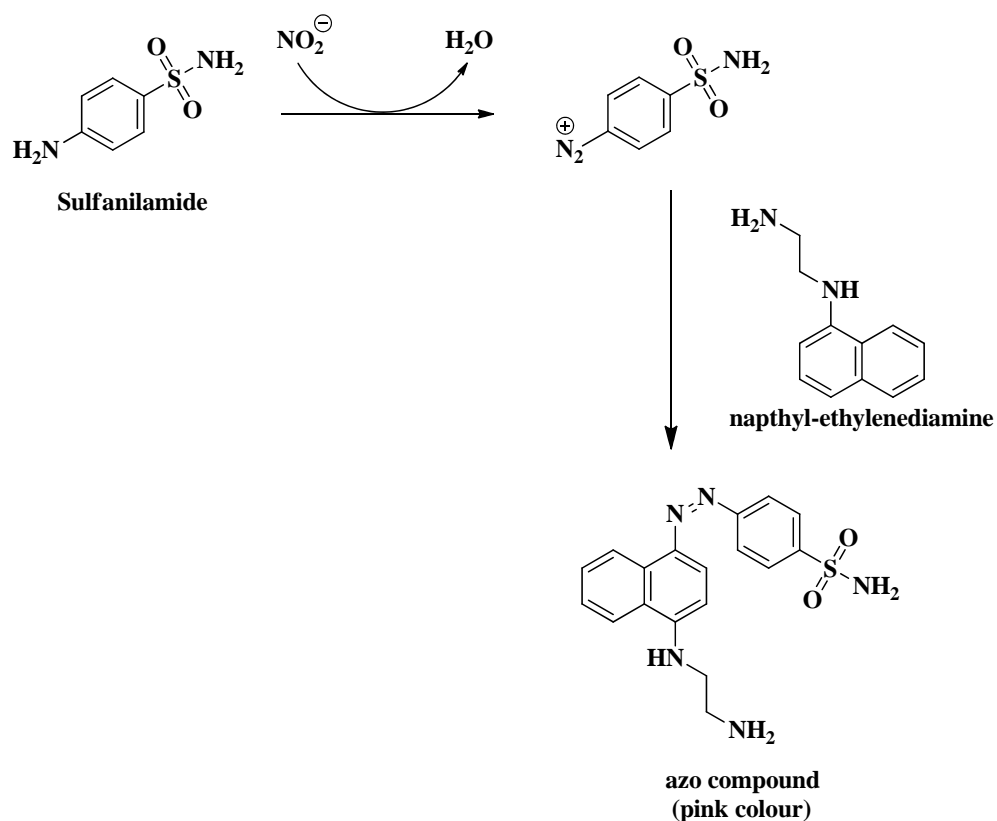


**Figure 2.2** A plot of concentration versus percentage inhibition of inhibitor

### 2.4.3 Nitric Oxide Inhibitory Activity

The potential anti-inflammatory activity of sample was assessed by evaluating its capacity to inhibit NO production in activated macrophages. Released nitrite in the culture medium, as an indicator of NO production, was measured using the colorimetric test based on the Griess reaction with some modification (Pacheco-Sanchez *et al.*, 2007). Nitrite is first treated with sulfanilamide (diazotizing reagent) to form a unstable diazonium salt. The intermediate was then reacted with N-naphthyl-ethylenediamine or NED, which was a coupling reagent to form a stable azo compound. The overall reaction is described in the scheme below.





**Scheme 2.4** Chemical reactions involved the measurement of nitrite using the Griess reagents system.

#### 2.4.3.1 Chemical Reagents

A murine macrophage cell line, RAW 264.7 (ATCC TIB-71), was obtained from the American Type Culture Collection. Dulbecco's modified Eagle's medium or DMEM/high glucose, fetal bovine serum (FBS), 4-(2-hydroxyethyl)-1-piperazineethane sulfonic acid (HEPES) and sodium pyruvate were obtained from Hyclone (Utah, USA). Streptomycin sulphate and Penicillin G (sodium salt) were purchased from M & H manufacturing (Samutprakarn, Thailand). 3-(4,5-dimethyl-2-thiazolyl)-2,5-diphenyl-2H-tetrazolium bromide (MTT) was purchased from USB Corporation (Ohio, USA). Lipopolysaccharide (LPS; *Samonella minnesota*), parthenolide was purchased from Sigma–Aldrich ChemieGmbH (Steinheim, Germany).

#### 2.4.3.2 Cell Culture and Treatment

A cell line was cultured in phenol red-free DMEM supplemented with 10% (v/v) FBS, 10 mM HEPES, 100 mM sodium pyruvate, 0.01% (w/v) penicillin G and 0.05% (w/v) streptomycin sulphate (DMEM complete medium).

All cells were grown at 37 °C under a humidified atmosphere accumulated with 5% (v/v) CO<sub>2</sub>, and were harvested by the addition of 10 mM cold phosphate buffer (pH 7.4) and gently aspirated before washing and dispersion into DMEM complete medium. 99 µL of the RAW 264.7 cell suspension were seeded per well of a 96-well microplate at 1×10<sup>4</sup> cells/well. 1 µL of the test sample in DMSO was added and incubated for 24 hours before being subjected to either the cytotoxic assay by MTT method or nitrite measurement. Cells were activated by adding 1 µL of LPS.

#### 2.4.3.3 Assay Method

The cytotoxic activity was evaluated by the reduction of MTT using the mitochondrial dehydrogenase of viable cells to give a blue formazan product, which can be measured spectrophotometrically. 50 µL of cells were seeded per well of a 96-well microplate at a concentration of 1×10<sup>4</sup> cells/well and then cultured for 4–6 hours at 37 °C to allow for recovery and surface adherence. Then, 1 µL of sample dissolved in DMSO at various concentrations was mixed into the well and cells were incubated at 37 °C for 72 hours with the addition of 10 µL of 12 mM MTT in phosphate buffer saline to cells for the last 4 hours of incubation. The medium was then carefully removed and replaced with 100 µL of 0.04 N hydrochloric–isopropanol and agitated to dissolve the formazan crystals (Mosmann, 1983). The absorbance of the dissolved formazan product was measured at 540 nm in microplate reader. Cell viability was calculated using the below equation.

$$\% \text{ cell viability} = \left( \frac{A_{\text{sample}}}{A_{\text{control}}} \right) \times 100 \quad (3)$$

A<sub>sample</sub> and A<sub>control</sub> are the absorbances from the mixture with or without the test sample added, respectively.

The potential anti-inflammatory activity of each sample was evaluated by determining its capacity to inhibit NO production in macrophages (Pacheco-Sanchez *et al.*, 2007). Released nitrite in the culture medium, as an indicator of NO production, was measured using the colorimetric test based on the Griess reaction. In the experiment, 50 µL of the prepared cell supernatant was mixed with 50 µL of 1% (w/v) sulfanilamide in 5% (v/v) phosphoric acid, incubated in the dark at room temperature for 10 min. Then 50 µL of a 0.1% (w/v) 0.1% N-naphthylenediamine dihydrochloride in water solution (NED) was added and incubated in the dark at room temperature for a further 10 mins. The nitrite concentration was then determined by measuring the absorbance at 540 nm in a

microplate reader using a standard calibration curve prepared from  $\text{NaNO}_2$  standards. The results were expressed as the percentage of NO production compared to the control from the equation (4) was shown below.

$$\% \text{ inhibition} = \left( \frac{\text{NO}_{2 \text{ control}} - \text{NO}_{2 \text{ sample}}}{\text{NO}_{2 \text{ control}}} \right) \times 100 \quad (4)$$

When  $\text{NO}_{2 \text{ control}}$  and  $\text{NO}_{2 \text{ sample}}$  are the amount of  $\text{NO}_2$  generated from the reaction in presence of the test sample and in absence of the test sample addition, respectively.

## CHAPTER III

### RESULTS AND DISCUSSION

According to the impressive preliminary screening result of anticholinesterase activity of *F. foveolata*, this plant was chosen for further investigating their biologically active principles.

#### 3.1 Primary Bioassay Screening Results of Crude Extracts

The vine of *F. foveolata* was extracted with appropriated solvents according to the procedure described in Scheme 2.1 of Chapter II. All extracts, hexane, CH<sub>2</sub>Cl<sub>2</sub> and BuOH extracts were then preliminarily tested for their anticholinesterase activity using microplate method. The results are shown in Table 3.1.

**Table 3.1** Anticholinesterase activities of *F. foveolata* extracts

Extract	% Inhibition*	
	AChE	BChE
Hexane extract	38.6	76.5
CH <sub>2</sub> Cl <sub>2</sub> extract	69.8	69.9
BuOH extract	78.1	91.1

\* At concentration of 1.0 mg/mL

From the results in Table 3.1, the BuOH extract displayed the most significant anticholinesterase activity and the CH<sub>2</sub>Cl<sub>2</sub> extract showed a moderate activity. Therefore both extracts were further studied to discover the active chemical constituents.

#### 3.2 Chemical Constituents from the Vine of *F. foveolata*

##### 3.2.1 Separation of the BuOH Extract

A part of the BuOH extract (434.1g) as a dark brown material was fractionated using Diaion column chromatography (CC) eluting with deionized (DI) water, MeOH and finally acetone, respectively. Each eluent was collected and then concentrated to a

small volume to obtain fractions A-C, respectively. The results of separation are shown in Table 3.2.

**Table 3.2** The separation of the BuOH extract from the vine of *F. foveolata*

Fraction	Eluent	Remark	Weight (g)
A	H <sub>2</sub> O	Dark brown syrup	20.8
B	MeOH	Dark brown syrup	87.2
C	acetone	Dark brown solid	4.0

Fraction B was subjected to vacuum CC (VCC) on silica gel eluted with a mixture of ethyl acetate (EtOAc), MeOH and H<sub>2</sub>O, respectively to yield fractions B1-B6. All fractions were further examined for anticholinesterase activity. The results of the inhibition test are shown in Table 3.3

**Table 3.3** The separation and anticholinesterase activity results of fraction B1-6

Fraction	Eluent (EtOAc:MeOH:H <sub>2</sub> O)	Remark	Weight (g)	% AChE inhibition*
B1	1:0:0	Dark brown syrup	47.0	54.4
B2	9:1:0	Dark brown syrup	11.6	40.2
B3	8:2:0.2	Dark brown syrup	31.2	43.8
B4	7:3:0.3	Dark brown syrup	16.3	29.1
B5	6:4:1	Dark brown syrup	17.7	20.8
B6	0:1:0	Dark brown syrup	4.1	18.7

\* At concentration of 1.0 mg/mL

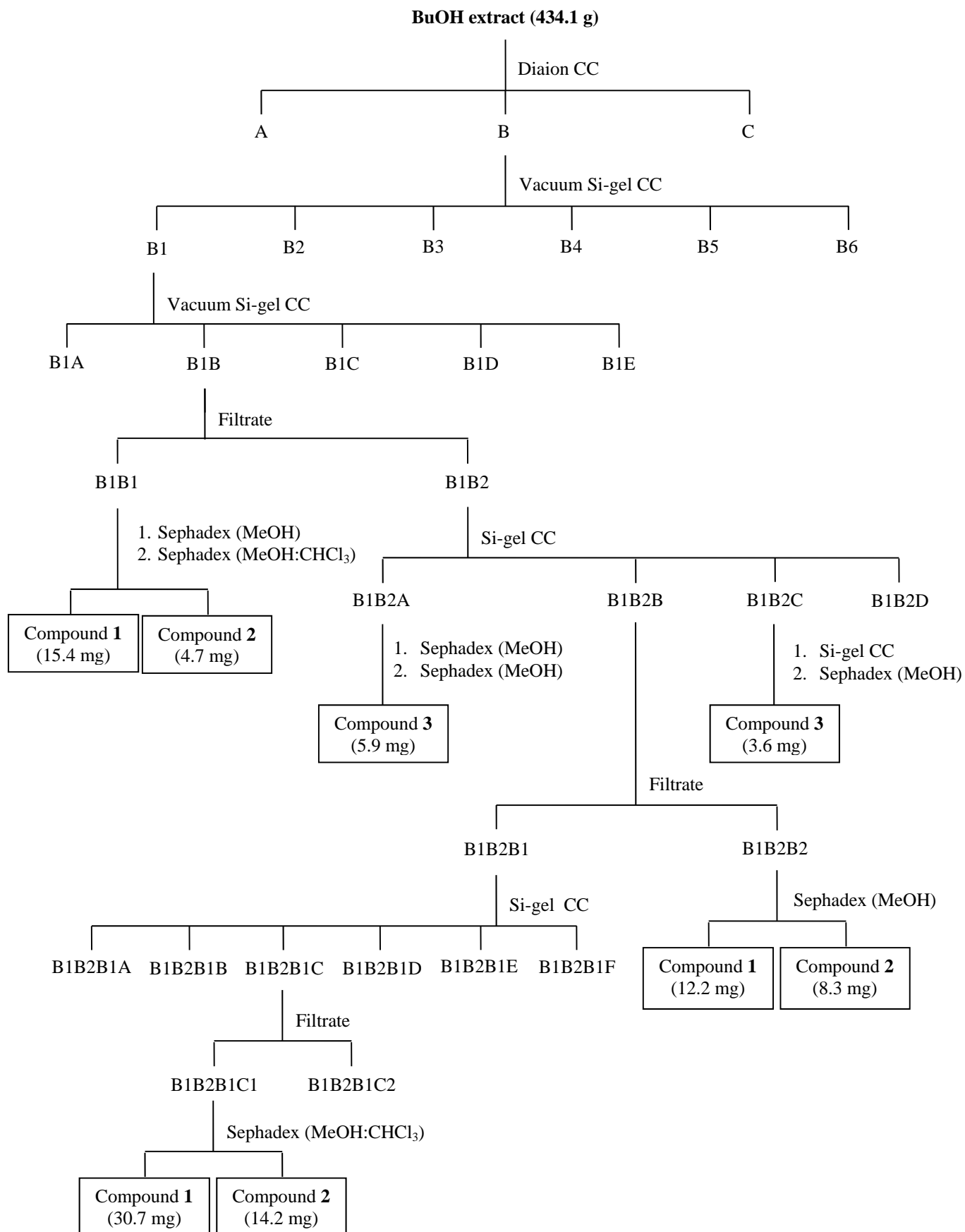
Fraction B1 was further separated by silica gel VCC eluting with an increasing polarity of hexane, EtOAc and MeOH, respectively to furnish sub-fractions B1A-B1E. During evaporating solvent from fraction B1B, it was noticed that some white powder solid precipitated. Thus fraction B1B was filtered to obtain solids (fraction B1B1) and the filtrate in fraction B1B2. Fraction B1B1 was further purified by sephadex LH-20 CC for 2 times; first CC was eluted with MeOH and second was eluted with 50% MeOH in chloroform (CHCl<sub>3</sub>) to give compounds **1** and **2**.

Fraction B1B2 was further separated by silica gel CC eluting with a gradient increasing polarity of hexane, EtOAc and MeOH mixture to furnish four sub-fractions B1B2A to B1B2D. Fraction B1B2A was subjected to sephadex LH-20 CC eluted with

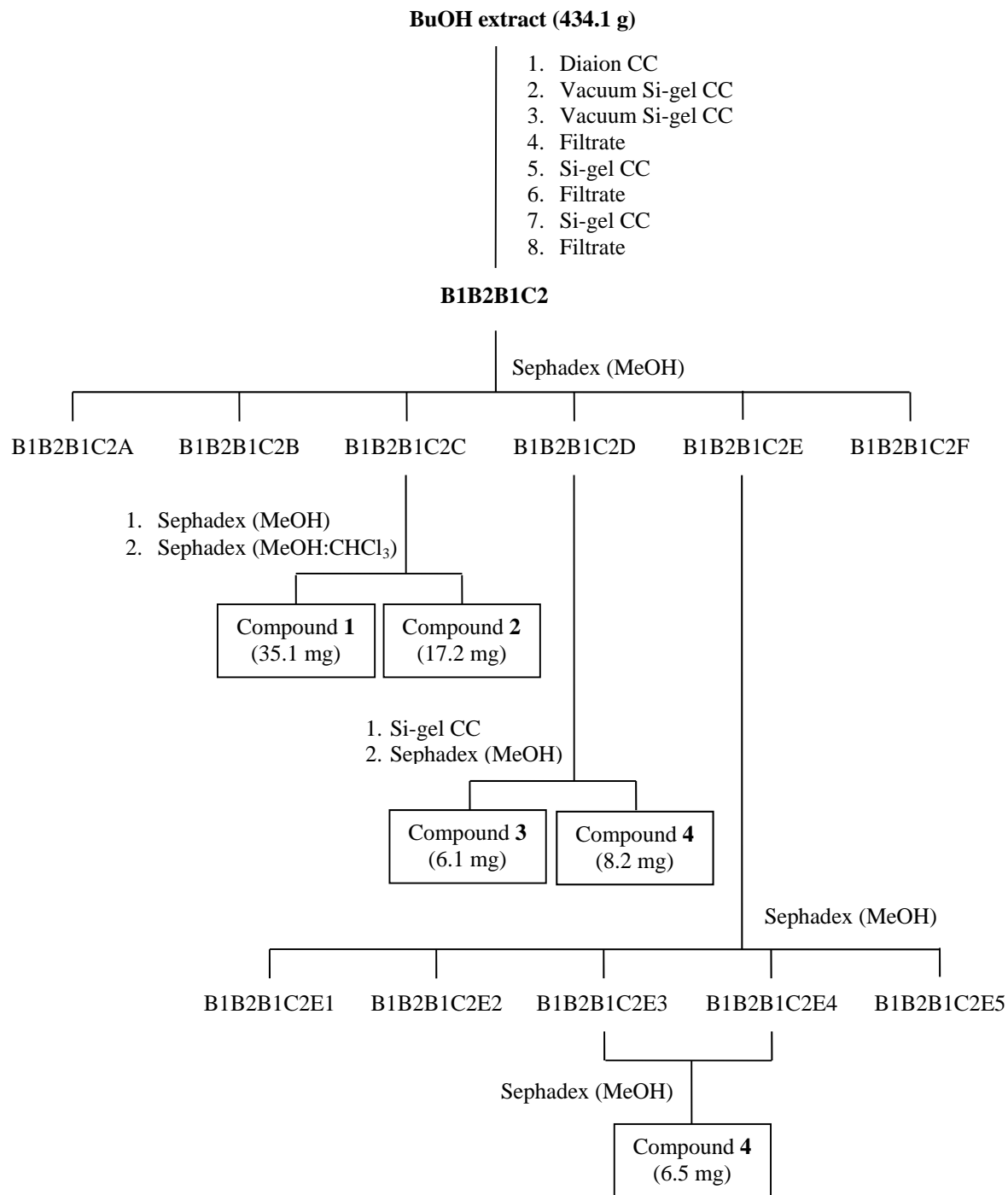
MeOH for twice to afford compound **3**. Fraction B1B2C was fractionated by silica gel CC with a gradient of hexane in EtOAc, EtOAc and MeOH in EtOAc, respectively and then purified on sephadex LH-20 CC with MeOH to afford compound **3**.

Fraction B1B2B was filtered to obtain 2 sub-fractions; B1B2B1 and B1B2B2. White solid in fraction B1B2B2 was purified over sephadex LH-20 CC eluting with 50% MeOH in CHCl<sub>3</sub> to give compounds **1** and **2**. Fraction B1B2B1 as a dark brown syrup was subjected on silica gel CC eluting with a gradient of hexane, EtOAc and MeOH by increasing polarity to furnish sub-fractions B1B2B1A to B1B2B1F. White solid was precipitated from fraction B1B2B1C, thus it was filtered to give fractions B1B2B1C1 and B1B2B1C2. Solid in fraction B1B2B1C1 was purified by sephadex LH-20 column CC with 50% MeOH in CHCl<sub>3</sub> to give compounds **1** and **2**, respectively. The results of separation are shown in Scheme 3.1.

Fraction B1B2B1C2 was repeatedly subjected to sephadex LH-20 eluted with MeOH to yield 6 sub-fractions, B1B2B1C2A to B1B2B1C2F. Fraction B1B2B1C2C was further separated by sephadex LH-20 chromatography for twice eluted with MeOH and 50% MeOH in CHCl<sub>3</sub>, respectively, to afford compounds **1** and **2**. Fraction B1B2B1C2D was separated by silica gel CC using a mixture of hexane, EtOAc and MeOH of increasing polarity as eluent and rechromatographed on a sephadex LH-20 column eluting with MeOH to furnish compounds **3** and **4**. Fractions B1B2B1C2E showed only one spot on TLC analysis. It was purified on sephadex LH-20 CC using MeOH to obtain five sub-fractions, B1B2B1C2E1 to B1B2B1C2E5. Fractions B1B2B1C2E3 and B1B2B1C2E4 were combined and purified by sephadex LH-20 CC with MeOH to give compound **4**. The results of separation of fraction B1B2B1C2 are shown in Scheme 3.2.



**Scheme 3.1** Isolated diagram of the BuOH extract from the vine of *F. foveolata*



**Scheme 3.2** Separation diagram of fraction B1B2B1C2 from BuOH extract



### 3.2.2 Separation of the CH<sub>2</sub>Cl<sub>2</sub> Extract

A part of CH<sub>2</sub>Cl<sub>2</sub> extract (42.0 g) as a brownish yellow material was fractionated using silica gel VCC eluting by an increase polarity of hexane, EtOAc, and MeOH, respectively. Each fraction was collected approximately 200 mL and then concentrated to a small volume. The fractions were combined monitoring by TLC results to obtain six fractions, D to I. The results of separation are shown in Table 3.4.

**Table 3.4** The separation of the CH<sub>2</sub>Cl<sub>2</sub> extract from the vine of *F. foveolata*.

<b>Fraction</b>	<b>Eluent</b> (Hexane:EtOAc)	<b>Remarks</b>	<b>Weight</b> (g)
D	7:3	yellow oil	1.7
E	6:4	brownish yellow syrup	7.4
F	4:6	brownish yellow syrup	6.5
G	4:6	dark brown syrup	18.5
H	3:7	dark brown syrup	24.2
I	0:1	dark brown syrup	1.7

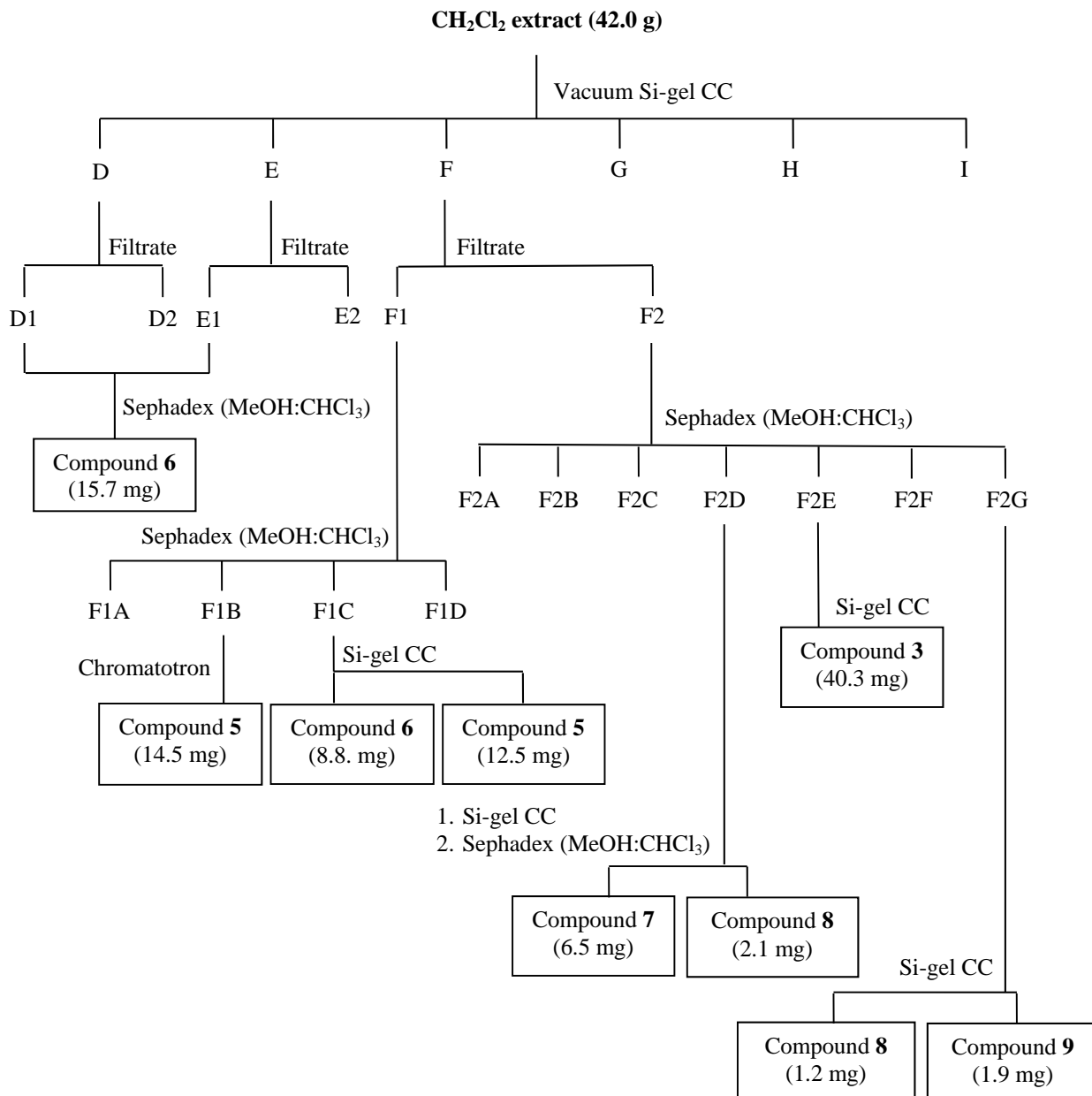
During evaporating solvent to a small volume, Fractions D and E gave some green platelets. These solids were filtrated to give fractions D1 and E1, respectively. According to TLC analysis, D1 and E1 were combined and then applied to a sephadex LH-20 CC eluting with 50% CHCl<sub>3</sub> in MeOH to give compound **6**.

Fraction F gave greenish white platelets, so this fraction was filtrated to give fractions F1 and F2. The solid in fraction F1 was re-chromatographed on a sephadex LH-20 CC with 50% MeOH in CHCl<sub>3</sub> as eluent to furnish fractions F1A to F1D. Fraction F1B was re-separated by chromatotron chromatography eluting with 10% EtOAc in hexane to afford compound **5**. Fraction F1C was subject to silica gel CC to furnish compounds **5** and **6**.

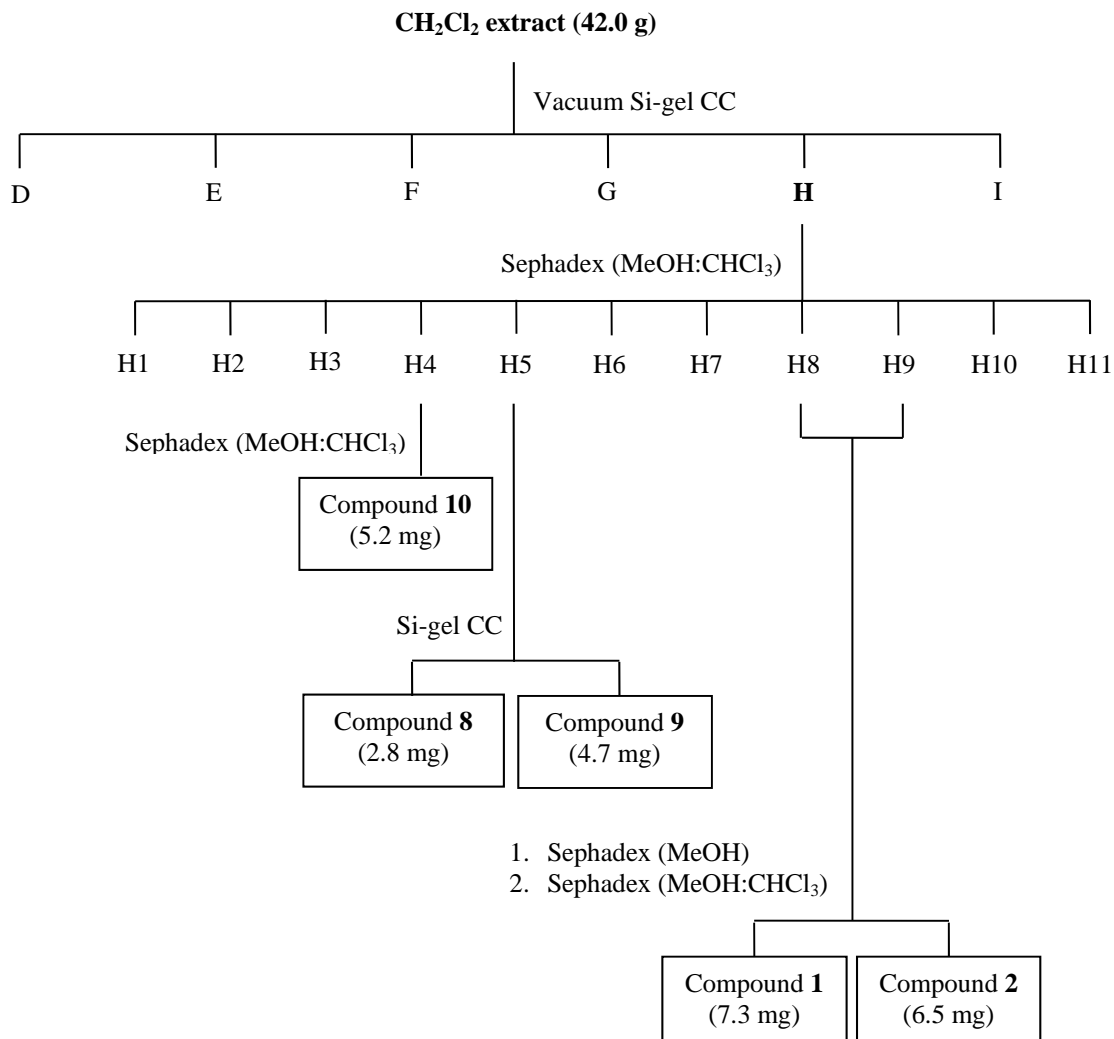
Fraction F2 as yellow syrup was subjected on a sephadex LH-20 CC eluting with 50% MeOH in CHCl<sub>3</sub> yielding seven fractions, F2A to F2G. Fraction F2D was further separated by silica gel CC using hexane–EtOAc gradient system and then purified by sephadex LH-20 column with 50% MeOH in CHCl<sub>3</sub> to afford compounds **7** and **8**. Fraction F2E was purified by silica gel flash CC using 50% EtOAc in hexane to give compound **3**. Fraction F2G was re-separated by silica gel CC using hexane–

EtOAc gradient system to yield compounds **8** and **9**. The separation diagram is shown in Scheme 3.3.

Fraction H was separated by sephadex LH-20 CC eluting by 50% MeOH in CHCl<sub>3</sub> to give fractions, H1 to H11. Fraction H3 was purified by sephadex LH-20 CC eluting by 50% MeOH in CHCl<sub>3</sub> to give compound **10**. Fraction H4 was applied to silica gel CC using a hexane–EtOAc gradient system to give compounds **8** and **9**, respectively. From the TLC result, fraction H8 had a similar spot to fraction H9. Thus, they were combined and purified by sephadex LH-20 CC eluting by 50% MeOH in CHCl<sub>3</sub> for twice to give compounds **1** and **2**. The separation diagram of fraction H is shown in Scheme 3.4.



**Scheme 3.3** Isolated diagram of the CH<sub>2</sub>Cl<sub>2</sub> extract from the vine of *F. foveolata*.



**Scheme 3.4** Separation diagram of fraction H from the CH<sub>2</sub>Cl<sub>2</sub> extract

### 3.2.3 Structural Elucidation of the Isolated Compounds

Ten compounds were isolated from the vine of *F. foveolata*. Their chemical structures were established by spectroscopic methods and comparing their data with those of literature reports.

#### 3.2.3.1 Structural Elucidation of Compounds 1-4

From the spectroscopic data of compounds **1-4**, the characteristic signals of *trans*-coupled olefinic protons were observed as two doublet signals at  $\delta_{\text{H}}$  6.70 and 7.50 ( $J = \sim 16.0$  Hz) which was associated with the carbon signal at  $\delta_{\text{C}} \sim 127.0$  and 130.0 in the HSQC spectrum. The spectrum data also showed the characteristic of the aromatic signals at  $\delta_{\text{H}} \sim 6.00$ -7.00 and  $\delta_{\text{C}} \sim 102.0$ -159.0. Thus, the core structures of compounds **1-4** were revealed as the *trans*-stilbene type skeleton. Their structures were further elucidated on the basis of the spectroscopic evidences comparing with those of literature data.

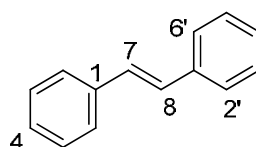


**Figure 3.1** A *trans*-stilbene skeleton

##### 3.2.3.1.1 Structural Elucidation of Compound 1

Compound **1** was obtained as pale yellow needle crystal (100.7 mg), m.p. 258.7-260.5°C. This compound showed a single spot on TLC with  $R_f$  value 0.43 (10% MeOH in  $\text{CHCl}_3$ ). It could be detected on TLC under UV light at 254 and 365 nm, which revealed the presence of a highly conjugated system in the molecule.

The  $^1\text{H-NMR}$  spectrum of compound **1** (Figure A-1) showed the pattern of a *trans*-stilbene skeleton at  $\delta_{\text{H}}$  6.75 (1H, *d*,  $J = 16.0$  Hz, H-7) and 6.91 (1H, *d*,  $J = 16.0$  Hz, H-8). The signals at  $\delta_{\text{H}}$  6.40 (2H, *d*,  $J = 2.0$  Hz, H-2 and H-6) and 6.11 (1H, *t*,  $J = 2.0$  Hz, H-4) was ascribed to one set of proton signals in the  $\text{A}_2\text{X}$  system on the 1, 3, 5-trisubstituted benzene ring. The presence of one set of proton signals in  $\text{A}_2\text{B}_2$  system on 1,4-disubstituted benzene ring at  $\delta_{\text{H}}$  7.30 (2H, *d*,  $J = 8.4$  Hz, H-2' and H-6') and 6.72 (2H, *d*,  $J = 8.4$  Hz, H-3' and H-5') were also observed in the spectrum. The  $^{13}\text{C-NMR}$  spectrum of compound **1** (Figure A-2) displayed ten carbon signals which could be assigned for aromatic carbons at  $\delta_{\text{C}}$  102.6-141.3 and two olefinic carbons at

$\delta_C$  127.0 (C-7) and 130.4 (C-8). The down-field chemical shift of carbons at  $\delta_C$  158.3 (C-4') and 159.6 (C-3 and C-5) were also assigned to three oxygenated carbons

According to the spectroscopic data of compound **1** compared with those of compounds in literature (Liu *et al.*, 2005), it could be confirmed that the structure of compound **1** was 3,4',5-trihydroxy-*trans*-stilbene or trivially named resveratrol. The comparison of spectral data is thus summarized in Table 3.5.

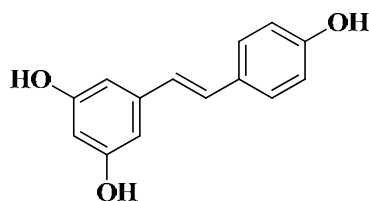


**Figure 3.2** Compound **1**: resveratrol

**Table 3.5** The  $^1\text{H}$  and  $^{13}\text{C}$ -NMR chemical shift assignments of compound **1** compared with those of resveratrol.

Position	Compound <b>1</b> (CD <sub>3</sub> OD)		Resveratrol (DMSO- <i>d</i> <sub>6</sub> )	
	$\delta_C$	$\delta_H$ (int., mult., <i>J</i> in Hz)	$\delta_C$	$\delta_H$ (int., mult., <i>J</i> in Hz)
1	141.3	-	139.2	-
2,6	105.8	6.40 (2H, <i>d</i> , 2.0)	104.3	6.37 (2H, <i>d</i> )
3,5	159.6	-	158.5	-
4	102.6	6.11 (1H, <i>t</i> , 2.0)	101.7	6.11 (1H, <i>s</i> )
7	127.0	6.75 (1H, <i>d</i> , 16.0)	125.6	6.78 (1H, <i>d</i> , 16.4)
8	130.4	6.91 (1H, <i>d</i> , 16.0)	127.8	6.90 (1H, <i>d</i> , 16.4)
1'	129.4	-	128.0	-
2',6'	128.8	7.30 (2H, <i>d</i> , 8.4)	127.8	7.39 (2H, <i>d</i> )
3',5'	116.5	6.72 (2H, <i>d</i> , 8.4)	115.5	6.73 (2H, <i>d</i> )
4'	158.3	-	157.2	-
OH-3	-	-	-	9.17 (2H, <i>s</i> )
OH-5	-	-	-	
OH-4'	-	-	-	

### 3.2.3.1.2 Structural Elucidation of Compound 2

Compound **2** was obtained as yellow amorphous powder (50.9 mg), m.p. 179.0-180.0°C. This compound showed a single spot on TLC with  $R_f$  value 0.57 (10% MeOH in  $\text{CHCl}_3$ ). It could be detected on TLC under UV light at 254 and 365 nm, which revealed the presence of a highly conjugated system in the molecule.

The  $^1\text{H-NMR}$  spectrum of compound **2** (Figure A-6) showed signals of a *trans*-stilbene skeleton at  $\delta_{\text{H}}$  6.82 (1H, *d*,  $J = 16.0$ , H-7) and 6.96 (1H, *d*,  $J = 16.0$ , H-8). The signals at  $\delta_{\text{H}}$  6.47 (2H, *d*,  $J = 2.0$  Hz, H-2 and H-6) and 6.17 (1H, *t*,  $J = 2.0$  Hz, H-4) were ascribed to the one set of proton signals in the  $\text{A}_2\text{X}$  system on the 1, 3, 5-trisubstituted benzene ring. The presence of one set of proton signals in ABX system on the 1,3,4-trisubstituted benzene ring at  $\delta_{\text{H}}$  7.10 (1H, *d*,  $J = 1.2$  Hz, H-2') and 6.77 (1H, *d*,  $J = 8.0$  Hz, H-5') and 6.95 (1H, *dd*,  $J = 1.2, 8.0$  Hz, H-6') were also observed in the spectrum. The  $^{13}\text{C-NMR}$  spectrum of compound **2** (Figure A-7) displayed signals of a methoxy carbon at  $\delta_{\text{C}}$  56.3 (OMe-3'), aromatic carbons at  $\delta_{\text{C}}$  102.6-147.6 and two olefinic carbons at  $\delta_{\text{C}}$  127.3 (C-7) and 129.6 (C-8). The down-field chemical shift of carbons at  $\delta_{\text{C}}$  147.6 (C-4') and 159.8 (C-3 and C-5) were also assigned to three oxygenated carbons.

The HMBC spectrum (Figure A-9) showed the clearly correlation between a methoxy group at  $\delta_{\text{H}}$  3.90 (OMe-3') and  $\delta_{\text{C}}$  149.1 (C-3'), which suggested that the methoxy group was attached to C-3' position. The correlation between H-5' and C-3', H-5' and C-4' including H-6' and C-4' was also confirmed the position of the methoxy and hydroxy groups on the aromatic ring.

According to the spectroscopic data of compound **2** compared with those of compounds in literature (Silayo *et al.*, 1999), it could be confirmed that the structure of compound **2** was 3, 4', 5-trihydroxy-3'-methoxy-*trans*-stilbene or trivially named isorhapontigenin. The comparison of spectral data is thus summarized in Table 3.6.

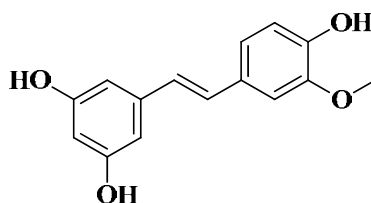


**Figure 3.3** Compound **2**: isorhapontigenin

**Table 3.6** The  $^1\text{H}$  and  $^{13}\text{C}$ -NMR chemical shift assignments of compound **2** compared with those of isorhapontigenin.

Position	Compound <b>2</b> ( $\text{CD}_3\text{OD}$ )		Isorhapontigenin ( $\text{acetone-}d_6$ )	
	$\delta_{\text{C}}$	$\delta_{\text{H}}$ (int., mult., $J$ in Hz)	$\delta_{\text{C}}$	$\delta_{\text{H}}$ (int., mult., $J$ in Hz)
1	141.2	-	140.6	-
2,6	105.8	6.47 (2H, <i>d</i> , 2.0)	105.7	6.61 (2H, <i>br d</i> , 1.8)
3,5	159.8	-	159.4	-
4	102.6	6.17 (1H, <i>t</i> , 2.0)	102.8	6.35 (1H, <i>br t</i> , 1.8)
7	127.3	6.82 (1H, <i>d</i> , 16.0)	127.5	6.92 (1H, <i>d</i> , 16.4)
8	129.6	6.96 (1H, <i>d</i> , 16.0)	129.1	7.00 (1H, <i>d</i> , 16.4)
1'	131.0	-	130.4	-
2'	110.3	7.10 (1H, <i>d</i> , 1.2)	112.4	7.12 (1H, <i>d</i> , 2.0)
3'	149.1	-	147.3	-
4'	147.6	-	148.3	-
5'	116.3	6.77 (1H, <i>d</i> , 8.0)	113.3	6.90 (1H, <i>d</i> , 8.1)
6'	121.2	6.95 (1H, <i>dd</i> , 1.2, 8.0)	119.9	6.97 (1H, <i>dd</i> , 8.2, 2.0)
OMe-3'	56.3	3.90 (3H, <i>s</i> )	56.2	3.80 (3H, <i>s</i> )

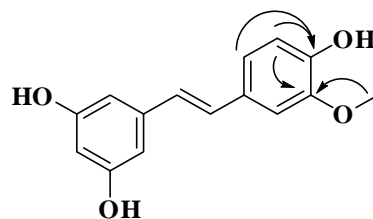


**Figure 3.4** Selected HMBC correlations of compound **2**



### 3.2.3.1.3 Structural Elucidation of Compound 3

Compound **3** was obtained as pale brown needle (55.1 mg), m.p. 150.7°C. This compound showed a single spot on TLC with  $R_f$  value 0.63 (10% MeOH in  $\text{CHCl}_3$ ). It could be detected on TLC under UV light at 254 and 365 nm, which revealed the presence of a highly conjugated system in the molecule.

The  $^1\text{H-NMR}$  spectrum of compound **3** (Figure A-11) revealed a *trans*-stilbene skeleton at  $\delta_{\text{H}}$  7.00 (1H, *d*,  $J = 16.0$  Hz, H-7) and 7.05 (1H, *d*,  $J = 16.0$  Hz, H-8). The signals at  $\delta_{\text{H}}$  6.49 (2H, *d*,  $J = 2.0$  Hz, H-2 and H-6) and 6.19 (1H, *t*,  $J = 2.0$  Hz, H-4) was ascribed to the one set of proton signals in the  $\text{A}_2\text{X}$  system on the 1, 3, 5-trisubstituted benzene ring. The presence of one set of proton signals on a phenyl ring at  $\delta_{\text{H}}$  7.51 (2H, *d*,  $J = 8.0$  Hz, H-2' and H-6'), 7.33 (2H, *t*,  $J = 8.0$  Hz, H-3' and H-5') and 7.23 (1H, *t*,  $J = 8.0$  Hz, H-4') were also observed in the spectrum. The  $^{13}\text{C-NMR}$  spectrum of compound **3** (Figure A-12) displayed ten carbon signals which could be assigned for aromatic carbons at  $\delta_{\text{C}}$  103.1-140.7 and two olefinic carbons at  $\delta_{\text{C}}$  129.9 (C-7) and 129.5 (C-8). The down-field chemical shift of carbons at  $\delta_{\text{C}}$  159.7 (C-3 and C-5) were also assigned to two oxygenated carbons.

According to the spectroscopic data of compound **3** compared with those of compounds in literature (Bachelor *et al.*, 1970), it could be confirmed that the structure of compound **3** was 3,5-dihydroxy-*trans*-stilbene or trivially named pinosylvin. The comparison of spectral data is thus summarized in Table 3.7.

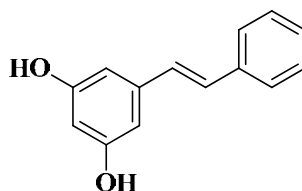


**Figure 3.5** Compound **3**: pinosylvin

**Table 3.7** The  $^1\text{H}$  and  $^{13}\text{C}$ -NMR chemical shift assignments of compound **3** compared with those of pinosylvin.

Position	Compound <b>3</b> (CD <sub>3</sub> OD)		Pinosylvin (CD <sub>3</sub> OD)	
	$\delta_{\text{C}}$	$\delta_{\text{H}}$ (int., mult., <i>J</i> in Hz)	$\delta_{\text{C}}$	$\delta_{\text{H}}$
1	140.7	-	140.0	-
2,6	106.5	6.49 (2H, <i>d</i> , 2.0)	106.2	6.54
3,5	159.7	-	156.9	-
4	103.1	6.19 (1H, <i>t</i> , 2.0)	102.4	6.26
7	129.9	7.00 (1H, <i>d</i> , 16.0)	128.0	6.88
8	129.5	7.05 (1H, <i>d</i> , 16.0)	129.5	6.97
1'	138.7	-	136.9	-
2',6'	127.5	7.51 (2H, <i>d</i> , 8.0)	126.6	7.42
3', 5'	129.7	7.33 (2H, <i>t</i> , 8.0)	128.7	7.30
4'	128.5	7.23 (1H, <i>br t</i> , 8.0)	127.8	7.22

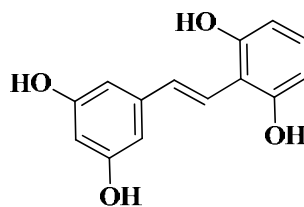
### 3.2.3.1.4 Structural Elucidation of Compound 4

Compound 4 was isolated as white needle (14.7 mg), m.p. 87.0-90.5°C. This compound showed a single spot on TLC with  $R_f$  value 0.68 (20% MeOH in  $\text{CHCl}_3$ ). It could be detected on TLC under UV light at 254 and 365 nm, which revealed the presence of a highly conjugated system in the molecule.

In the  $^1\text{H-NMR}$  spectrum indicated that compound 4 (Figure A-16) possessed a *trans*-stilbene skeleton at  $\delta_{\text{H}}$  7.47 (1H, *d*,  $J = 16.4$  Hz, H-7) and 7.39 (1H, *d*,  $J = 16.4$  Hz, H-8). The signals at  $\delta_{\text{H}}$  6.46 (2H, *d*,  $J = 2.0$  Hz, H-2 and H-6) and 6.14 (1H, *t*,  $J = 2.0$  Hz, H-4) was ascribed to one set of proton signals in the  $\text{A}_2\text{X}$  system on the 1, 3, 5-trisubstituted benzene ring. The presence of one set of proton signals in  $\text{AB}_2$  system on 1, 2, 3-trisubstituted benzene ring at  $\delta_{\text{H}}$  6.33 (2H, *d*,  $J = 8.0$  Hz, H-3' and H-5') and 6.83 (1H, *t*,  $J = 8.0$  Hz, H-4') were also observed in the spectrum. The  $^{13}\text{C-NMR}$  spectrum (Figure A-17) showed signals of aromatic carbons at  $\delta_{\text{C}}$  102.2-143.2 and two olefinic carbons at  $\delta_{\text{C}}$  121.7 (C-7) and 132.0 (C-8). The down-field chemical shift of carbons at  $\delta_{\text{C}}$  159.5 (C-3 and C-5), 158.0 (C-6') and 158.1 (C-2') were also assigned to four oxygenated carbons.

In the HMBC experiment (Figure A-19), the correlations between *trans*-olefinic protons H-7 and C-2, C-1' or H-8 and C-2' were observed. The correlation between protons and carbons on each aromatic ring was also displayed. Therefore, the 3',5'-dihydroxybenzene ring was connected at C-7 and a 2',6'-dihydroxybenzene ring was connected at C-8.

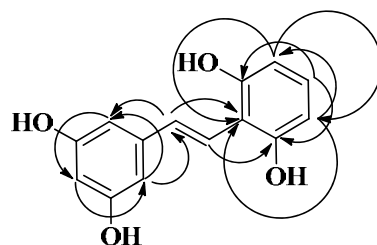
Based on these data, compound 4 was characterized as 2',3,5,6'-tetrahydroxy-*trans*-stilbene or trivially named gnetol. The spectral data is thus summarized in Table 3.8. Gnetol had previously report by Zaman *et al.* (1983), however it could not access the spectroscopic data from that publication to compare the data of compound 4.



**Figure 3.6** Compound 4: gnetol

**Table 3.8** The  $^1\text{H}$ ,  $^{13}\text{C}$ -NMR and HMBC assignments of compound **4**

Position	Compound <b>4</b> ( $\text{CD}_3\text{OD}$ )		
	$\delta_{\text{C}}$	$\delta_{\text{H}}$ (int., mult., $J$ in Hz)	HMBC
1	143.2	-	-
2	105.7	6.46 (1H, <i>d</i> , 2)	C7,C3,C4,C6
3	159.5	-	-
4	102.2	6.14 (1H, <i>t</i> , 2)	C2,C3,C5,C6
5	159.5	-	-
6	105.7	6.46 (1H, <i>d</i> , 2)	C7,C2,C4,C5
7	132.0	7.47 (1H, <i>d</i> , 16.8)	C1',C8,C2
8	121.7	7.39 (1H, <i>d</i> , 16.4)	C1,C7,C2',C5'
1'	113.2	-	-
2'	158.1	-	-
3'	107.9	6.33 (1H, <i>d</i> , 8)	C1',C2',C5'
4'	128.8	6.83 (1H, <i>t</i> , 8)	C2',C6'
5'	107.9	6.33 (1H, <i>d</i> , 8)	C1',C3',C6'
6'	158.0	-	-

**Figure 3.7** Selected HMBC correlations of compound **4**.

### 3.2.3.2 Structural Elucidation of Compounds 5-6

#### 3.2.3.2.1 Structural Elucidation of Compound 5

Compound **5** was obtained as white amorphous powder (27.0 mg), m.p. 85.0-87.5°C. This compound showed a single spot on TLC with  $R_f$  value 0.26 (in 100%  $\text{CH}_2\text{Cl}_2$ ). It could be detected on TLC under UV light at 254 and 365 nm, which revealed the presence of a conjugated system in the molecule.

The  $^1\text{H-NMR}$  spectra of compound **5** (Figure A-21) showed the characteristic signals of ferulate moiety (Figure 3.8); one set of proton signals in ABX system at  $\delta_{\text{H}}$  6.97 (1H, *s*), 6.84 (1H, *d*,  $J = 8.0$  Hz), 7.00 (1H, *dd*,  $J = 1.6, 8.0$  Hz), *trans*-olefinic bond proton signals at  $\delta_{\text{H}}$  6.22 (1H, *d*,  $J = 16.0$  Hz), 6.54 (1H, *d*,  $J = 16.0$  Hz) and a methoxy group signal at  $\delta_{\text{H}}$  3.86 (3H, *s*). The  $^{13}\text{C-NMR}$  spectrum of compound **5** (Figure A-22) showed an ester carbon signal at  $\delta_{\text{C}}$  166.6, two olefinic and eight aromatic carbons at  $\delta_{\text{C}}$  114.8-148.0. The correlations of this ferulate moiety were confirmed by the presence of correlations in the HMBC data (Figure A-24).

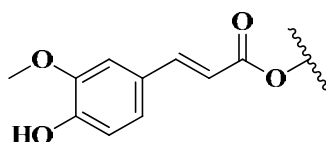


**Figure 3.8** A structure of ferulate moiety

Two highly deshielded protons at  $\delta_{\text{H}}$  4.12 (2H, *t*,  $J = 6.6$  Hz) and 3.57 (2H, *t*,  $J = 6.6$  Hz) showed correlations with  $\delta_{\text{C}}$  63.6 (C-1') and 62.1 (C-24'), respectively, which could be assigned as two oxygenated methylene groups. The deshielded signal of  $\delta_{\text{H}}$  4.12 (2H, *t*,  $J = 6.6$  Hz) had a long range coupling with a carbonyl carbon at  $\delta_{\text{C}}$  166.4. Thus the oxygenated methylene group at  $\delta_{\text{H}}$  4.12 was connected with an ester group of the ferulate moiety while another oxygenated methylene group was an hydroxyl methylene group attach at the end of molecule.

The envelop signals at  $\delta_{\text{H}}$  1.18-1.62 which had one bond coupling with  $\delta_{\text{C}}$  24.7.-63.6 in the HSQC data (Figure A-23) could be assign as a long chain methylene moiety. The number of carbons in this moiety was further determined by using the positive ESI-MS technique (Figure A-26). The observation molecular peak plus Na  $[\text{M}+\text{Na}]^+$  was found at  $m/z$  569.16. Thus the molecular weight of compound **5** was 546 g/mol. This result led to the presence of 24 methylene carbons in this moiety.

According to the spectroscopic data of compound **5** compared with those of compounds in literature (Xiang *et al.*, 2008), it was found that the NMR data of

compound **5** was in agreement with those of 24'-hydroxy-tetracosyl ferulate. The comparison of spectral data of both compounds is summarized in Table 3.9.

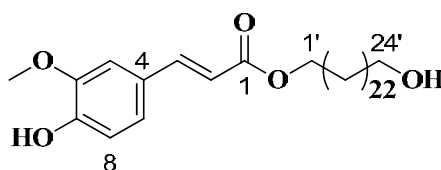


**Figure 3.9** Compound **5**: 24'-hydroxy-tetracosyl ferulate

**Table 3.9** The  $^1\text{H}$  and  $^{13}\text{C}$ -NMR chemical shift assignment of compound **5** compared with those of 24'-hydroxy-tetracosyl ferulate.

Position	Compound <b>5</b> ( $\text{CDCl}_3$ )		24'-Hydroxy-tetracosyl ferulate ( $\text{CDCl}_3$ )	
	$\delta_{\text{C}}$	$\delta_{\text{H}}$ (int., mult., $J$ in Hz)	$\delta_{\text{C}}$	$\delta_{\text{H}}$ (int., mult., $J$ in Hz)
1	166.4	-	167.4	-
2	114.6	6.22 (1H, <i>d</i> , 16.0)	115.6	6.31 ( <i>d</i> , 15.8)
3	143.6	7.54 (1H, <i>d</i> , 16.0)	144.7	7.62 ( <i>d</i> , 15.8)
4	126.0	-	127.0	-
5	108.2	6.97 (1H, <i>s</i> )	109.4	7.05 ( <i>d</i> , 1.9)
6	145.7	-	146.8	-
7	146.8	-	148.0	-
8	113.6	6.84 (1H, <i>d</i> , 8.0)	114.8	6.93 ( <i>d</i> , 8.2)
9	122.0	7.00 (1H, <i>dd</i> , 1.6,8.0)	123.0	7.08 ( <i>dd</i> , 1.9,8.2)
1'	63.6	4.12 (2H, <i>t</i> , 6.4)	64.6	4.20 ( <i>t</i> , 6.8)
2'	27.7	1.62 ( <i>m</i> )	28.8	1.69 ( <i>m</i> )
3'	25.0	1.30 ( <i>m</i> )	26.0	1.38 ( <i>m</i> )
4'-21'	28.2-28.7	1.18 ( <i>m</i> )	29.3-29.7	1.27 ( <i>m</i> )
22'	24.7	1.30 ( <i>m</i> )	25.7	1.38 ( <i>m</i> )
23'	31.8	1.48 ( <i>m</i> )	32.8	1.58 ( <i>m</i> )
24'	62.1	3.57 (2H, <i>t</i> , 6.8)	63.1	3.65 ( <i>t</i> , 6.7)
6-OMe	54.9	3.86 (3H, <i>s</i> )	55.9	3.94 ( <i>s</i> )

### 3.2.3.2.2 Structural Elucidation of Mixture 6

Mixture **6**, which was isolated as an inseparable mixture of two ferulic acid ester, was obtained as pale-greenish amorphous (24.5 mg), m.p. 115.7-116.5°C. This compound showed a superimposed spot on TLC with  $R_f$  value of 0.57 in  $\text{CH}_2\text{Cl}_2$ . The UV spectrum exhibited absorption at 245, 295 and 320 nm in  $\text{CHCl}_3$ .

The  $^1\text{H-NMR}$  spectra of mixture **6** (Figure A-27) were identical with those of compound **5** except for the absence of a strongly deshielded triplet signal at  $\delta_{\text{H}} \sim 3.50$ . However, there are no additional signals for this molecule including the absence of a methyl group. Therefore, it could be implied that each end of the long chain moiety connected by a ferulate part.

The number of methylene carbons was further determined by using the positive ESI-Qq-TOFMS technique (Figure A-32). The observation molecular peak plus proton  $[\text{M}+\text{H}]^+$  was found at  $m/z$  695.4507 (calculated for  $\text{C}_{42}\text{H}_{63}\text{O}_8^+$ , 695.4517) and 723.4820 (calculated for  $\text{C}_{44}\text{H}_{67}\text{O}_8^+$ , 723.4830). Thus the mixture **6** was characterized as a mixture of two compounds which their molecular weights were 694 and 722 and g/mol, respectively. This result confirmed the presence of 22 and 24 methylene carbons between two ferulate moieties in each compounds respectively.

According to the spectroscopic data of mixture **6**, the molecular formula was determined as  $\text{C}_{42}\text{H}_{62}\text{O}_8$  and  $\text{C}_{44}\text{H}_{66}\text{O}_8$  on the basis of spectrometry. Thus that the mixture **6** was composed of 1,22-docosanediol diferulate (**6a**) and 1,24-tetracosanediol diferulate (**6b**). The former was a novel compound while the latter was a known compound which previously isolated from *Hyoscyamus niger* seeds (Ma *et al.*, 2002). The HMBC (Figure A-30) and COSY (Figure A-31) correlations are shown in Figure 3.11 and the spectral data is summarized in Table 3.10.

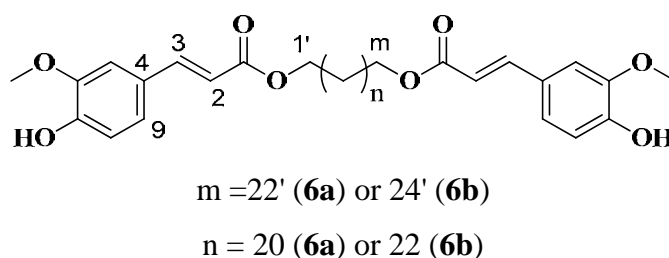


**Figure 3.10** Mixture **6**: A mixture of 1,22-docosanediol diferulate (**6a**) and 1,24-tetracosanediol diferulate (**6b**)

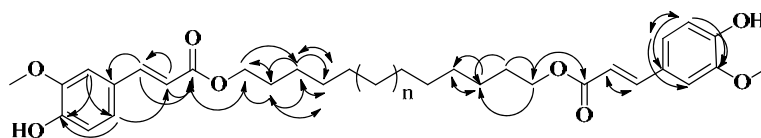


**Figure 3.11** HMBC (→) and COSY (↔) correlations of mixture **6** ( $n = 11$  or  $13$ )

**Table 3.10** The  $^1\text{H}$ ,  $^{13}\text{C}$ -NMR, HMBC and  $^1\text{H}$ - $^1\text{H}$  COSY assignments of compound **6a**

Position	compound <b>6a</b> ( $\text{CDCl}_3$ )			
	$\delta_{\text{C}}$	$\delta_{\text{H}}$ (int., mult., $J$ in Hz)	HMBC	COSY
1	166.6	-	-	-
2	115.7	6.22 (1H, <i>d</i> , 16.0)	C-1,C-4	H-3
3	144.8	7.54 (1H, <i>d</i> , 16.0)	C-1,C-3,C-5,C-9	H-2
4	127.1	-	-	-
5	109.3	6.97 (1H, <i>s</i> )	C-7,C-9	-
6	146.9	-	-	-
7	148.0	-	-	-
8	114.8	6.85 (1H, <i>d</i> , 8.0)	C-4,C-6	H-9
9	123.2	7.00 (1H, <i>d</i> , 8.0)	C-2,C-5,C-7,C-8	H-8
1',22'	64.8	4.12 (2H, <i>t</i> , 6.8)	C-1,C-2',C-21	H-2',H-21'
2',21'	28.9	1.62 (2H, <i>m</i> )	{ C-1',C-3', C-20',C-22'	{ H-1',H-3' H-20',H-22'
3',20'	26.1	1.30 ( <i>m</i> )	{ C-2',C-4' C-19',C-21'	{ H-2',H-4', H-19',H-21'
4'-19'	29.7-29.8	1.18 ( <i>m</i> )	C-3' – C-20'	H-3',H-20'
OMe-6	56.0	3.86 (3H, <i>s</i> )	C-6	-
OH-7	-	5.81 (1H, <i>s</i> )	-	-



**Table 3.11** The  $^1\text{H}$  and  $^{13}\text{C}$ -NMR chemical shift assignments of compound **6b** compared with those of 1,24-tetracosanediol diferulate.

Position	Compound <b>6b</b> ( $\text{CDCl}_3$ )		1,24-Tetracosanediol diferulate ( $\text{CDCl}_3$ )	
	$\delta_{\text{C}}$	$\delta_{\text{H}}$ (int., mult., $J$ in Hz)	$\delta_{\text{C}}$	$\delta_{\text{H}}$ (int., mult., $J$ in Hz)
1	166.6	-	167.3	-
2	115.7	6.22 (2H, <i>d</i> , 16.0)	115.6	6.29 (2H, <i>d</i> , 15.6)
3	144.8	7.54 (2H, <i>d</i> , 16.0)	144.5	7.61 (2H, <i>d</i> , 15.6)
4	127.1	-	126.9	-
5	109.3	6.97 (2H, <i>s</i> )	109.2	7.04 (2H, <i>d</i> , 2.0)
6	146.9	-	146.6	-
7	148.0	-	147.8	-
8	114.8	6.85 (1H, <i>d</i> , 8.0)	114.6	6.92 (2H, <i>d</i> , 8.4)
9	123.2	7.00 (1H, <i>d</i> , 8.0)	122.9	7.07 (2H, <i>dd</i> , 2.0, 8.4)
1', 24'	64.8	4.12 (2H, <i>t</i> , 6.8)	64.6	4.19 (4H, <i>t</i> , 6.6)
2', 23'	28.9	1.62 (2H, <i>m</i> )	28.8	1.68 4.19 (4H, <i>p</i> , 7.2)
3', 22'	26.1	1.30 ( <i>m</i> )	26.1-29.7	1.25-1.40 ( <i>m</i> )
4'-21'	29.7-29.8	1.18 ( <i>m</i> )		
OMe-6	56.0	3.86 (6H, <i>s</i> )	56.0	3.93 (6H, <i>s</i> )
OH-7	-	5.81 (2H, <i>s</i> )	32.8	5.88 ( <i>br s</i> )

### 3.2.3.4 Structural Elucidation of Compounds 7-10

From the spectroscopic data of compounds **7-10**, the  $^{13}\text{C}$ -NMR spectra together with the HMBC correlations indicated that these compounds had 15 carbons as core structure and one of them was a carbonyl carbon at  $\delta_{\text{C}} \sim 180.0$ . The  $^1\text{H}$ -NMR data clearly showed the signals of aromatic protons at  $\delta_{\text{H}} \sim 6.5$ - $8.0$  which were associated with the carbon aromatic signals at  $\delta_{\text{C}} \sim 90.0$ - $130.0$  assigned by the HSQC spectra. Thus, these compounds were assigned as the flavone skeleton. Their structures were further elucidated on the basis of spectroscopic evidences comparing with literature data.

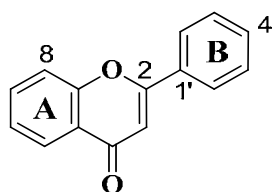


**Figure 3.12** A flavone skeleton

#### 3.2.3.4.1 Structural Elucidation of Compound 7

Compound **7** was obtained as yellow amorphous (6.5 mg), m.p.  $297.8^\circ\text{C}$ . This compound showed a single spot on TLC with  $R_f$  value 0.59 (10% MeOH in  $\text{CHCl}_3$ ).

The  $^1\text{H}$ -NMR spectrum of compound **7** (Figure A-34) showed a sharp singlet of a hydroxyl group at  $\delta_{\text{H}} 13.12$  (1H, *s*, 5-OH) which indicated the strong hydrogen bonding to a carbonyl group at  $\delta_{\text{C}} 183.6$  (C-4). Two singlet signals at  $\delta_{\text{H}} 6.67$  (1H, *s*, H-6) and  $6.80$  (1H, *s*, H-8) showed one bond connection with carbons at  $\delta_{\text{C}} 105.5$  (C-6) and  $94.9$  (C-8) determined by the HSQC spectrum (Figure A-36). In the HMBC spectrum (Figure A-37), the correlation of H-6 and H-8 with carbon signal at  $\delta_{\text{C}} 105.6$  (C-4a),  $167.1$  (C-7) could be assigned on the A-ring of the flavones skeleton. Meanwhile, the HMBC spectrum also showed a methoxy group signal at  $\delta_{\text{H}} 3.88$  (3H, *s*) correlated to  $\delta_{\text{C}} 132.2$  (C-3). Thus the position the methoxy group was on C-3. Two multiplet signals at  $\delta_{\text{H}} 7.61$  (3H, *m*, H-2', H-4' and H-6') and  $8.08$  (2H, *m*, H-3', 5') indicated that the B-ring contain one substituent.

According to the spectroscopic data of compound **7**, it could be characterized as 5,7-dihydroxy-3-methoxyflavone or galangin 3-methyl ether. The spectral data of compound **7** and galangin 3-methyl ether reported in the literature (Urbatsch *et al.*, 1975) are summarized in Table 3.12.

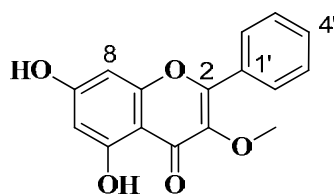


**Figure 3.13** Compound 7: galangin 3-methyl ether

**Table 3.12** The  $^1\text{H}$  and  $^{13}\text{C}$ -NMR chemical shift assignments of compound 7 compared with those of galangin 3-methyl ether.

Position	Compound 7 ( $\text{CDCl}_3$ )		Galangin 3-methyl ether ( $\text{C}_6\text{D}_6$ )
	$\delta_{\text{C}}$	$\delta_{\text{H}}$ (int., mult., $J$ in Hz)	$\delta_{\text{H}}$ (int., mult., $J$ in Hz)
2	157.9	-	-
3	167.1	-	-
4	183.6	-	-
4a	105.6	-	-
5	164.7	-	-
6	105.5	6.67 (1H, <i>s</i> )	6.63 ( <i>d</i> ,2)
7	132.2	-	-
8	94.9	6.80 (1H, <i>s</i> )	6.84 ( <i>d</i> ,2)
8a	154.0	-	-
1'	131.1	-	-
2',6'	130.0	7.61 (3H, <i>m</i> )	7.55,7.95 (5H, <i>m</i> )
4'	132.7		
3',5'	127.2	8.08 (2H, <i>m</i> )	
OH-5	-	13.12 (1H, <i>s</i> )	-
OMe-7	60.7	3.88 (3H, <i>s</i> )	3.81

### 3.2.3.4.2 Structural Elucidation of Compound 8

Compound **8** was obtained as yellow crystals (6.1 mg), m.p. 160.0-161.0°C. This compound showed a single spot on TLC with  $R_f$  value 0.61 (30% EtOAc in hexane). It could be detected on TLC under UV light.

The NMR spectroscopic data of compound **8** was similar to those of **7** with the exception of singlet signal at  $\delta_H$  6.71 (1H, s). The  $^1H$ -NMR spectrum of compound **8** (Figure A-39) showed a sharp singlet signal of a hydroxyl group at  $\delta_H$  12.74 (1H, s, OH-5), an AB spin system of aromatic protons in the A-ring at  $\delta_H$  6.23 (1H, *d*,  $J = 2$  Hz, H-6) and 6.63 (1H, *d*,  $J = 2$  Hz, H-8), the presence of aromatic protons in the B-ring at  $\delta_H$  7.49 (3H, *m*, H-2', H-4' and H -6') and 7.97 (2H, *m*, H-3' and H-5') and a methoxy group at  $\delta_H$  3.82 (3H, *s*) which correlated to  $\delta_C$  166.8 (C-7). The HSQC spectrum (Figure A-41) clearly showed the connection of an aromatic proton signal at  $\delta_H$  6.71 (1H, *s*) with the carbon signal at  $\delta_C$  106.3 (C-3).

By comparison of spectral data with those of compounds in literature, compound **8** was 5-hydroxy-7-methoxyflavone or tectochrysin. The spectral data of compound **8** and tectochrysin reported in the literature (Sutthanut *et al.*, 2007) are summarized in Table 3.13.

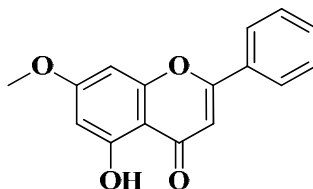


**Figure 3.14** Compound **8**: tectochrysin

**Table 3.13** The  $^1\text{H}$  and  $^{13}\text{C}$ -NMR chemical shift assignments of compound **8** compared with those of tectochrysin.

Position	Compound <b>8</b> ( $\text{CDCl}_3$ )		Tectochrysin ( $\text{CDCl}_3$ )	
	$\delta_{\text{C}}$	$\delta_{\text{H}}$ (int., mult., $J$ in Hz)	$\delta_{\text{C}}$	$\delta_{\text{H}}$ (int., mult., $J$ in Hz)
2	164.9	-	163.8	-
3	106.3	6.71 (1H, <i>s</i> )	105.7	6.64 (1H, <i>s</i> )
4	183.3	-	182.4	-
4a	106.2	-	105.6	-
5	161.7	-	162.1	-
6	98.9	6.23 (1H, <i>d</i> , 2.0)	98.1	6.36 (1H, <i>d</i> , 2.0)
7	166.8	-	165.5	-
8	93.4	6.63 (1H, <i>d</i> , 2.0)	92.6	6.48 (1H, <i>d</i> , 2.0)
8a	156.6	-	157.7	-
1'	132.2	-	131.2	-
2',6'	127.3	[ 7.49 (3H, <i>m</i> )	126.2	[ 7.52 (3H, <i>m</i> )
4'	132.8		131.5	
3',5'	130.0	7.97 (2H, <i>m</i> )	129.0	7.87 (2H, <i>m</i> )
OH-5	-	12.74 (1H, <i>s</i> )	-	12.73 (1H, <i>s</i> )
OMe-7	56.5	3.82 (3H, <i>s</i> )	55.7	3.88 (3H, <i>s</i> )

### 3.2.3.4.3 Structural Elucidation of Compound 9

Compound **9** was obtained as yellow short needle (6.6 mg), m.p. 129.0°C. This compound showed a single spot on TLC with  $R_f$  value 0.33 (10% EtOAc in hexane).

The NMR spectroscopic data of compound **9** were superimposed with those of **7** with except for the presence of additional one methoxy group signal at  $\delta_H$  3.82 (1H, *s*). The  $^1H$ -NMR spectrum of compound **9** (Figure A-44) indicated a sharp singlet of a hydroxyl group at  $\delta_H$  12.53 (1H, *s*, OH-5), an AB spin system of aromatic protons in the A-ring at  $\delta_H$  6.23 (1H, *d*,  $J = 2$  Hz, H-6) and 6.63 (1H, *d*,  $J = 2$  Hz, H-8), the presence of aromatic protons in the B-ring at  $\delta_H$  7.47 (3H, *m*, H-2', H-4' and H-6') and 7.99 (2H, *m*, H-3' and H-5') and another methoxy group at  $\delta_H$  3.88 (3H, *s*) which correlated to  $\delta_C$  166.8 (C-7). The HMBC spectrum (Figure A-47) clearly showed the connection of a methoxy signal at  $\delta_H$  3.82 (1H, *s*) with the carbon signal at  $\delta_C$  140.5 (C-3).

By comparison of spectral data, compound **9** was identified as 5-hydroxy-3,7-dimethoxyflavone. The spectral data of compound **9** and those of 5-hydroxy-3,7-dimethoxyflavone reported in the literature (Sutthanut *et al.*, 2007) are summarized in Table 3.14.

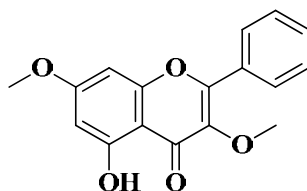


**Figure 3.15** Compound **9**: 5-hydroxy-3,7-dimethoxyflavone

**Table 3.14** The  $^1\text{H}$  and  $^{13}\text{C}$ -NMR chemical shift assignments of compound **9** compared with those of 5-hydroxy-3,7-dimethoxyflavone.

Position	Compound <b>9</b> (acetone- $d_6$ )		5-Hydroxy-3,7-dimethoxyflavone ( $\text{CDCl}_3$ )	
	$\delta_{\text{C}}$	$\delta_{\text{H}}$ (int., mult., $J$ in Hz)	$\delta_{\text{C}}$	$\delta_{\text{H}}$ (int., mult., $J$ in Hz)
2	156.3	-	155.5	-
3	140.5	-	139.4	-
4	178.3	-	178.6	-
4a	107.3	-	105.9	-
5	162.8	-	161.7	-
6	98.6	6.23 (1H, $d$ , 2.0)	97.7	6.28 (1H, $d$ , 2.0)
7	166.8	-	165.3	-
8	92.9	6.57 (1H, $d$ , 2.0)	91.9	6.38 (1H, $d$ , 2.0)
8a	158.0	-	155.6	-
1'	131.4	-	130.2	-
2',6'	129.5	7.47 (3H, $m$ )	128.4	7.48 (3H, $m$ )
4'	131.8		130.7	
3',5'	129.2	7.99 (2H, $m$ )	128.1	8.03 (2H, $m$ )
OMe-3	60.5	3.82 (3H, $s$ )	60.1	3.82 (3H, $s$ )
OH-5	-	12.53 (1H, $s$ )	-	12.55 (1H, $s$ )
OMe-7	56.5	3.88 (3H, $s$ )	55.6	3.85 (3H, $s$ )

#### 3.2.3.4.4 Structural Elucidation of Compound 10

Compound **10** was obtained as yellow powder (5.2 mg), m.p. 313.5-313.7 °C. This compound showed a single spot on TLC with  $R_f$  value 0.43 (10% MeOH in  $\text{CHCl}_3$ ).

The NMR spectroscopic data of compound **10** were similar to those of **7**, except the proton signals in the B-ring. The  $^1\text{H-NMR}$  spectrum (Figure A-49) showed the presence of aromatic protons in ABX system at  $\delta_{\text{H}}$  7.69 (1H, *d*,  $J = 2.0$  Hz, H-2') and 6.86 (1H, *d*,  $J = 8.4$  Hz, H-5') and 7.57 (1H, *dd*,  $J = 2.0, 8.4$  Hz, H-6') in the B-ring, which were assigned as H-2', H-5' and H-6', respectively.

By comparison of spectral data with those of quercetin in literature, compound **10** was identified as 3,3',4',5,7-pentahydroxyflavone or quercetin. The spectral data of compound **10** and quercetin reported in the literature (Wawer and Zielinska, 1997; Xiao *et al.*, 2006) are thus summarized in Table 3.15.

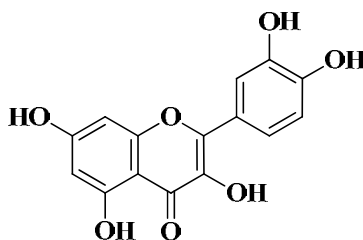


**Figure 3.16** Compound **10**: quercetin



**Table 3.15** The  $^1\text{H}$  and  $^{13}\text{C}$ -NMR chemical shift assignments of compound **10** compared with those of quercetin.

Position	Compound 10 (acetone- $d_6$ )		Quercetin	
	$\delta_{\text{C}}$	$\delta_{\text{H}}$ (int., mult., $J$ in Hz)	$\delta_{\text{C}}^*$	$\delta_{\text{H}}$ (int., mult., $J$ in Hz)**
2	146.9	-	146.9	-
3	136.8	-	135.9	-
4	176.2	-	176.0	-
4a	104.1	-	103.1	-
5	162.3	-	156.3	-
6	99.1	6.13 (1H, <i>d</i> , 2.0)	98.3	6.27 (1H, <i>br s</i> )
7	165.0	-	164.0	-
8	94.4	6.39 (1H, <i>d</i> , 2.0)	93.5	6.53 (1H, <i>br s</i> )
8a	157.7	-	160.8	-
1'	123.7	-	122.2	-
2'	115.7	7.69 (1H, <i>d</i> , 2.0)	115.2	7.81 (1H, <i>br s</i> )
3'	145.8	-	145.2	-
4'	148.3	-	147.8	-
5'	116.2	6.86 (1H, <i>d</i> , 8.4)	115.7	6.99 (1H, <i>d</i> , 8.0)
6'	121.4	7.57 (1H, <i>dd</i> , 2.0, 8.4)	120.1	7.70 (1H, <i>d</i> , 8.0)
OH-5	-	12.05 (1H, <i>s</i> )	-	-

\*Measured in (DMSO- $d_6$ )

\*\*Measured in (acetone- $d_6$ )

### 3.3 Biological Activity Study of Isolated Compounds from the Vine of *F. foveolata*

As aforementioned results, the separation of the *F. foveolata* vine led to the isolation of ten compounds. These compounds were further studied for their bioactivities; anticholinesterase,  $\alpha$ -glucosidase inhibitory and anti-inflammatory activities.

#### 3.3.1 The Results of Cholinesterase Inhibitory Activity Test

The cholinesterase inhibitory activities of compounds **1-10** isolated from *F. foveolata* were evaluated by colorimetric method. Since galantamine and eserine has been reported as potential AChE agents, these compounds were used as standard in this experiment.

The inhibitory activity in Table 3.16 revealed that most of tested compounds showed low activities against AChE and BChE, except for compounds **1-4** exhibited high inhibition toward BChE at the final concentration of 0.1 mg/mL. Regarding the results, the quantitative analysis for determination  $IC_{50}$  values of compounds **1-4** against AChE and BChE was then performed using spectrophotometric method as described in Chapter II. The  $IC_{50}$  values of tested compounds were calculated from the Prism program and tabulated in Table 3.16. In addition, the structural activity relationship of all isolated stilbenes toward BChE was also observed.

According to the results in Table 3.17, compound **4** possessed the highest activity with the  $IC_{50}$  value of 1.27  $\mu$ M which was more effective than that of standard compounds, galantamine and eserine. The position and number of hydroxyl groups of stilbenes seem to affect to BChE inhibitory action. The absence of hydroxyl groups in a phenyl ring of compound **3** was significant decreasing the activity compared to compound **4**. Additionally, the presence of a methoxy group at 3'-position reduced the activity (compound **1** vs. compound **2**).

Stilbenes were known to display a variety of pharmacological properties (Xiao *et al.*, 2008), and some stilbenes-oligomers were presented as potent AChE inhibitors e.g. (+)- $\alpha$ -viniferin (Sung *et al.*, 2002) and neohopeaphenol (Liu *et al.*, 2005). However, inhibitory effect of stilbenes toward BChE has not been reported yet. Thus, the result of this study was found that compound **4** could be a candidate for further study and improvement to be an effective drug for treatment of AD.

**Table 3.16** Cholinesterase inhibitory activity of the isolated compounds at final concentration of 0.1 mg/mL

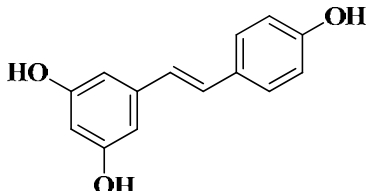
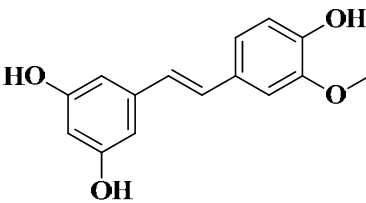
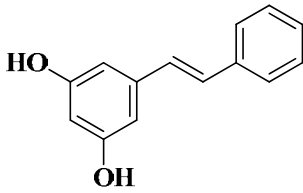
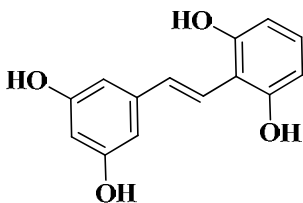
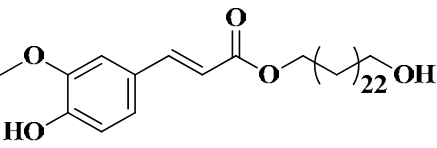
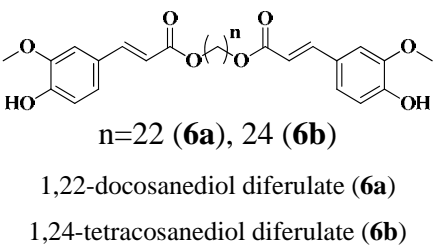
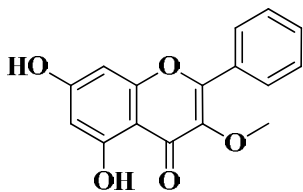
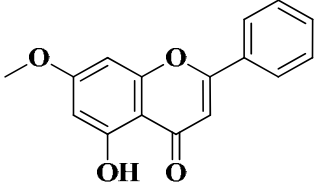
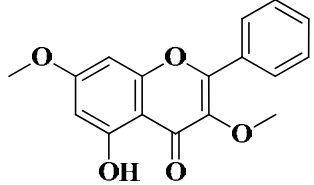
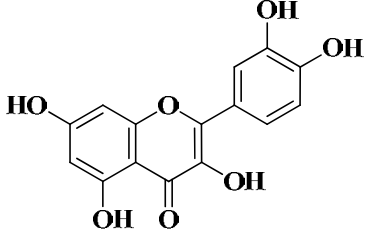
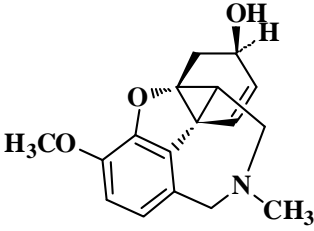
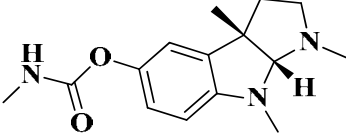
Compound	Structure	% Inhibition*	
		AChE	BChE
resveratrol (1)		17.69 ± 0.20	90.10 ± 1.16
isorhaponigetin (2)		20.90 ± 1.40	88.30 ± 0.79
pinosylvin (3)		22.11 ± 0.73	94.71 ± 0.48
gnetol (4)		19.02 ± 0.38	89.2 ± 0.98
24'-hydroxy-tetracosyl ferulate (5)		N.I.	N.I.
mixture (6)	 n=22 ( <b>6a</b> ), 24 ( <b>6b</b> ) 1,22-docosanediol diferulate ( <b>6a</b> ) 1,24-tetracosanediol diferulate ( <b>6b</b> )	N.I.	N.I.
galangin 3-methyl ether (7)		16.64 ± 0.14	25.98 ± 0.91

Table 3.16 Continued

Compound	Structure	% Inhibition*	
		AChE	BChE
tectochrysin (8)		1.48 ± 0.53	6.25 ± 0.66
5-hydroxy-3,7-dimethoxyflavone (9)		4.46 ± 1.98	6.25 ± 2.66
quercetin (10)		18.81 ± 0.23	30.96 ± 0.08
galantamine		95.59 ± 1.41	93.1 ± 0.39
eserine		97.93 ± 2.23	92.17 ± 0.79

\*Results are expressed as mean ± SD (n=3), N.I. = No inhibition

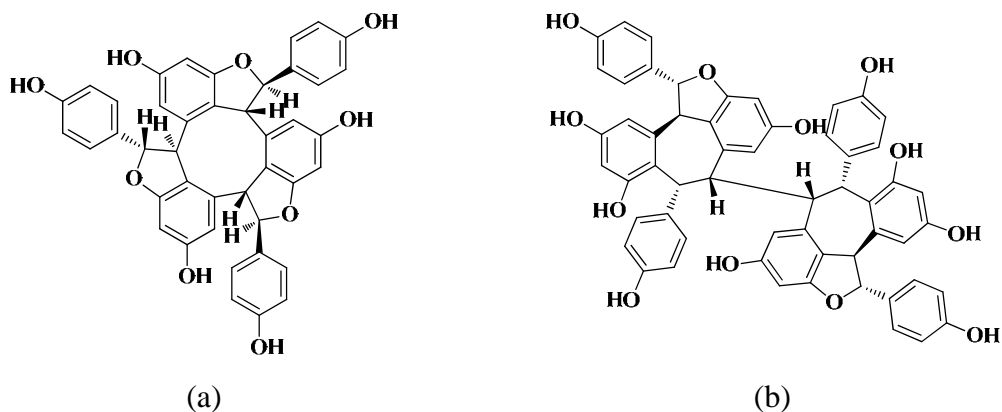
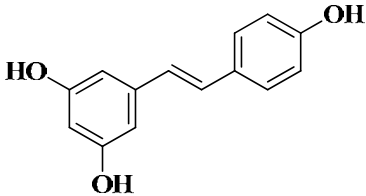
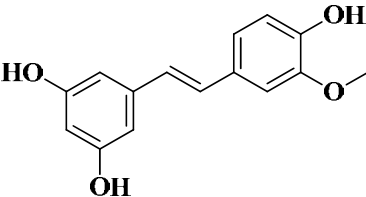
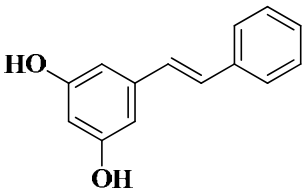
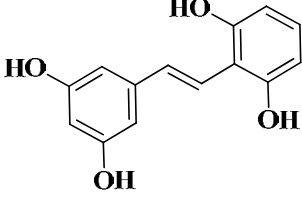
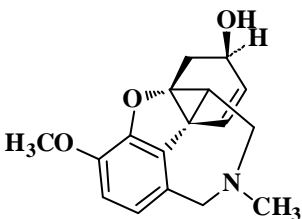
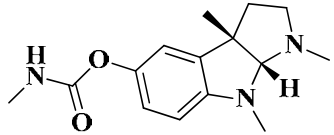


Figure 3.17 Structure of stilbene-oligomer, (+)- $\alpha$ -viniferin (a), neohopeaphenol (b)

**Table 3.17** The IC<sub>50</sub> values of cholinesterase inhibitory activity of isolated stilbenes.

Compound	Structure	IC <sub>50</sub> (μM)	
		AChE	BChE
resveratrol (1)		> 400	15.89 ± 3.3
isorhaponigetin (2)		> 400	96.13 ± 6.6
pinosylvin (3)		> 400	45.78 ± 5.5
gnetol (4)		> 400	1.27 ± 0.6
galantamine		5.60 ± 0.7	26.30 ± 3.9
eserine		3.33 ± 0.02	10.21 ± 0.06

### 3.3.2 The Results of $\alpha$ -Glucosidase Inhibitory Activity Test

The  $\alpha$ -glucosidase inhibitory activity of compounds isolated from the vine of *F. foveolata* was evaluated by colorimetric method (Pullela *et al.*, 2006) with slight modification. Acarbose, an antidiabetes drug, was used as standard compound. The results are shown in Table 3.18.

**Table 3.18** The  $IC_{50}$  values of  $\alpha$ -glucosidase inhibitory effect of the isolated compounds

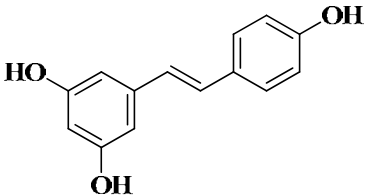
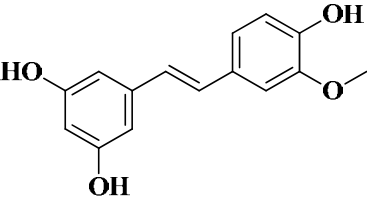
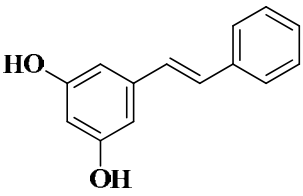
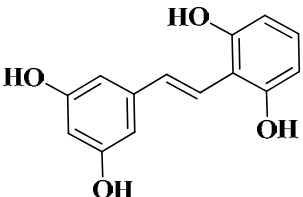
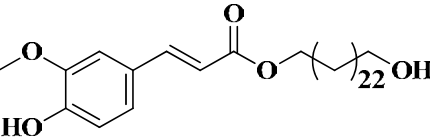
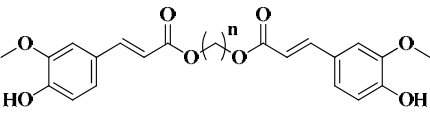
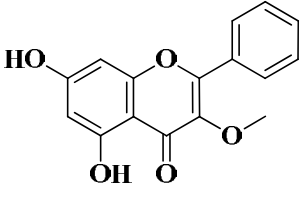
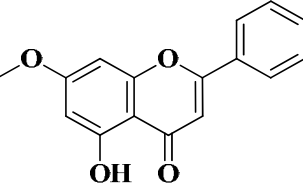
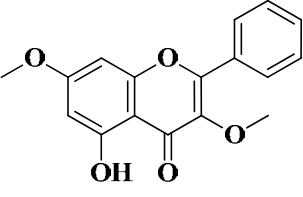
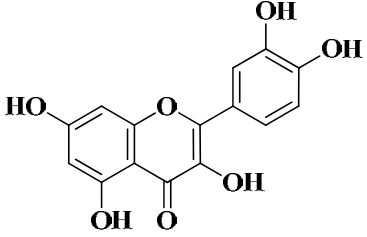
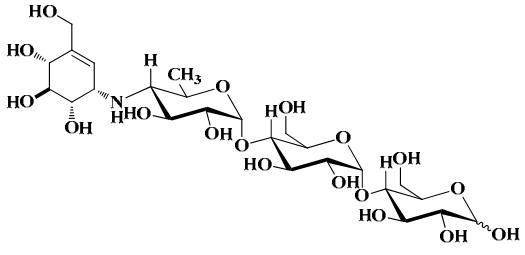
Compound	Structure	$IC_{50}$ ( $\mu$ M)
resveratrol (1)		$41.66 \pm 0.20$
isorhaponigetin (2)		$93.79 \pm 2.20$
pinosylvin (3)		$249.05 \pm 0.73$
gnetol (4)		$17.21 \pm 0.38$
24'-hydroxy-tetracosyl ferulate (5)		$>700$
mixture (6)	 n=22 ( <b>6a</b> ), 24 ( <b>6b</b> ) 1,22-docosanediol diferulate ( <b>6a</b> ) 1,24-tetracosanediol diferulate ( <b>6b</b> )	$>700$

Table 3.18 continued

Compound	Structure	IC <sub>50</sub> (μM)
galangin 3-methyl ether (7)		>700
tectochrysin (8)		126.80 ± 0.53
5-hydroxy-3,7-dimethoxyflavon (9)		>700
quercetin (10)		5.62 ± 0.14
acarbose		0.7 mM

According to the result in Table 3.18, compound **10** showed the highest inhibitory effect with the IC<sub>50</sub> value of 5.62 μM, followed by compound **4** with the IC<sub>50</sub> value 17.21 μM. The activities of both compounds were higher than that of the standard control acarbose (IC<sub>50</sub> 0.7 mM).

Among of the isolated stilbenes, the structure-activity trends of compounds **1-4** upon on α-glucosidase inhibition could be summarized. The appearance and the number of the hydroxy groups in a benzene ring played a key role in the inhibitory activity as seen in the low activity of compound **3** comparing to those of compounds **1**, **2** and **4**. Furthermore, compounds **1** and **2** showed the different inhibitory effect. It

could be indicated that the presence of a methoxy group significantly reduced the activity. For stilbene compounds, the monomeric stilbene, resveratrol, was reported recently to possess similar *in vitro* activity, similar to that found in this work (Kageura *et al.*, 2001; Lam *et al.*, 2008).

From the literature review, the  $\alpha$ -glucosidase inhibitory activity of flavones was affected by the number of hydroxyl groups on either A or B-rings. The absence of a hydroxyl group at position 5, 6 or 7 of the A-ring decreased the activity (Borges de Melo *et al.*, 2006). Another study reported that a methoxy group at position 5 had increase the activity comparing with a hydroxyl group at this position (Azuma *et al.*, 2011). However, the results of this study could not confirm this assumption.

However, the activity results of compounds **7-9** showed some crucial information. The substituents as a methoxy groups at position 3 seem to decrease the activity. Nevertheless, compound **10** exhibited higher inhibition than compounds **7-9**. This might be implied that the hydroxyl groups on the B-ring affected the activity which consistent with the results in the literature (Azuma *et al.*, 2011).

### 3.3.3 The Results of Nitric Oxide Inhibitory Activity Test

Seven isolated compounds, compounds **1-4**, **8-10** were evaluated their anti-inflammatory activity by the *in vitro* assay based on the inhibition of LPS-induced NO production from macrophages.

Results of activity test from isolated stilbenes, compounds **1-4** were shown in Figure 3.18. The effect on cell viability was determined with MTT assay test. The compounds were tested for their acute toxicity on cell lines. At different concentrations, compounds **1** and **2** showed more than 80% cell survival (non-toxic concentrations), while compounds **3** and **4** exhibited high cytotoxic effects on the macrophage with the IC<sub>50</sub> of 64.70 and 94.77  $\mu$ M, respectively.

For compounds **3** and **4**, it showed the potent inhibition activity in a dose-dependent, while compounds **1** and **2** showed low activity. Although compounds **3** and **4** had the high inhibition effect, it was also higher toxicity toward macrophages.



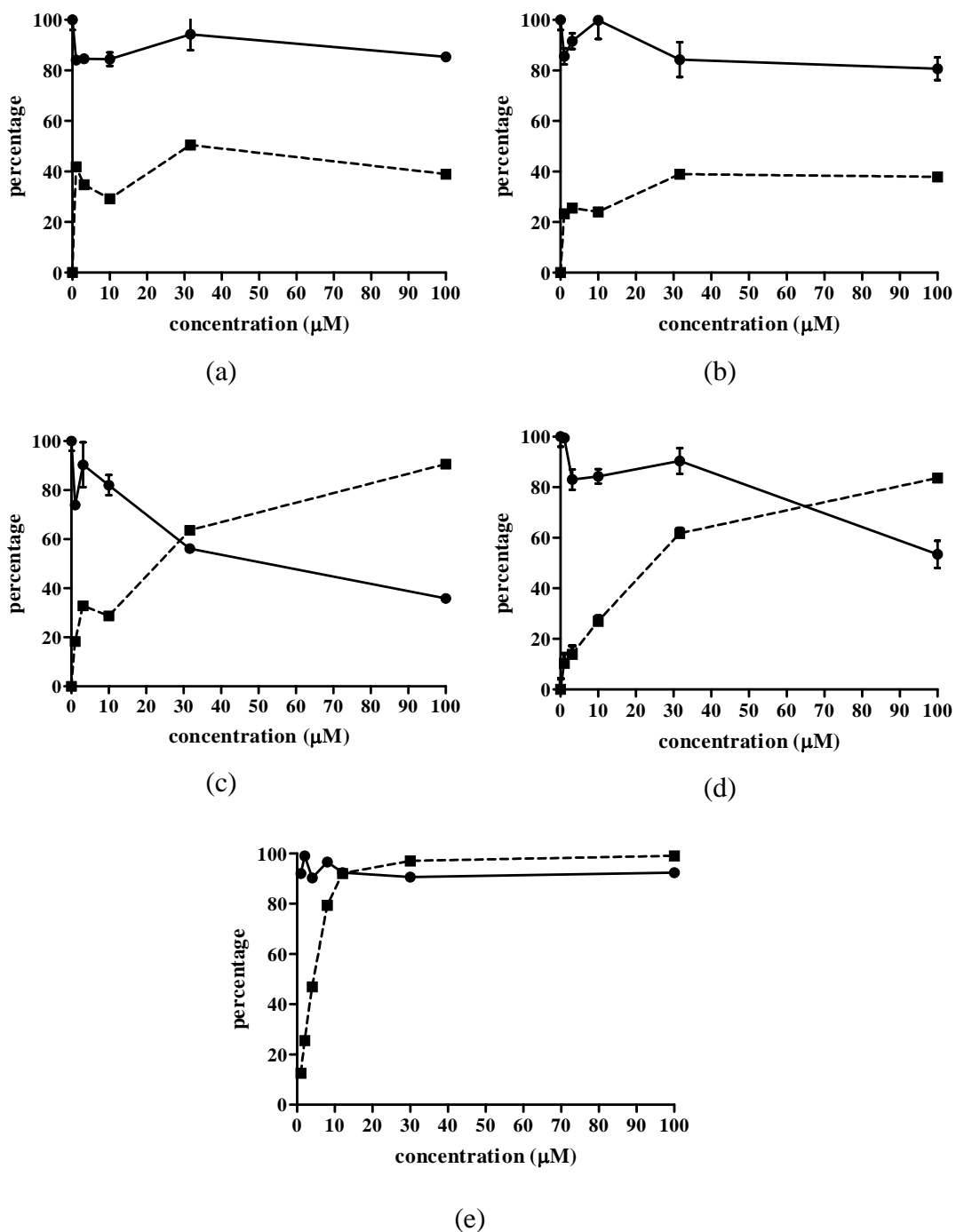
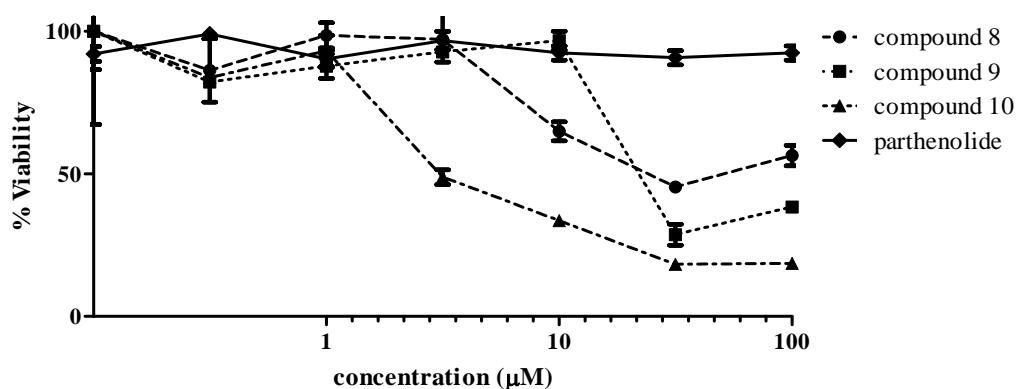


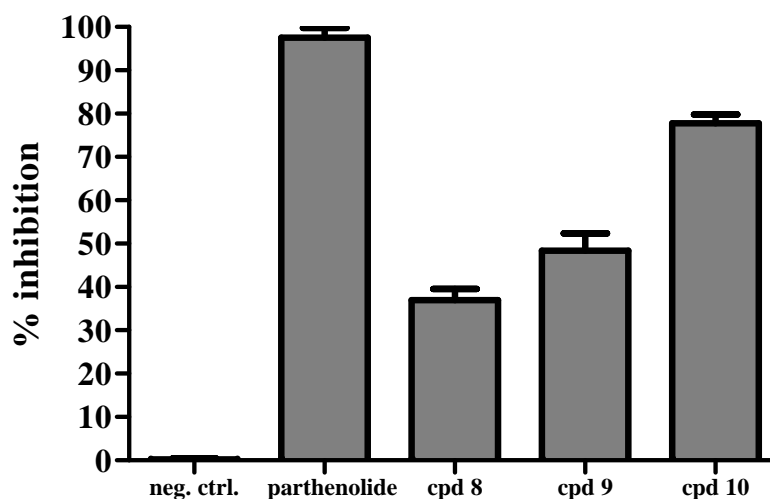
**Figure 3.18** Anti-inflammatory activity and cytotoxicity of compounds **1** (a), **2** (b), **3** (c), **4** (d) and parthenolide standard (e). Data are shown as the mean ( $\pm 1$  S.E.M.) percentage of anti-inflammatory activity, derived from three replications.

----- % inhibition      ————— % viability

Compounds **8-10** were subsequently tested for their acute toxicities and NO inhibitory activities on cell lines. As a result in Figure 3.19, compounds **8-10** showed cytotoxic effect on the cell lines with  $IC_{50}$  of 26.88, 57.19 and 12.86  $\mu\text{M}$ , respectively. NO inhibitory effects of compounds **8-10** were evaluated at concentration of 5.0  $\mu\text{g/mL}$  which was a less toxicity concentration. Among these compounds, compound **10** exhibited the highest anti-inflammatory activity followed by compounds **9** and **8**, respectively.



(a)



(b)

**Figure 3.19** Cytotoxicity (a) and anti-inflammatory activity (b) of compounds **8-10** and parthenolide standard. Data are shown as the mean ( $\pm 1$  S.E.M.) percentage of anti-inflammatory activity, derived from three replications.

## CHAPTER IV

### CONCLUSION

During the course of this research, chemical constituents and biological activities of the vine of *F. foveolata* were thoroughly investigated. Ten compounds were obtained and their structures were elucidated by means of physical properties and spectroscopic evidences.

Isolated substances were then evaluated for their bioactivities: cholinesterase inhibitory activity against AChE and BChE,  $\alpha$ -glucosidase inhibitory and anti-inflammatory activities. The chemical structures of the isolated substances and their bioactivities were accumulated in Table 4.1.

This study is the first report of *F. foveolata* constituents including their bioactivities. According to the results of this study, compound **4** or gnetol exhibited higher inhibitory activity than standard compounds towards BChE and  $\alpha$ -glucosidase. However, only few publications have limited in the literature of the activities of gnetol. Ohguchi *et al.* (2003) have shown that gnetol possesses strong inhibitory action on tyrosinase, the rate limiting enzyme in melanin synthesis. Moreover, gnetol (**4**) significantly suppressed melanin biosynthesis in murine B16 melanoma cells. In addition, gnetol also showed significant antioxidant activity (Sri-in, 2007). Based on these results, this compound has potential for use as a bioactive agent and also appears to be a great candidate for clinical trials treatment including AD and diabetes patients.

As for compound **10** or quercetin, it showed stronger activity than standard compounds in  $\alpha$ -glucosidase inhibitory activity. It would be a lead compound suitable for designing new potent  $\alpha$ -glucosidase inhibitors. In addition, *F. foveolata* may be useful as a medicinal food or as a source of natural  $\alpha$ -glucosidase inhibitors for use in suppressing postprandial hyperglycemia in the management of diabetes.

**Table 4.1** Isolated compounds from *F. foveolata* and their bioactivities

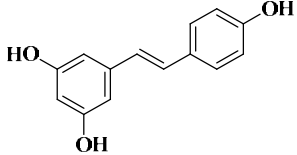
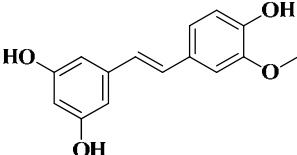
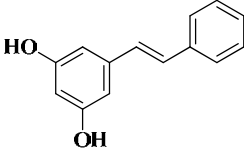
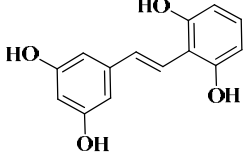
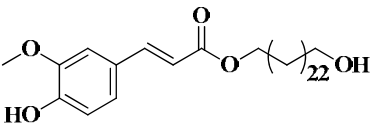
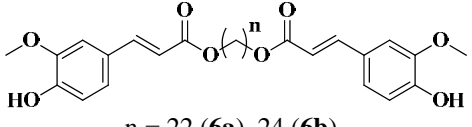
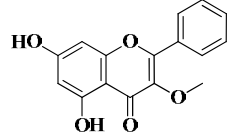
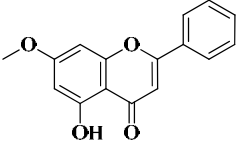
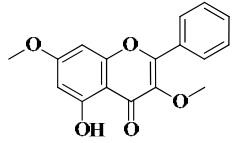
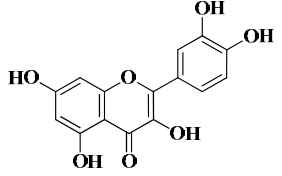
Substance	Remark	Weight (mg), % Yield*	Melting point (°C)	Anticholinesterase inhibition**		$\alpha$ -Glucosidase inhibition (IC <sub>50</sub> , $\mu$ M)	NO inhibition***
				AChE	BChE		
 resveratrol (1)	pale yellow crystals	100.7, 2.32 x 10 <sup>-2</sup>	258.7-260.5	17.69 $\pm$ 0.20	90.10 $\pm$ 1.16 (IC <sub>50</sub> = 15.9 $\mu$ M)	41.66 $\pm$ 0.20	39.84 $\pm$ 5.09
 isorhaponigetin (2)	yellow amorphous powder	50.9, 1.17 x 10 <sup>-2</sup>	179.0-180.0	20.90 $\pm$ 1.40	88.30 $\pm$ 0.79 (IC <sub>50</sub> = 96.1 $\mu$ M)	93.79 $\pm$ 2.20	30.39 $\pm$ 2.86
 pinosylvin (3)	pale brown needle crystals	55.1, 1.27. x 10 <sup>-2</sup>	150.7	22.11 $\pm$ 0.73	94.71 $\pm$ 0.48 (IC <sub>50</sub> = 48.8 $\mu$ M)	249.05 $\pm$ 0.73	46.69 $\pm$ 4.28
 gnetol (4)	white crystals	14.7, 3.39 x 10 <sup>-3</sup>	87.0-90.5	19.02 $\pm$ 0.38	89.2 $\pm$ 0.98 (IC <sub>50</sub> = 1.3 $\mu$ M)	17.21 $\pm$ 0.38	45.66 $\pm$ 0.76

Table 4.1 continued

Substance	Remark	Weight (mg), % Yield*	Melting point (°C)	Anticholinesterase inhibition**		$\alpha$ -Glucosidase inhibition (IC <sub>50</sub> , $\mu$ M)	NO inhibition***
				AChE	BChE		
 24'-hydroxy-tetracosyl ferulate ( <b>5</b> )	white amorphous powder	27.0, 6.43 x 10 <sup>-2</sup>	85.0-87.5	N.I.	N.I.	>700	N/T
 n = 22 ( <b>6a</b> ), 24 ( <b>6b</b> ) 1,22-docosanediol diferulate ( <b>6a</b> ) 1,24-tetracosanediol diferulate ( <b>6b</b> )	greenish white amorphous powder	24.5, 5.83 x 10 <sup>-2</sup>	115.0-116.5	N.I.	N.I.	>700	N/T
 galangin 3-methyl ether ( <b>7</b> )	yellow amorphous powder	6.5, 1.54 x 10 <sup>-2</sup>	297.8	16.64 ± 0.14	25.98 ± 0.91	>700	N/T

**Table 4.1** continued

Substance	Remark	Weight (mg), % Yield*	Melting point (°C)	Anticholinesterase inhibition**		$\alpha$ -Glucosidase inhibition (IC <sub>50</sub> , $\mu$ M)	NO inhibition***
				AChE	BChE		
 tectochrysin (8)	yellow crystals	6.1, 1.45 x 10 <sup>-2</sup>	160.0-161.0	1.48 ± 0.53	6.25 ± 0.66	126.80 ± 0.53	36.95 ± 2.56
 5-hydroxy-3,7-dimethoxyflavone (9)	yellow crystals	6.6, 1.57 x 10 <sup>-2</sup>	129.0	4.46 ± 1.98	6.25 ± 2.66	>700	48.34 ± 4.04
 quercetin (10)	yellow amorphous powder	5.2, 1.23 x 10 <sup>-2</sup>	313.5-313.7	18.81 ± 0.23	30.96 ± 0.08	5.62 ± 0.14	77.80 ± 2.03

Note:

N.I. = no inhibition

N/T = not test

\* The percentage of yield substances was calculated based on the crude extract.

\*\* At concentration of 0.1 mg/mL

\*\*\* At concentration of 5.0  $\mu$ g/mL

## REFERENCES

- Adisakwattana, S., Sookkongwaree, K., Roengsumran, S., Petsom, A., Ngamrojnavanich, N., Chavasiri, W., Deesamer, S. and Yibchok-anun, S. Structure-activity relationships of *trans*-cinnamic acid derivatives on  $\alpha$ -glucosidase inhibition. *Bioorg. Med. Chem. Lett.* 14 (2004): 2893-2896.
- Azuma, T., Kayano, S., Matsumura, Y., Konishi, Y., Tanaka, Y. and Kikuzaki, H. Antimutagenic and  $\alpha$ -glucosidase inhibitory effects of constituents from *Kaempferia parviflora*. *Food Chem.* 125 (2011): 471-475.
- Bachelor, F.W., Loman, A.A. and Snowdon, L.R. Synthesis of pinosylvin and related heartwood stilbenes. *Can. J. Chem.* 48 (1970): 1554.
- Bischoff, H. Pharmacology of alpha-glucosidase inhibition. *Eur. J. Clin. Invest.* 24 (1994): 3-10.
- Borges de Melo, E., Da Silveira Gomes, A. and Carvalho, I.  $\alpha$ - and  $\beta$ -Glucosidase inhibitors: Chemical structure and biological activity. *Tetrahedron* 62 (2006): 10277-10302.
- Bryan, N.S., Rassaf, T., Maloney, R.E., Rodriguez, C.M., Saijo, F., Rodriguez, J.R. and Feelisch, M. Cellular targets and mechanisms of nitros(yl)ation: An insight into their nature and kinetics in vivo. *Proc. Natl. Acad. Sci. USA.* 101 (2004): 4308-4313.
- Chen, X., Zheng, Y. and Shen, Y. A new method for production of valienamine with microbial degradation of acarbose. *Biotechnol. Prog.* 21 (2005): 1002-1003.
- Ellman, G., Courtney, K.D., Andres, V. and Featherstone, R.M. A new and rapid colorimetric determination of acetylcholinesterase activity. *Biochem. Pharmacol.* 7 (1961): 88-95.
- Ferrero-Miliani, L., Nielsen, O.H., Andersen, P.S. and Girardin, S.E. Chronic inflammation: Importance of NOD2 and NALP3 in interleukin-1beta generation. *Clin. Exp. Immunol.* 147 (2007): 227-235.
- Gemma, S., Gabellieri, E., Huleatt, P., Fattorusso, C., Borriello, M., Catalanotti, B., Butini, S., De Angelis, M., Novellino, E., Nacci, V., Belinskaya, T., Saxena, A. and Campiani, G. Discovery of huperzine a-tacrine hybrids as potent inhibitors of human cholinesterases targeting their midgorge recognition sites. *J. Med. Chem.* 49 (2006): 3421-3425.

- Gravier-Pelletier, C., Maton, W., Dintinger, T., Tellier, C. and Le Merrer, Y. Synthesis and glycosidase inhibitory activity of aminocyclitols with a C6- or a C7-ring. *Tetrahedron* 59 (2003): 8705-8720.
- Goodwin, D.C., Landino, L.M. and Marnett, L.J. Effects of nitric oxide and nitric oxide-derived species on prostaglandin endoperoxide synthase and prostaglandin biosynthesis. *FASEB J.* 13 (1999): 1121–1136.
- Hermel, A.P. and Mathur, R. *Davidson's Diabetes Mellitus: Diagnosis and treatment*. 5<sup>th</sup> ed. Philadelphia: Saunders, 2004.
- Holden, M. and Kelly, C. Use of cholinesterase inhibitors in dementia. *Adv. Psychiatr. Tr.* 8 (2002): 89-96.
- Ingkaninan, K., Temkitthawon, P., Chuenchom, K., Yuyaem, T. and Thongnoi, W. Screening for acetylcholinesterase inhibitory activity in plants used in Thai traditional rejuvenating and neurotonic remedies. *J. Ethnopharmacol.* 89 (2003): 261-264.
- Kageura, T., Matsuda, H., Morikawa, T., Toguchida, I., Harima, S., Oda, M. and Yoshikawa, M. Inhibitors from rhubarb on lipopolysaccharide-induced nitric oxide production in macrophages: Structural requirements of stilbenes for the activity. *Bioorg. Med. Chem.* 9 (2001): 1887-1893.
- Krentz, A.J. and Bailey, C.J. Oral antidiabetic agents: Current role in type 2 diabetes mellitus. In Leroith, D., Taylor, S.I. and Olefsky, J.M. (eds.), *Diabetes mellitus: A fundamental and clinical text*. 3<sup>rd</sup> ed. Philadelphia: Lippincott Williams & Wilkins, 2004.
- Lam, S.H., Chen, J.M., Kang, C.J., Chen, C.H. and Lee S.S.  $\alpha$ -Glucosidase inhibitors from the seeds of *Syagrus romanzoffiana*. *Phytochemistry* 69 (2008): 1173-1178.
- Liu, R., Chu, X. and Sun, A. Preparative isolation and purification of five compounds from the Chinese medicinal herb *Polygonum cuspidatum* Sieb. et Zucc by high-speed counter-current chromatography. *J. Chromatogr. A* 1097 (2005): 33–39.
- López-Franco, O., Hernández-Vargas, P., Ortiz-Muñoz, G., Sanjuán, G., Suzuki, Y., Ortega, L., Blanco, J. and Egido, J. Parthenolide modulates the NF-kappa B-mediated inflammatory responses in experimental atherosclerosis. *Arterioscler. Thromb. Vasc. Biol.* 26(8) (2006): 1864–1870.
- Ma, C.Y., Williams, I.D. and Che, C.T. Withanolides from *Hyoscyamus niger* seeds. *J. Nat. Prod.* 62(10) (1999): 1445-1447.



- Mac Micking, J., Xie, Q.W. and Nathan, C. Nitric oxide and macrophage function. *Annu. Rev. Immunol.* 15 (1997): 323–350.
- Madidol University, Department of Pharmaceutical Botany. *Siam medicinal plants: National wisdom*. 2<sup>nd</sup> ed. Bangkok: Amarin Printing & Publishing Public, 1995.
- Meek, P.D., McKeithan, K. and Schumock, G.T. Economic considerations in Alzheimer's disease. *Pharmacotherapy* 2 (1998): 68-73, 79-82.
- Menichini, F., Tendis, R., Bonesi, M., Loizzo, M.R., Conforti, F., Statti, G., Cindio, B.D., Houghton, P.J. and Menichini, F. The influence of fruit ripening on the phytochemical content and biological activity of *Capsicum chinense* Jacq, cv *Habanero*. *Food Chem.* 114 (2009): 553–560.
- Minghetti, L., Polazzi, E., Nicolini, A., Creminon, C. and Levi, G. Interferon- $\gamma$  and nitric oxide down-regulate lipopolysaccharide-induced prostanoid production in cultured rat microglial cells by inhibiting cyclooxygenase-2 expression. *J. Neurochem.* 66 (1996): 1963–1970.
- Mosmann, T. Rapid colorimetric for cellular growth and survival: Application to proliferation and cytotoxicity assays. *J. Immunol. Meth.* 65 (1983): 55–63.
- Mukherjee, P.K., Kumar, V., Mal, M. and Houghton, P.J. In vitro acetylcholinesterase inhibitory activity of the essential oil from *Acorus calamus* and its main constituents. *Planta Med.* 73 (2007): 283-285.
- Nolan, J.J. Insulin sensitizers: A new era in the management of type 2 diabetes. In Betteridge, D.J. (eds.) *Diabetes: Current perspectives*. London: Martin Dunitz, 2000.
- Ogawa, S., Asada, M., Ooki, Y., Mori, M., Itoh, M. and Korenaga, T. Design and synthesis of glycosidase inhibitor 5-amino-1,2,3,4-cyclohexanetetrol derivatives from (-)-vibo-quercitol. *Bioorg. Med. Chem.* 13 (2005): 4306-4314.
- Ohguchi, K., Tanaka, T., Iliya, I., Ito, T., Iinuma, M., Matsumoto, K., Akao, Y. and Nozawa, Y. Gnetol as a potent tyrosinase inhibitor from genus *Gnetum*. *Biosci. Biotechnol. Biochem.* 67(3) (2003): 663-665.
- Pacheco-Sanchez, M., Boutin, Y., Angers, P., Gosselin, A. and Tweddell, R.J. Inhibitory effect of CDP, a polysaccharide extracted from the mushroom *Collybia dryophila*, on nitric oxide synthase expression and nitric oxide production in macrophages. *Eu. J. Pharmacol.* 555 (2007): 61–66.

- Palasuwan, A., Soogarun, S., Lertlum, T., Pradniwat, P. and Wiwanitkit, V. Inhibition of Heinz body induction in an *in vitro* model and total antioxidant activity of medicinal Thai plants. *Asian Pac. J. Cancer Prevent.* 6 (2005): 458-463.
- Pullela, S.V., Tiwari, A.K., Vanka, U.S., Vummenthula, A., Tatipaka, H.B., Dasari, K.R., Khan, I.A. and Janaswamy, M.R. HPLC assisted chemobiological standardization of  $\alpha$ -glucosidase-I enzyme inhibitory constituents from *Piper longum* Linn-an Indian medicinal plant. *J. Ethnopharmacol.* 108 (2006): 445–449.
- Rhabasa-Lhoret, R. and Chiasson, J. Alpha-glucosidase inhibitors. In Defronzo, R.A., Ferrannini, E., Keen, H. and Zimmet, P. (eds.), *International textbook of diabetes mellitus*. London: John Wiley, 2004.
- Silayo, A., Ngadjui, B.T. and Abegaz, B.M. Homoisoflavonoids and stilbenes from the bulbs of *Scilla nervosa subsp. rigidifolia*. *Phytochemistry* 52(5) (1999): 947-955.
- Singab, A.N.B., El-Beshbishy, H.A., Yonekawa, M., Nomura, T. and Fukai, T. Hypoglycemic effect of Egyptian *Morus alba* root bark extract: Effect on Diabetes and lipid peroxidation of streptozotocin-induced diabetic rats. *J. Ethnopharmacol.* 100 (2005): 333-338.
- Song, Y.S., Park, E.H., Hur, G.M., Ryu, Y.S., Kim, Y.M. and Jin, C. Ethanol extract of propolis inhibits nitric oxide synthase gene expression and enzyme activity. *J. Ethnopharmacol.* 80 (2002): 155–161.
- Sri-in, P. *Bioactive compounds from the roots of Gnetum macrostachyum*. Master's Thesis, Department of Chemistry, Faculty of Science, Chulalongkorn University, 2007.
- Sung, S.H., Kang, S.Y., Lee, K.Y., Park, M.J., Kim, J.H., Park, J.H., Kim, Y.C., Kim, J. and Kim, Y.C. (+)- $\alpha$ -Viniferin, a stilbene trimer from *Caragana chamlaque*, inhibits acetylcholinesterase. *Biol. Pharm. Bull.* 25 (2002): 125-127.
- Sutthanut, K., Sripanidkulchai, B., Yenjai, C. and Jay, M. Simultaneous identification and quantitation of 11 flavonoid constituents in *Kaempferia parviflora* by gas chromatography. *J. Chromatogr. A* 1143 (2007): 227–233.
- Temkitthawon, P., Viyoch, J. and Ingkaninan, K. Screening for PDE inhibitory activity from Thai traditional plant used as rejuvenation and aphrosiac agents. *Planta Med.* 72 (2006): 47.

- Tringali, C. *Bioactive compounds from natural sources*. 1<sup>st</sup> ed. London: Taylor & Francis, 2001.
- Urbatsch, L.E., Mabry, T.J., Miyakado, M., Ohno, N. and Yoshioka, H. Flavonol methyl ethers from *Ericameria diffusa*. *Phytochemistry* 15 (1976): 440-441.
- Viegas, C. Jr., Bolzani, V.S., Pimentel, L.S.B., Castro, N.G., Cabral, R.F., Costa, R. S., Floyd, C., Rocha, M.S., Young, M.C.M., Barreiro, E.J. and Fraga, C.A.M. New selective acetylcholinesterase inhibitors designed from natural piperidine alkaloids. *Bioorg. Med. Chem.* 13 (2005): 4184-4190.
- Wawer, I. and Zielinska, A. <sup>13</sup>C-CP-MAS-NMR studies of flavonoids. I. Solid-state conformation of quercetin, quercetin 5'-sulphonic acid and some simple polyphenols. *Solid State Nucl. Magn. Reson.* 10 (1997): 33-38.
- Weinberger, B., Heck, B.E., Laskin, D.L. and Laskin J.D. Nitric oxide in the lung: Therapeutic and cellular mechanisms of action. *Pharmacol. Therapeut.* 84 (1999): 401-411.
- Wutthamawech, W. *Medicinal plants Encyclopedia*. 1<sup>st</sup> ed. Bangkok: Odeon Store, 1997.
- Xiang, W.S., Wang, J.D., Wang, X.J. and Zhang, J. Two new components from *Gnetum pendulum*. *J. Asian Nat. Prod. Res.* 10 (2008): 1081-1085.
- Xiao, K., Zhang, H.J., Xuan, L.J., Zhang, J., Xu, Y.M. and Bai, D.L. Stilbenoids: Chemistry and bioactivities. *Stud. Nat. Prod. Chem.* 34 (2008): 453-646.
- Xiao, Z.P., Wu, H.K., Wu, T., Shi, H., Hang, B. and Aisa, H.A. Kaempferol and quercetin flavonoids from *Rosa rugosa*. *Chem. Nat. Compd.* 42 (2006): 736-737.
- Yun, J.M., Kwon, H. and Hwang, J.K. 2003. In vitro anti-inflammatory activity of panduratin A isolated from *Kaempferia pandurata* in RAW 264.7 cells. *Planta Med.* 69 (2003): 1102-1108.
- Zaman, A., Prakash, S., Wizarat, K., Joshi, B.S., Gawad, D.H and Likhate, K. Isolation and structure of gnetol, a novel stilbene from *Gnetum ula*. *Indian J. Chem., Sect B* 22(2) (1983): 101-104.
- Zechel, D.L. and Withers, S.G. Glycosidase mechanisms: Anatomy of a finely tuned catalyst. *Acc. Chem. Res.* 33 (2000): 11-18.

## **APPENDIX**

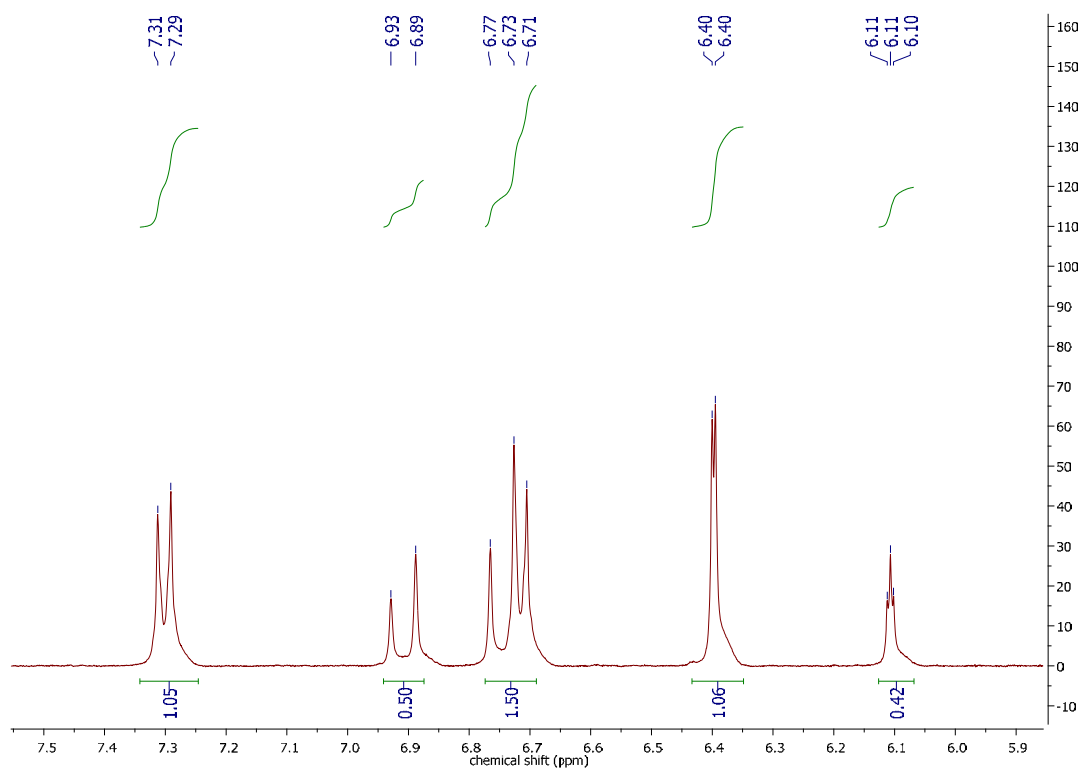


**Figure A-1** The  $^1\text{H-NMR}$  spectrum of compound 1

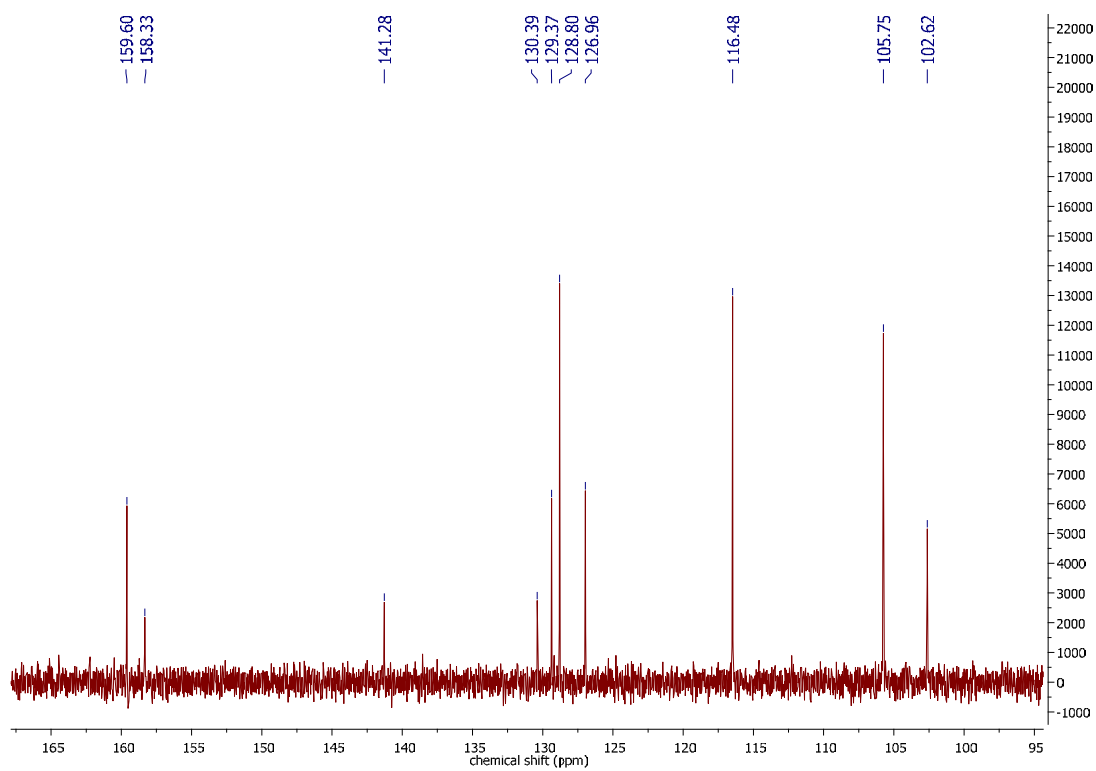


**Figure A-2** The  $^{13}\text{C-NMR}$  spectrum of compound 1

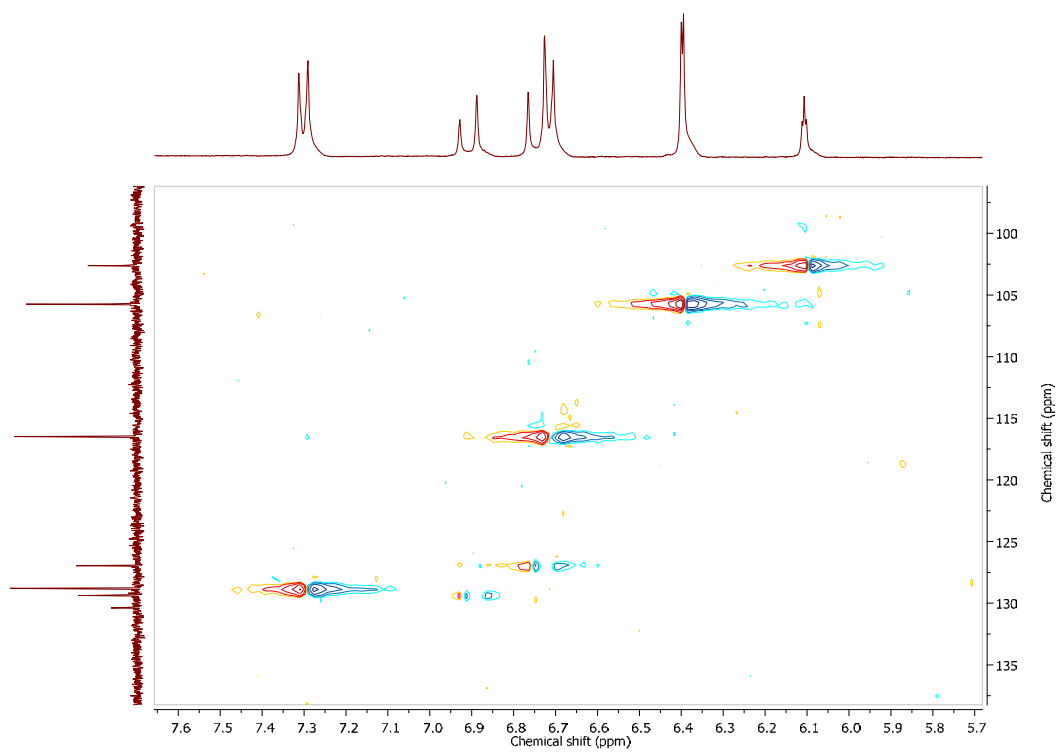


**Figure A-3** The HSQC spectrum of compound **1**

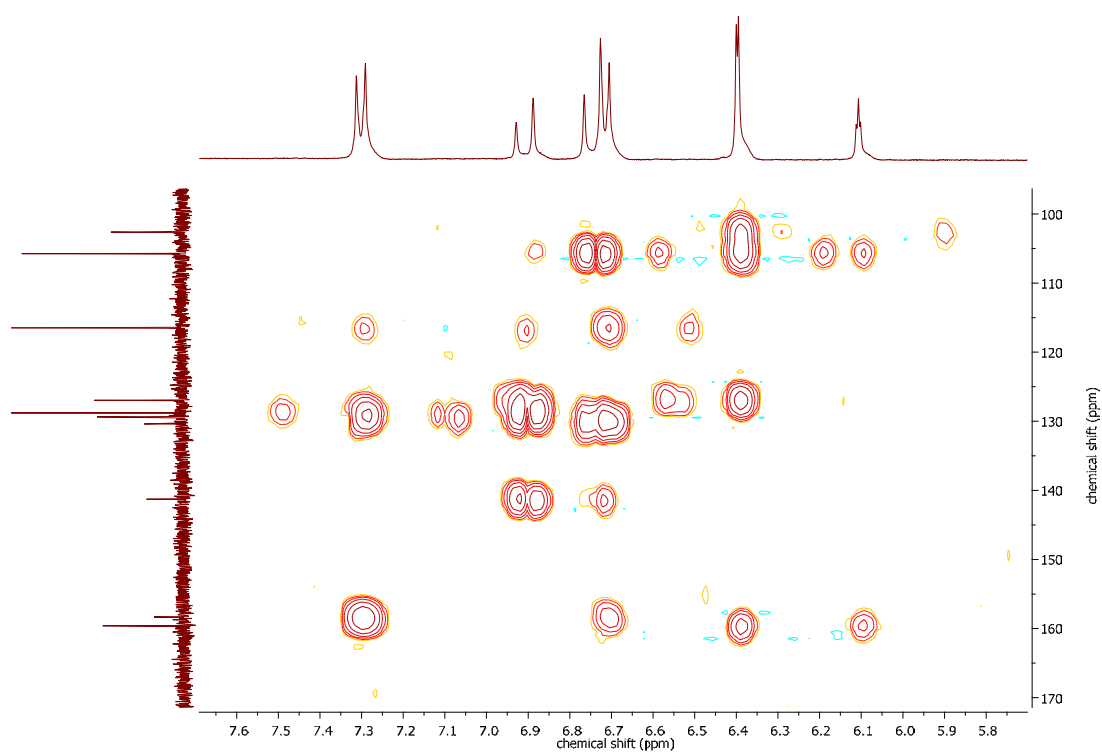


**Figure A-4** The HMBC spectrum of compound **1**

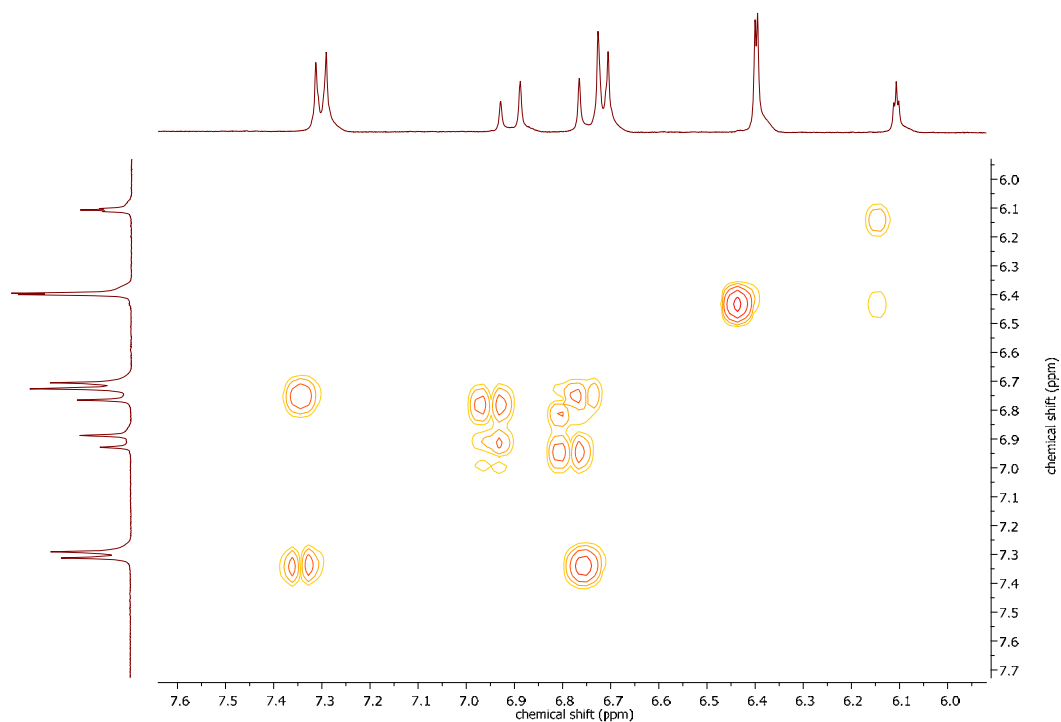


**Figure A-5** The COSY spectrum of compound **1**

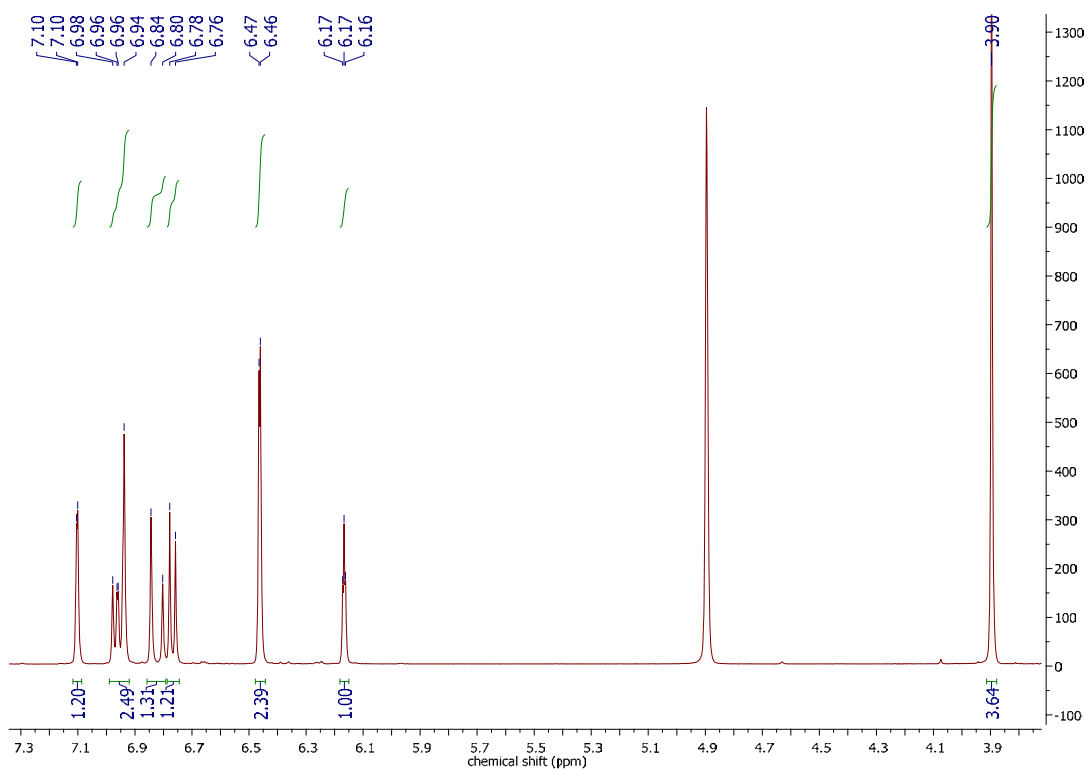


**Figure A-6** The <sup>1</sup>H-NMR spectrum of compound **2**

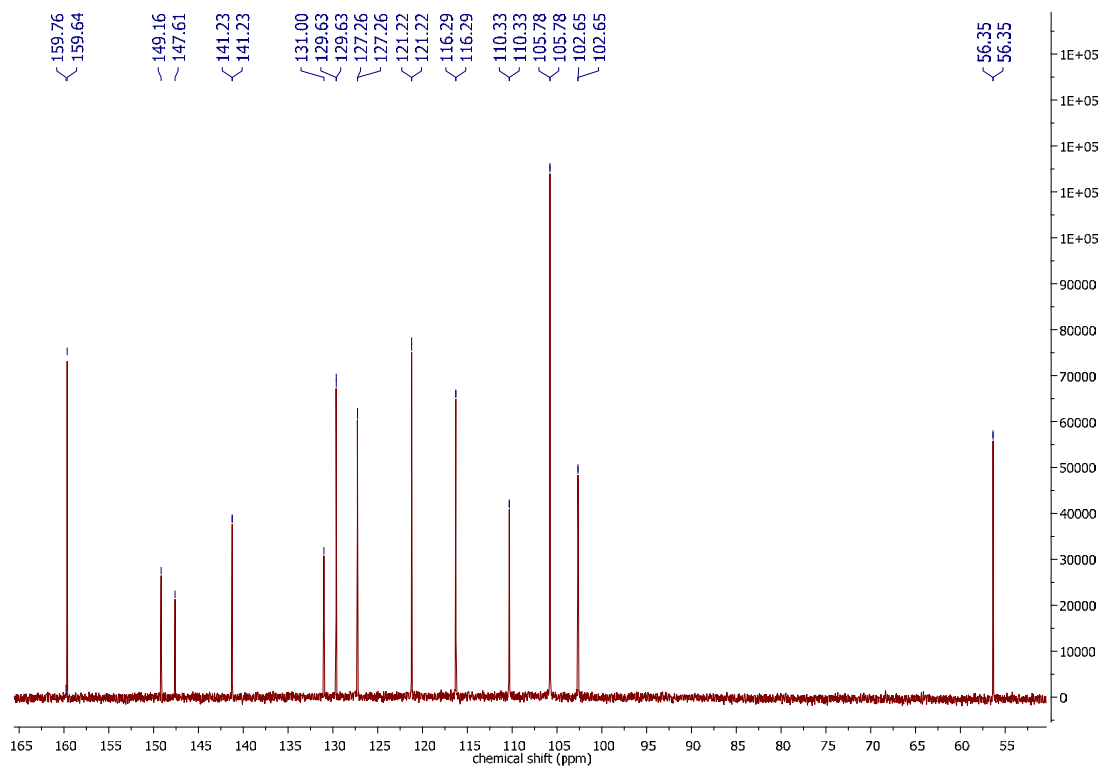


Figure A-7 The  $^{13}\text{C}$ -NMR spectrum of compound 2

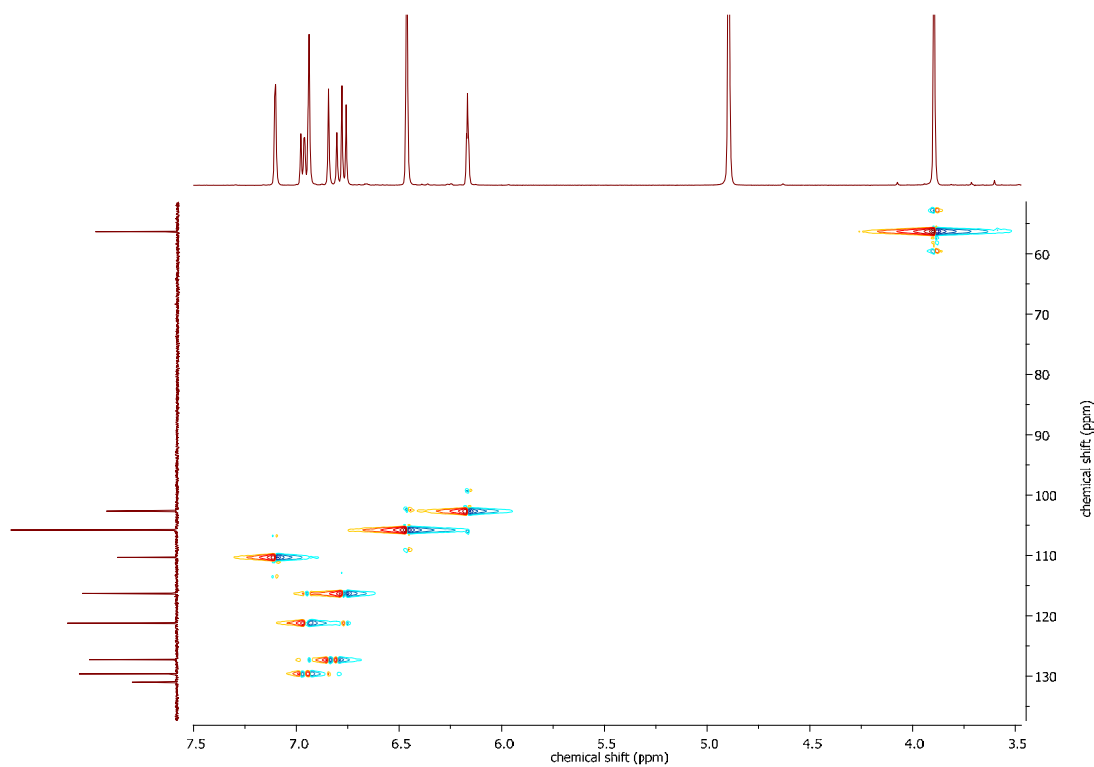
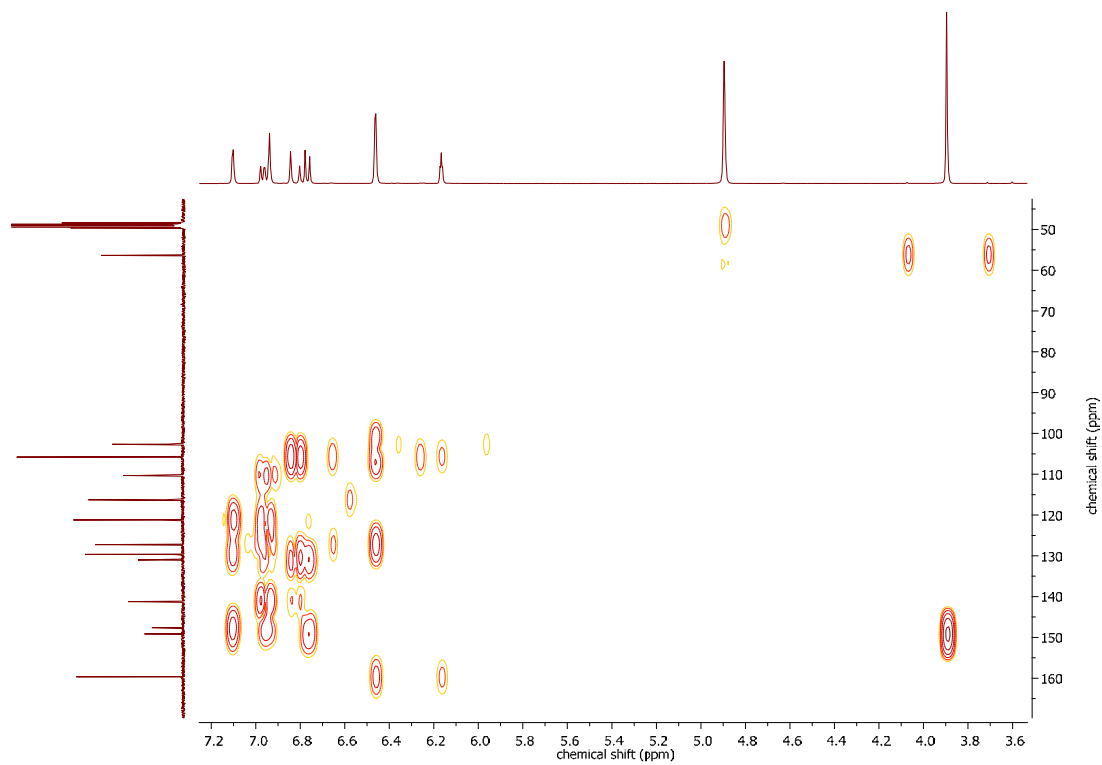
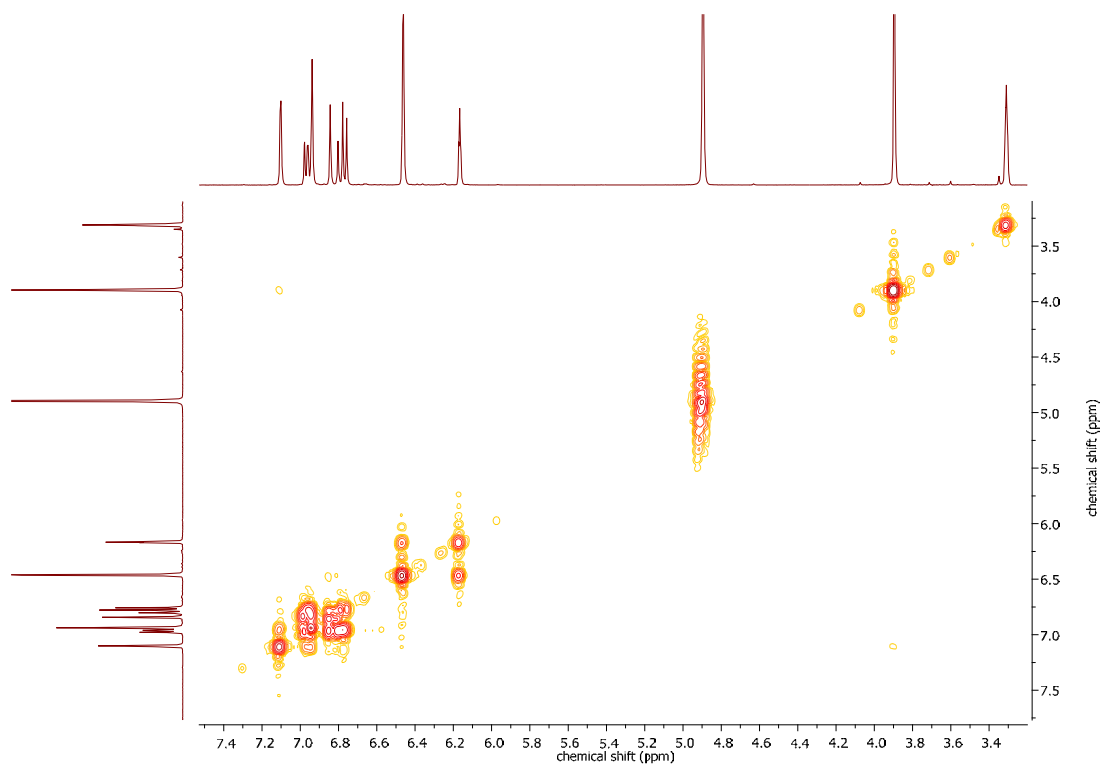


Figure A-8 The HSQC spectrum of compound 2





**Figure A-9** The HMBC spectrum of compound **2**



**Figure A-10** The COSY spectrum of compound **2**

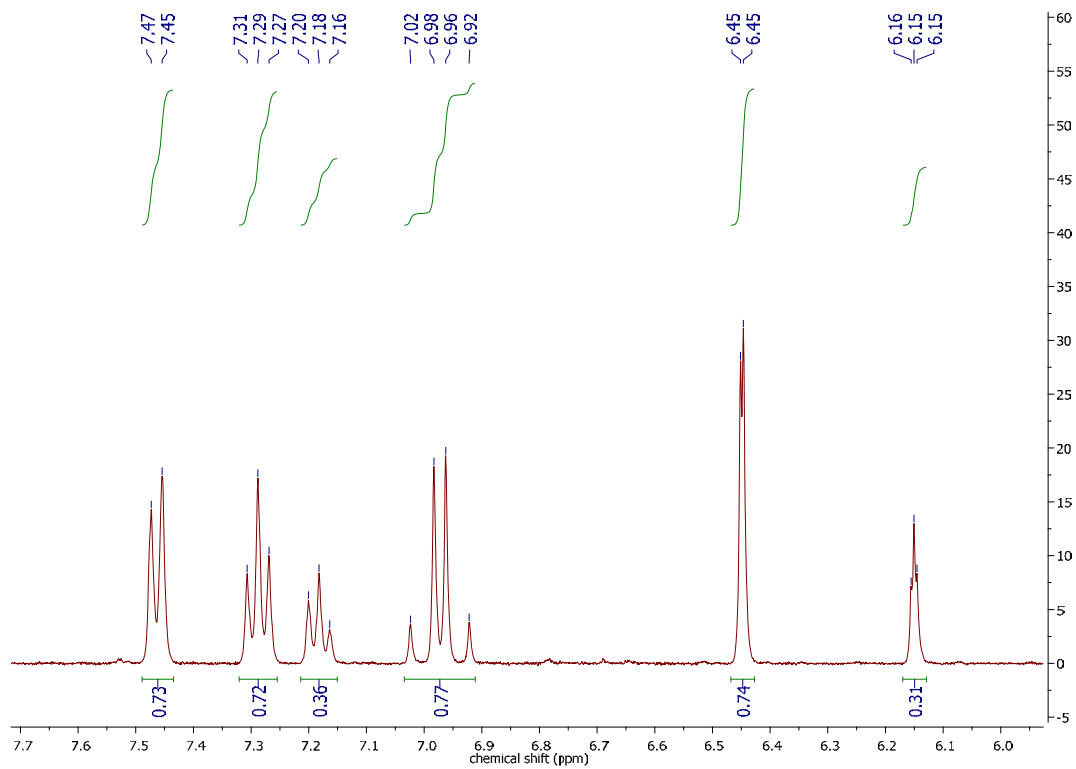


Figure A-11 The  $^1\text{H-NMR}$  spectrum of compound **3**

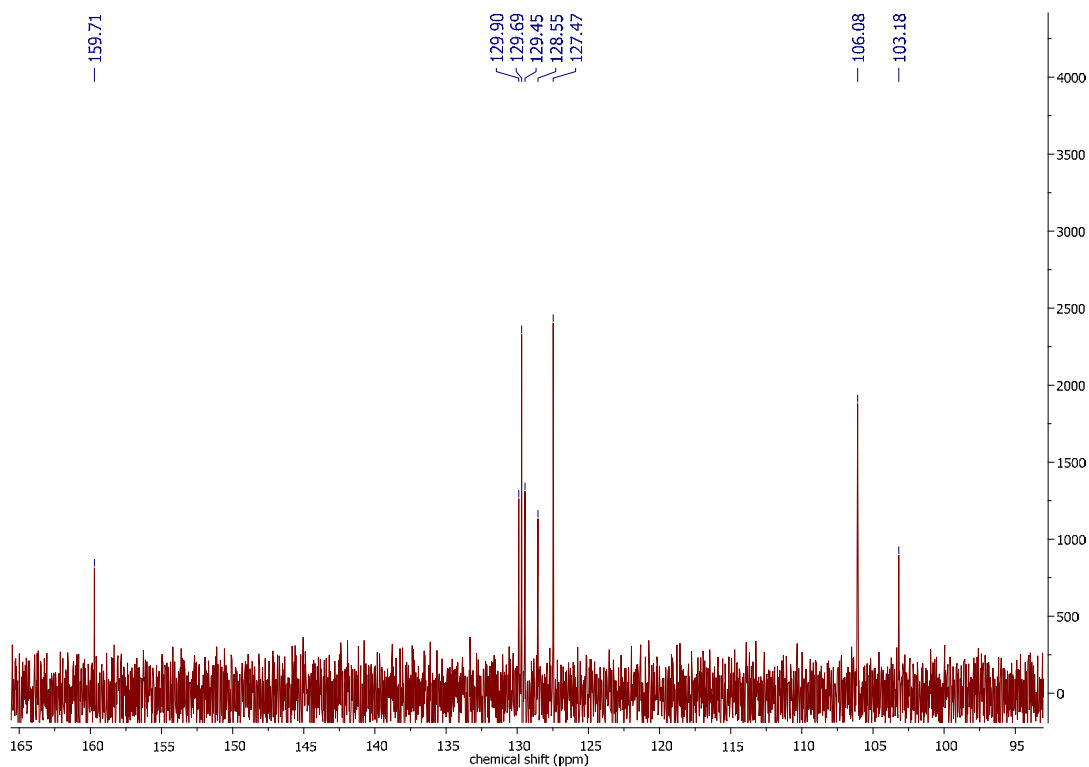
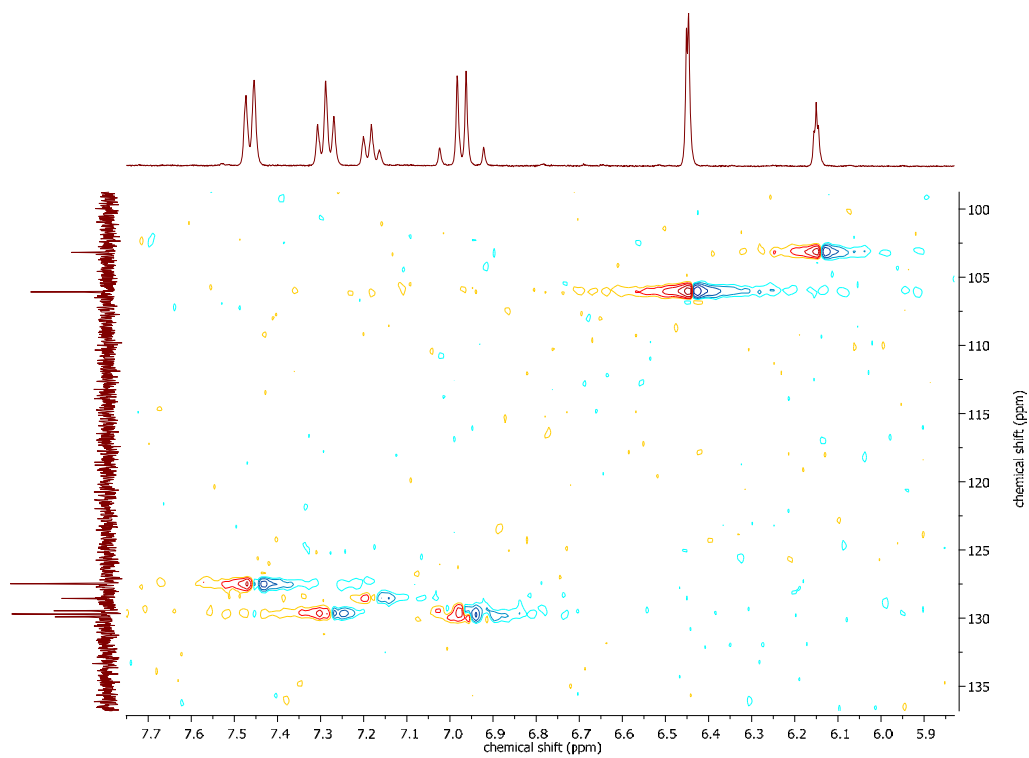
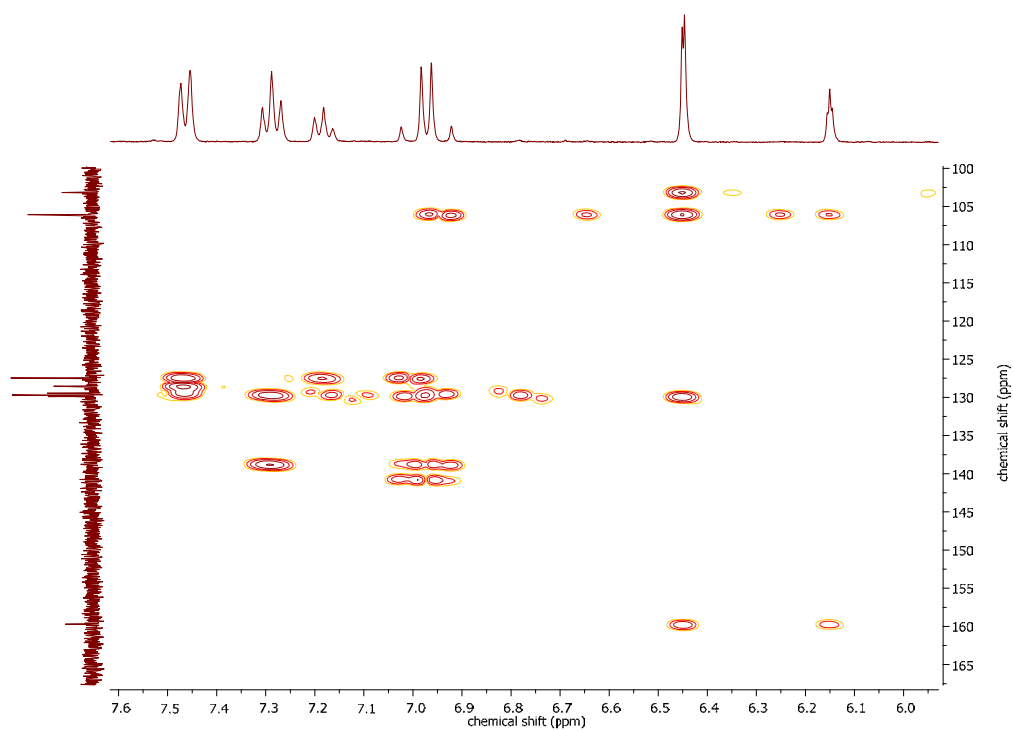


Figure A-12 The  $^{13}\text{C-NMR}$  spectrum of compound **3**



**Figure A-13** The HSQC spectrum of compound **3**



**Figure A-14** The HMBC spectrum of compound **3**

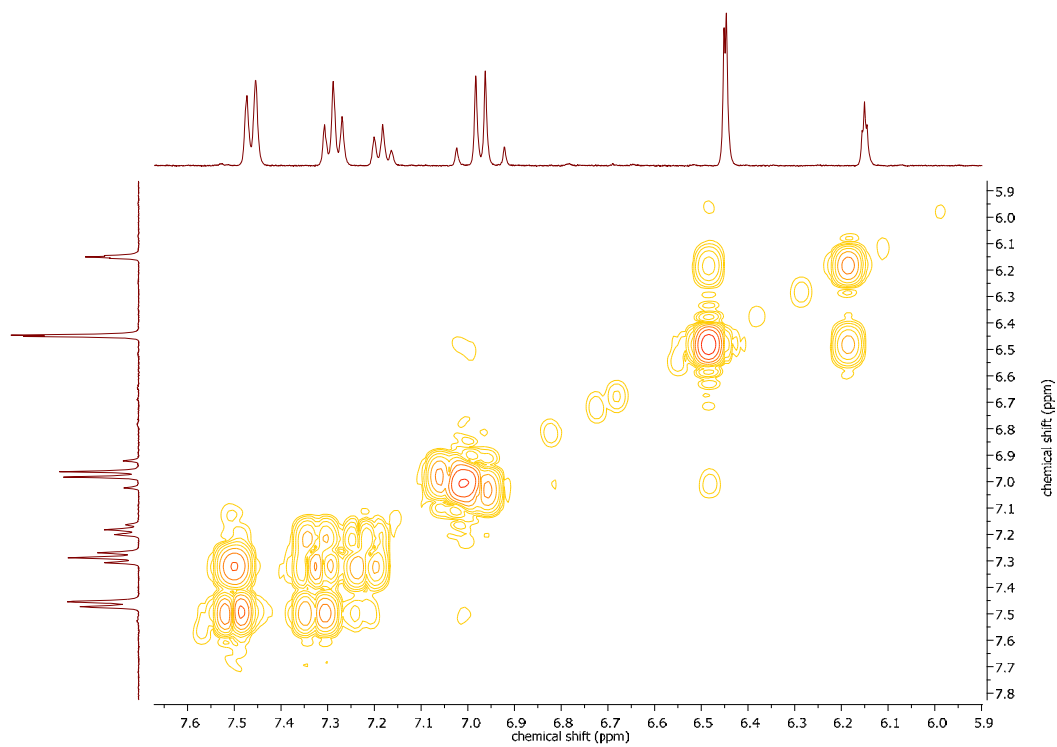


**Figure A-15** The COSY spectrum of compound **3**

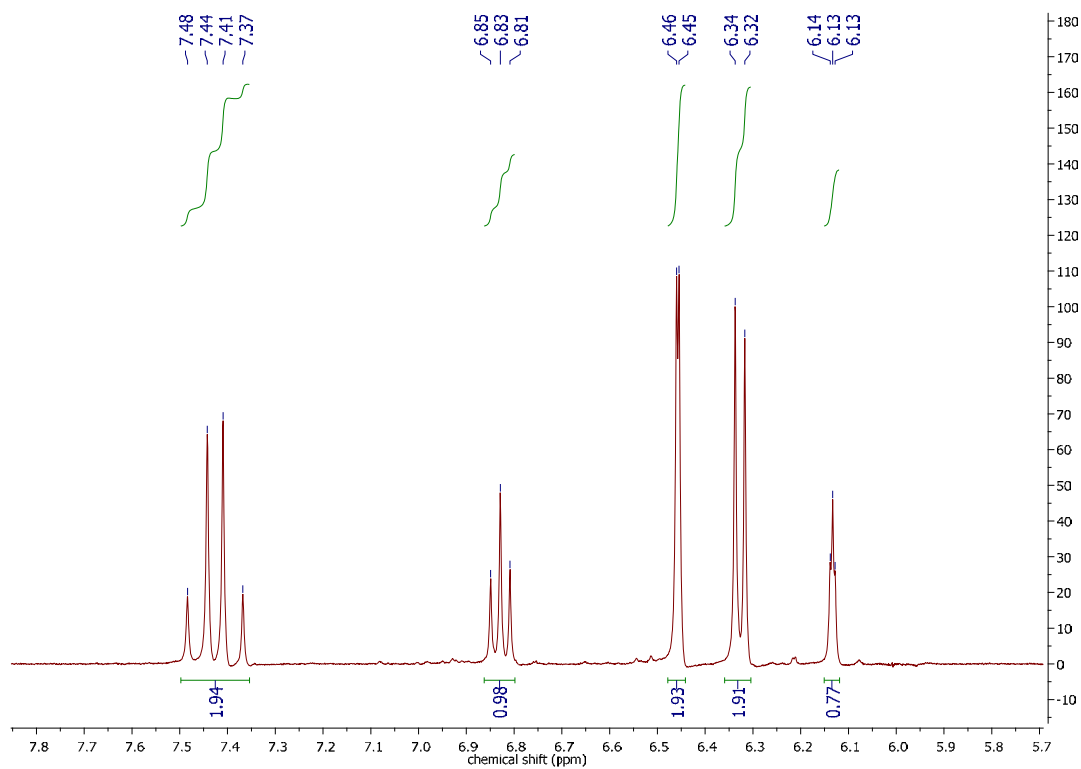


**Figure A-16** The  $^1\text{H}$ -NMR spectrum of compound **4**

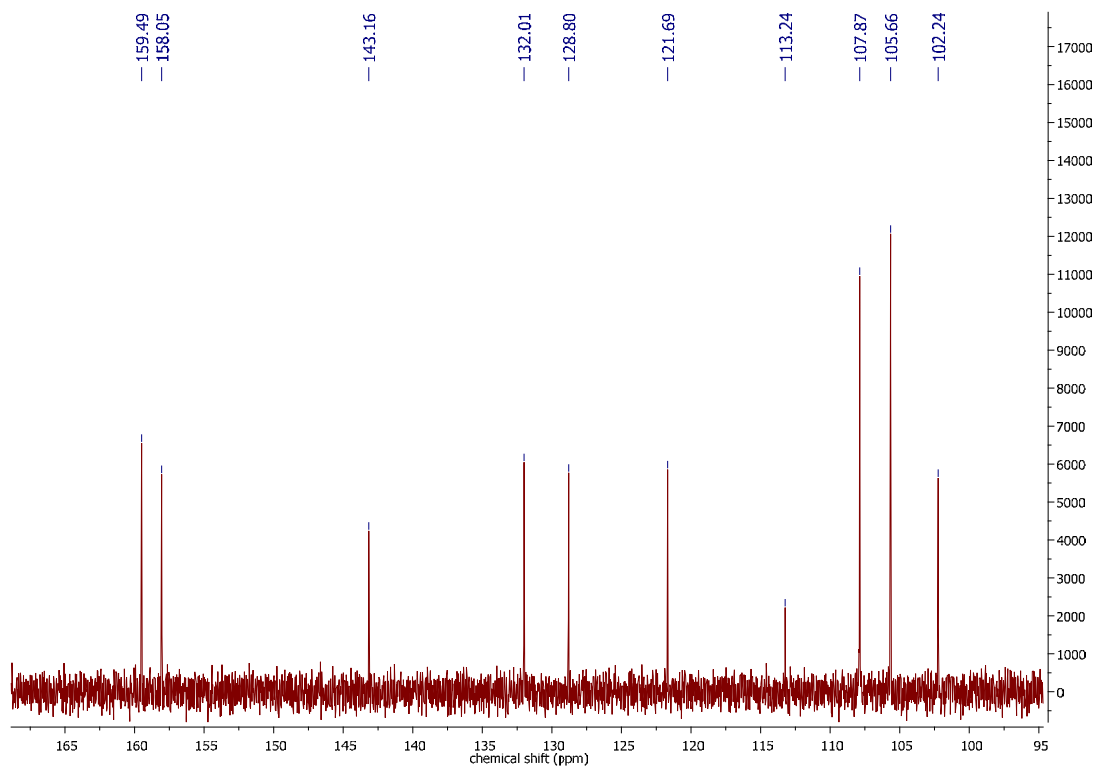


Figure A-17 The  $^{13}\text{C}$ -NMR spectrum of compound 4

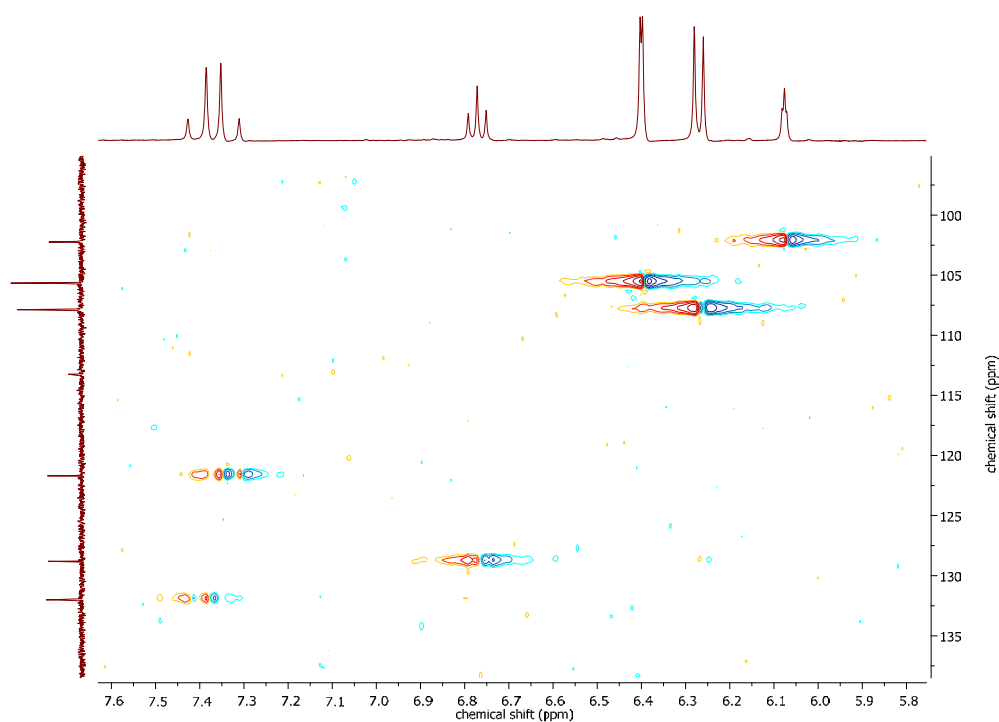
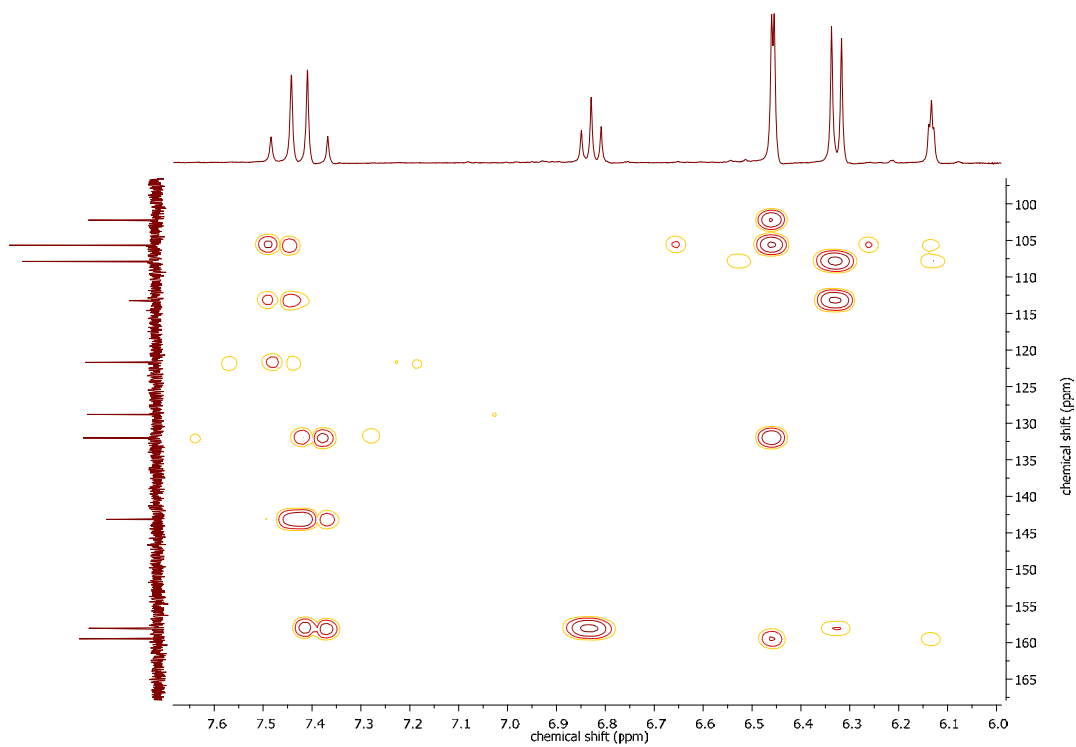
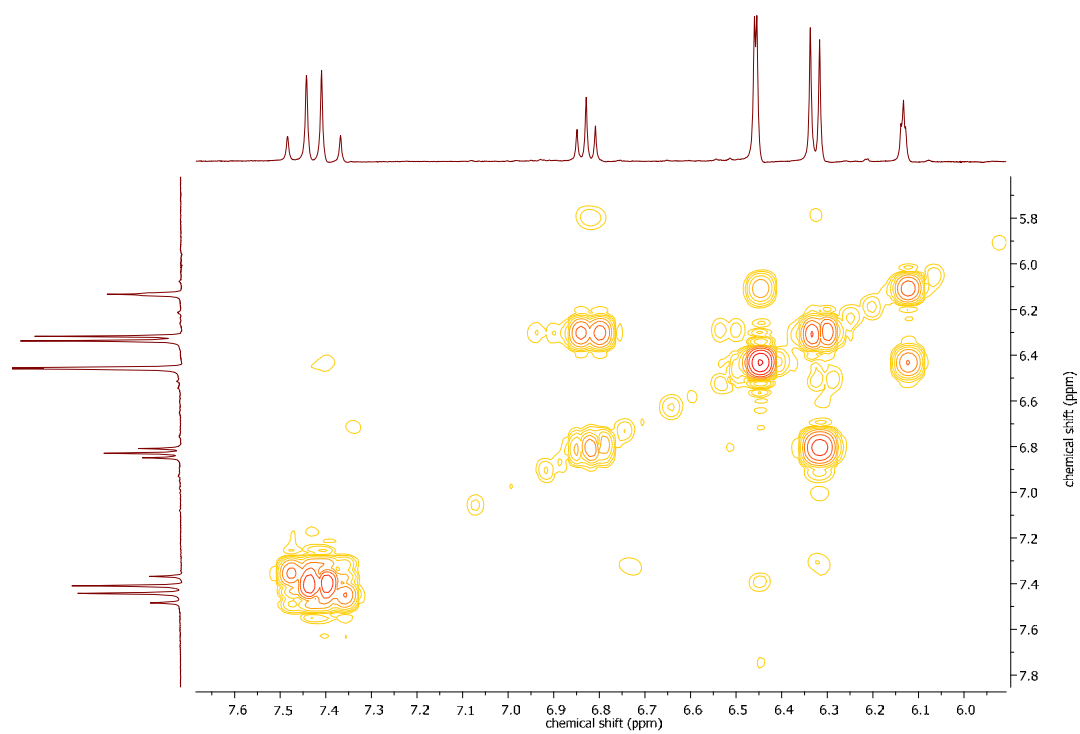


Figure A-18 The HSQC spectrum of compound 4



**Figure A-19** The HMBC spectrum of compound **4**



**Figure A-20** The COSY spectrum of compound **4**

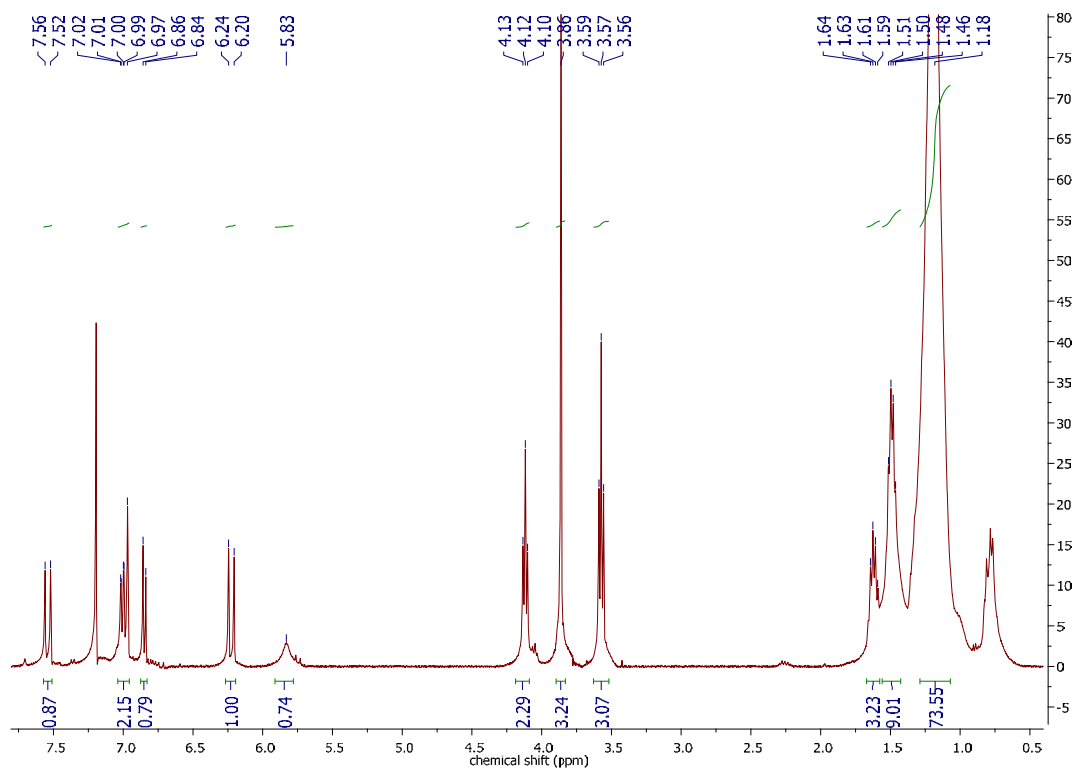


Figure A-21 The  $^1\text{H-NMR}$  spectrum of compound 5

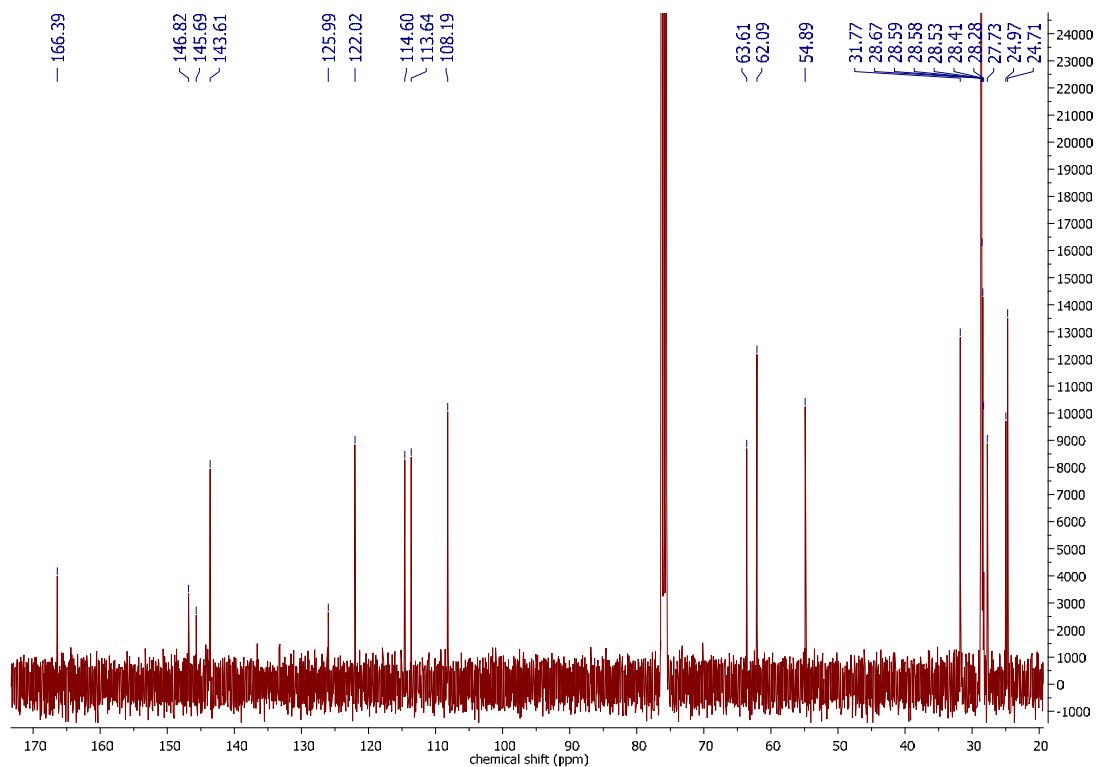
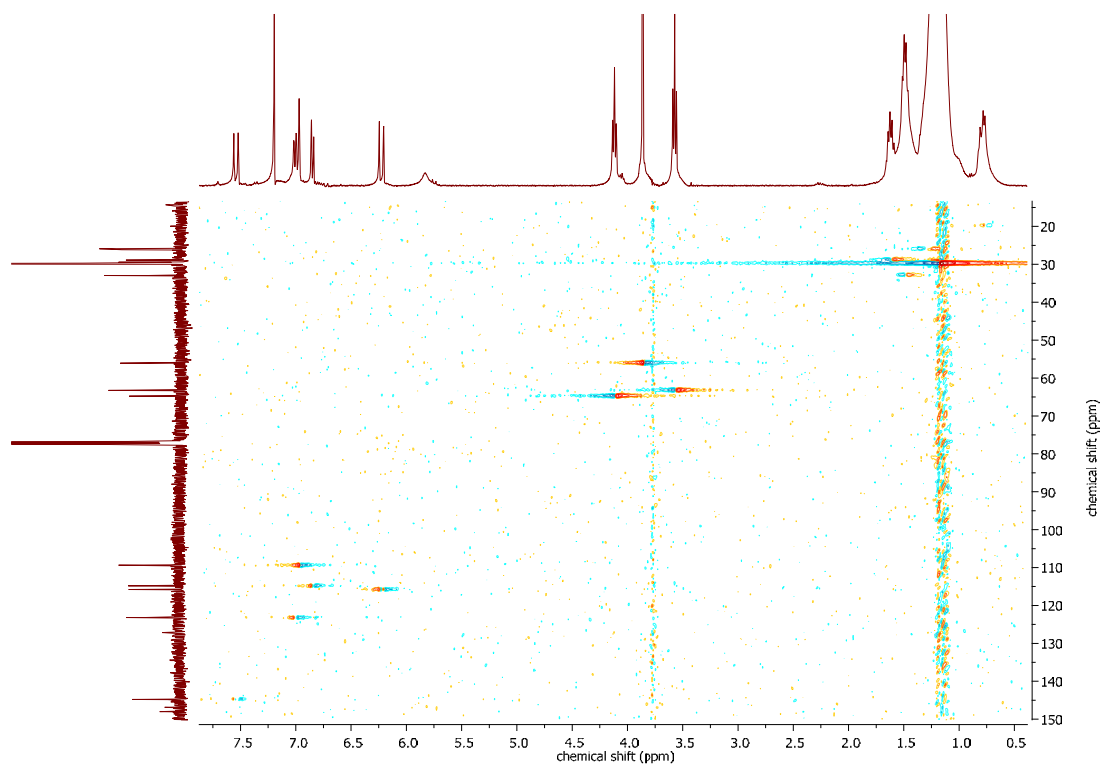
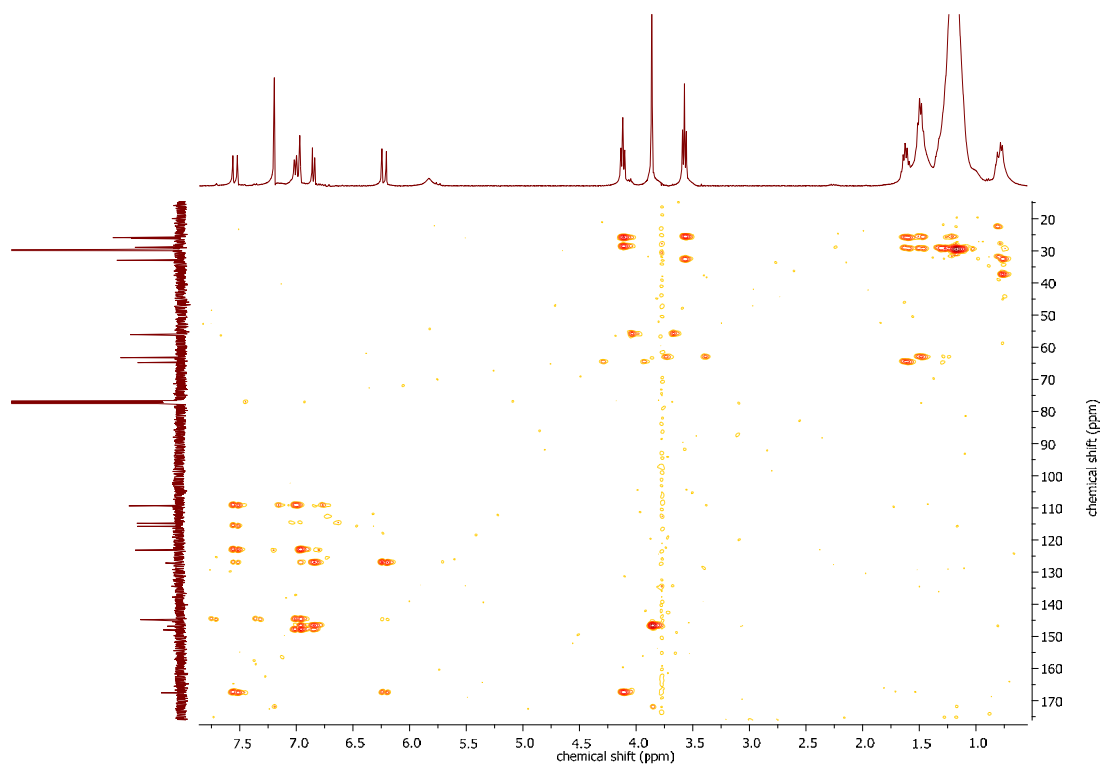


Figure A-22 The  $^{13}\text{C-NMR}$  spectrum of compound 5



**Figure A-23** The HSQC spectrum of compound **5**



**Figure A-24** The HMBC spectrum of compound **5**



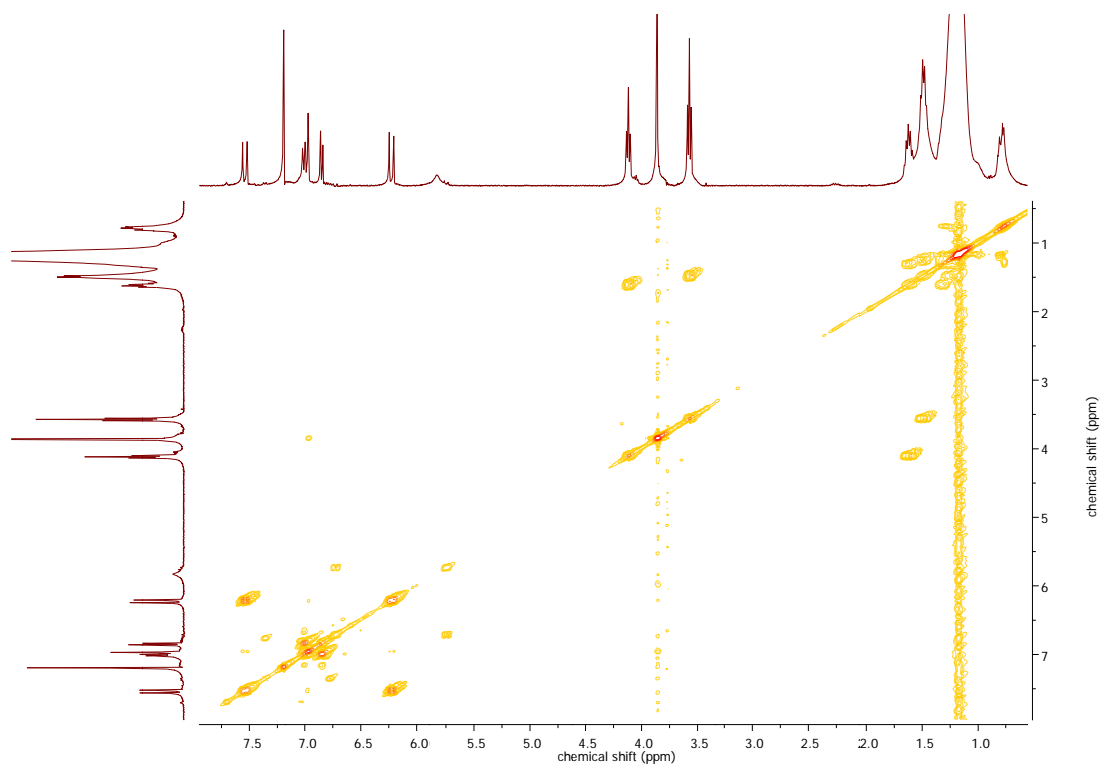


**Figure A-25** The COSY spectrum of compound **5**

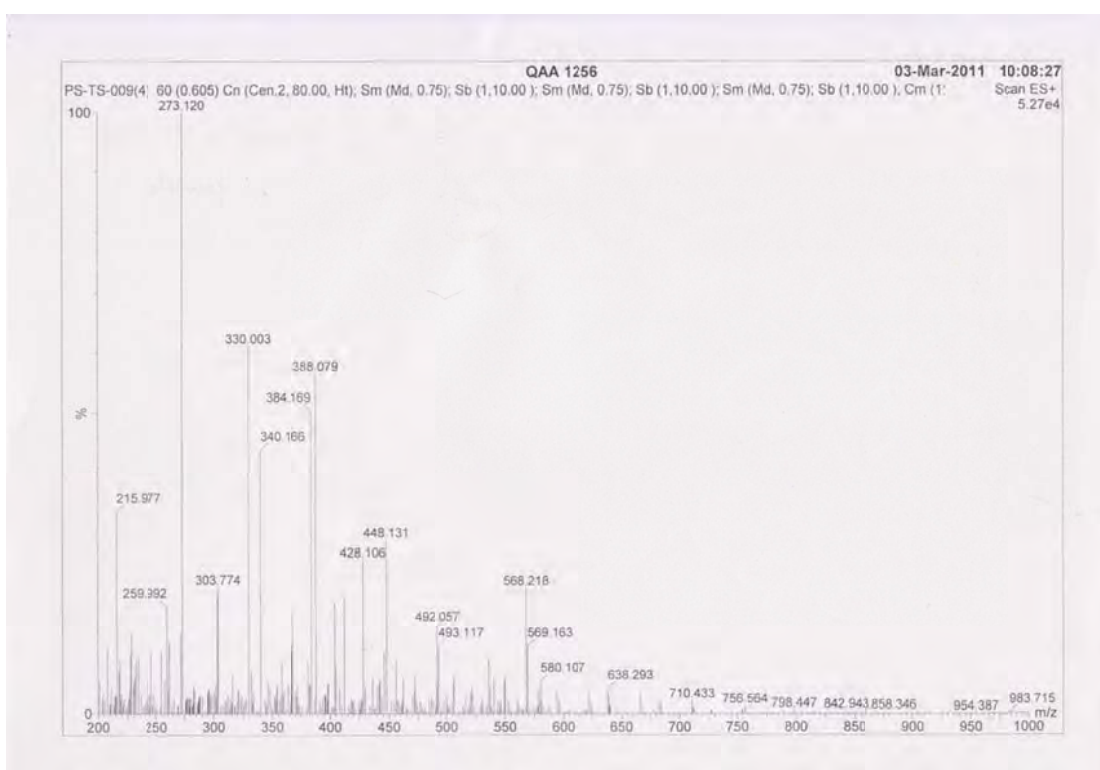


**Figure A-26** The positive mass spectrum of compound **5**

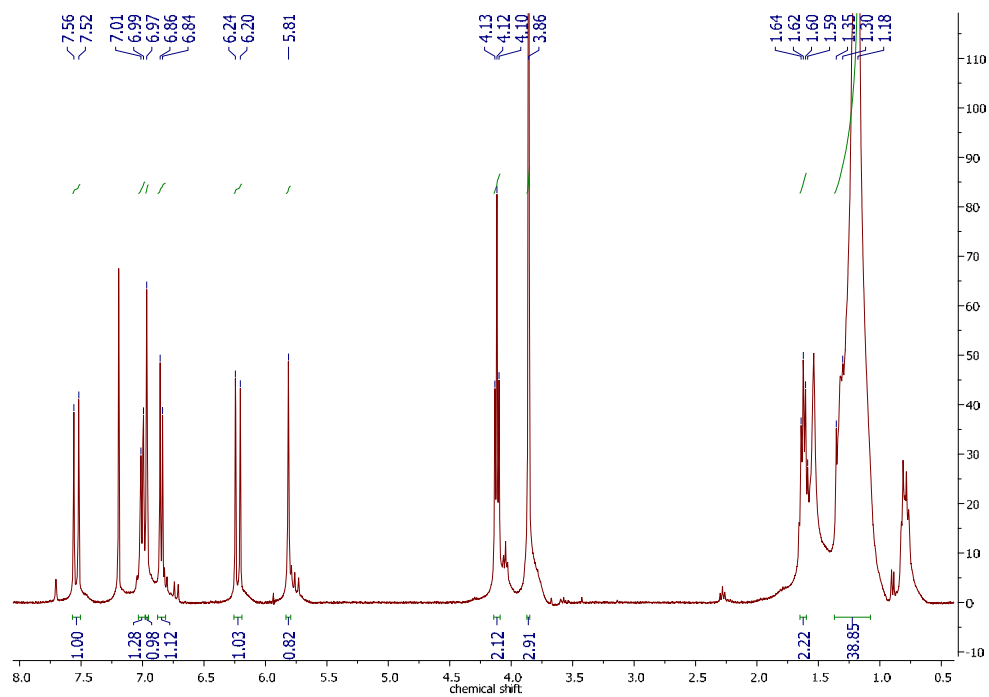


Figure A-27 The  $^1\text{H-NMR}$  spectrum of mixture 6

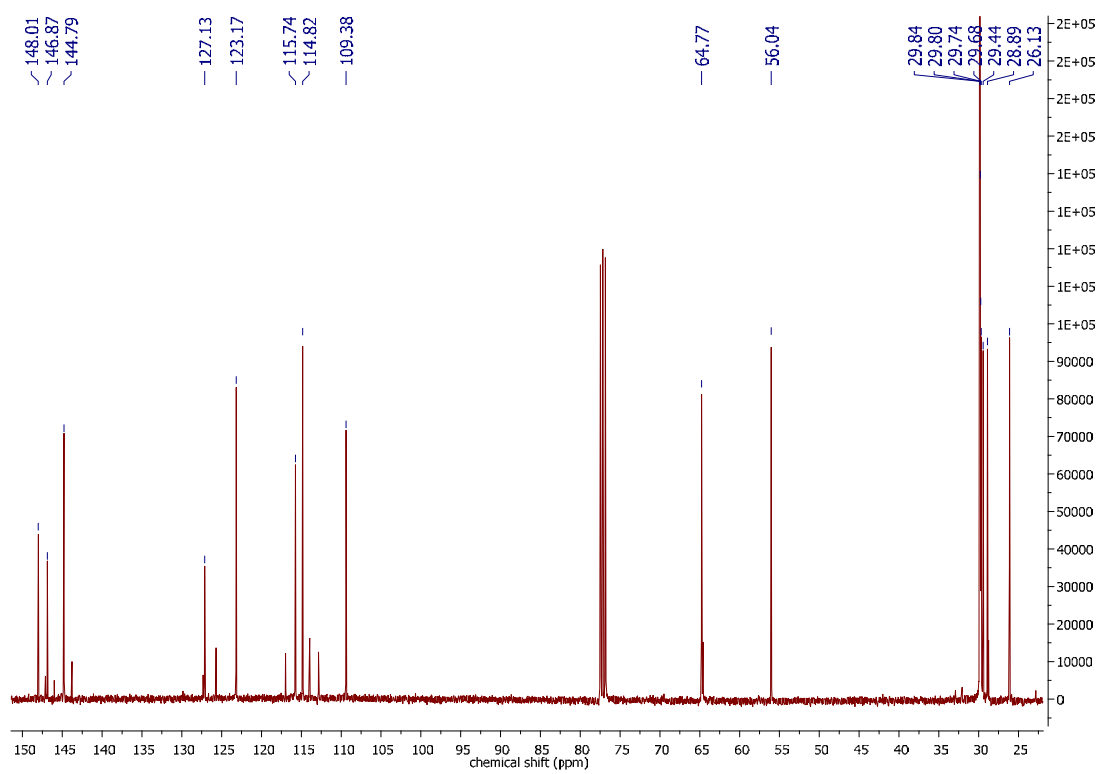
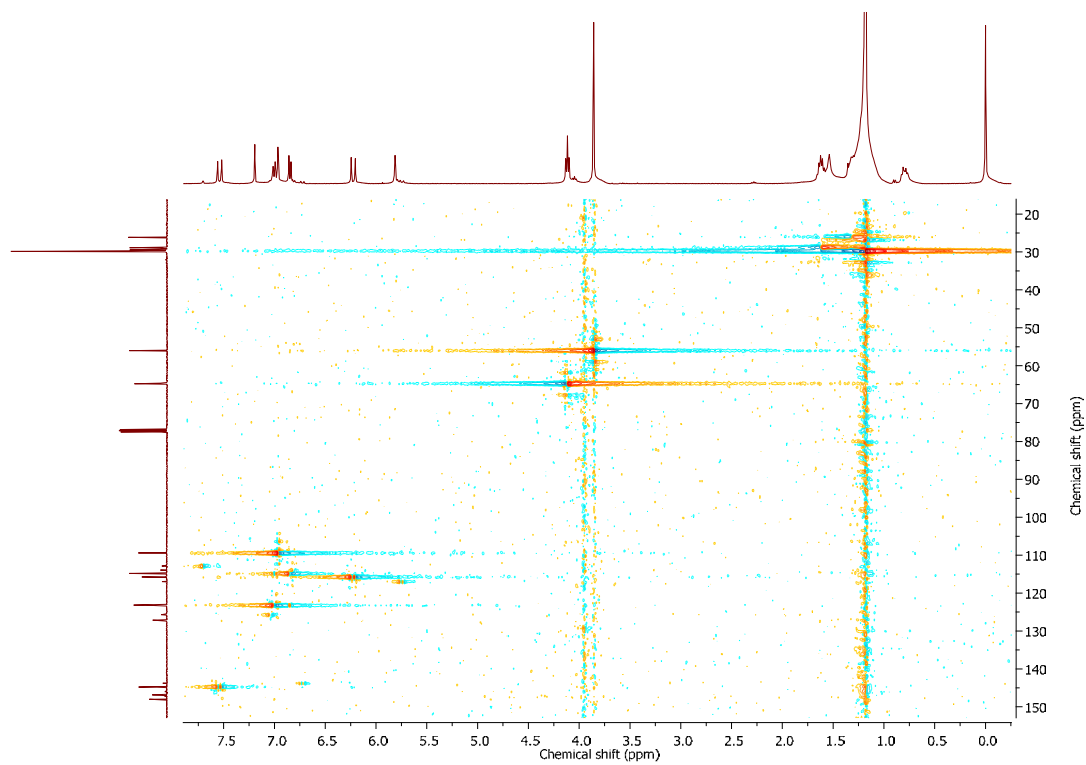
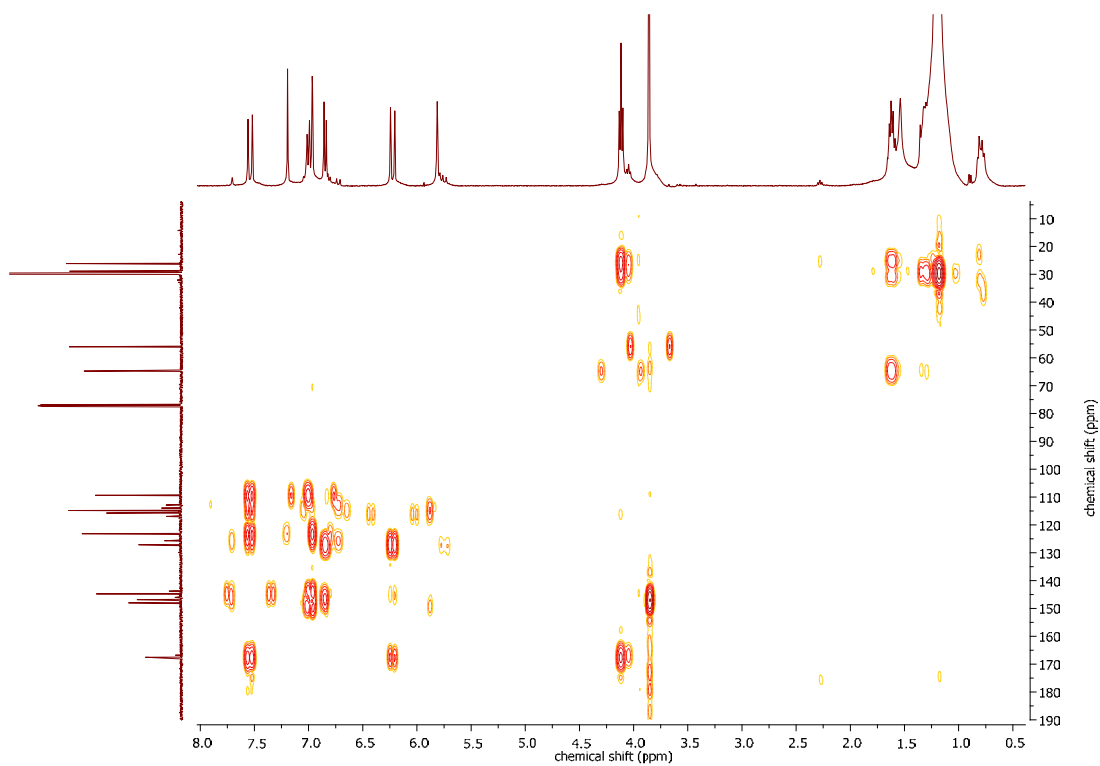


Figure A-28 The  $^{13}\text{C-NMR}$  spectrum of mixture 6



**Figure A-29** The HSQC spectrum of mixture **6**



**Figure A-30** The HMBC spectrum of mixture **6**

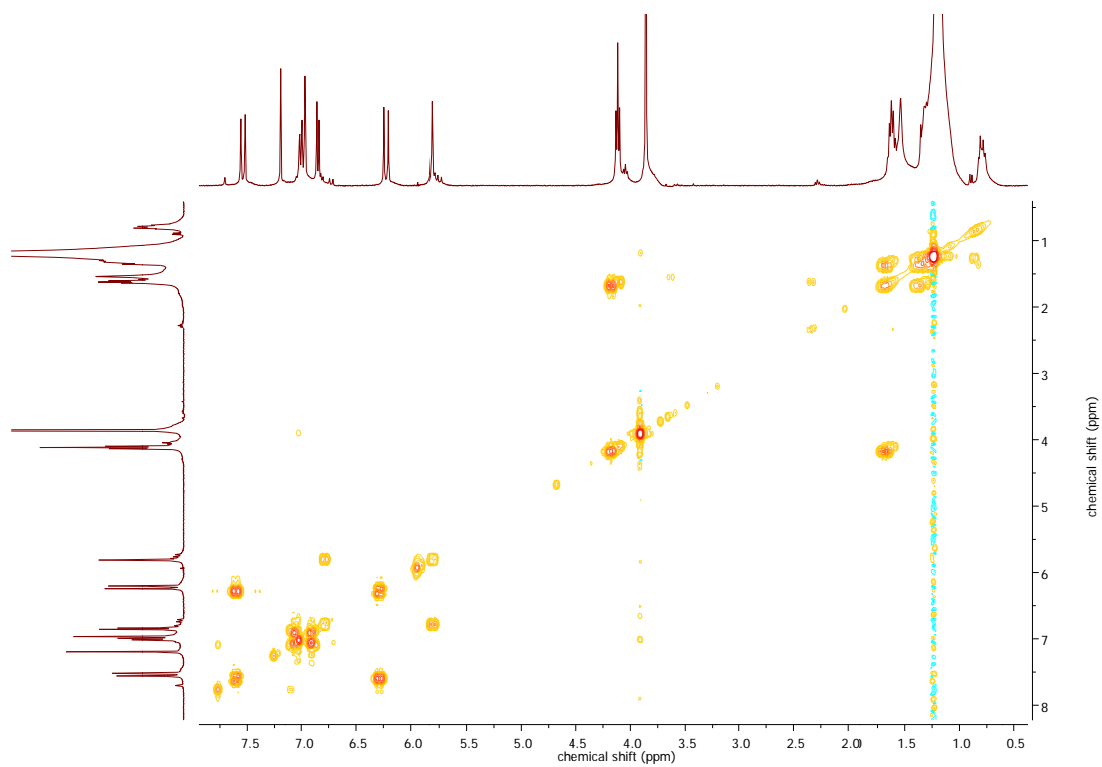


**Figure A-31** The COSY spectrum of mixture **6**

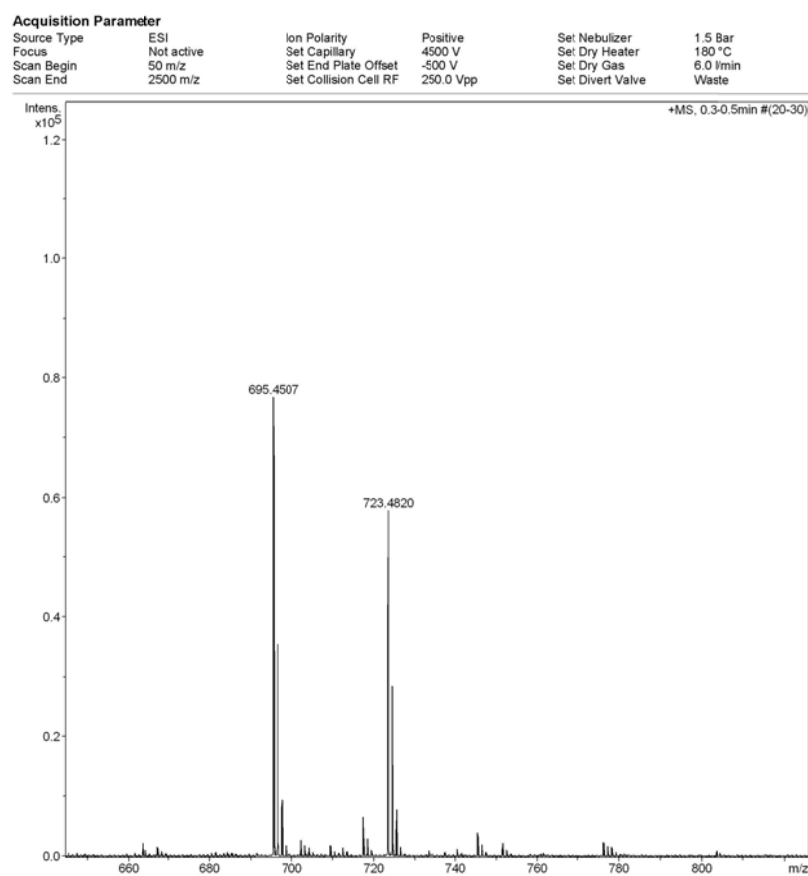
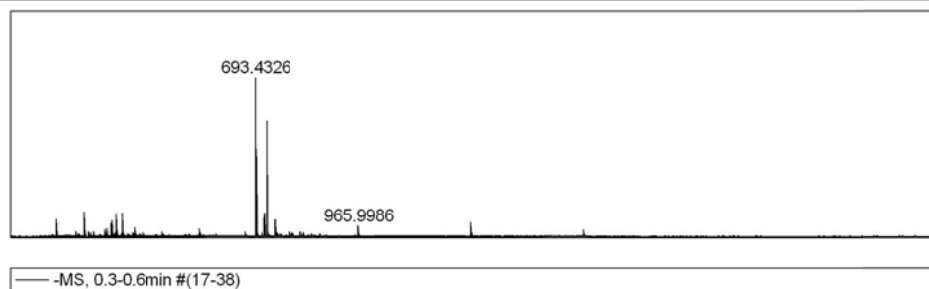


**Figure A-32** The positive mass spectrum of mixture **6**

**Acquisition Parameter**

Source Type	ESI	Ion Polarity	Negative	Set Nebulizer	1.5 Bar
Focus	Not active	Set Capillary	2500 V	Set Dry Heater	180 °C
Scan Begin	50 m/z	Set End Plate Offset	-500 V	Set Dry Gas	6.0 l/min
Scan End	2500 m/z	Set Collision Cell RF	250.0 Vpp	Set Divert Valve	Waste



#	m/z	I
1	693.4326	1246
2	721.4655	907

**Figure A-33** The negative mass spectrum of mixture **6**

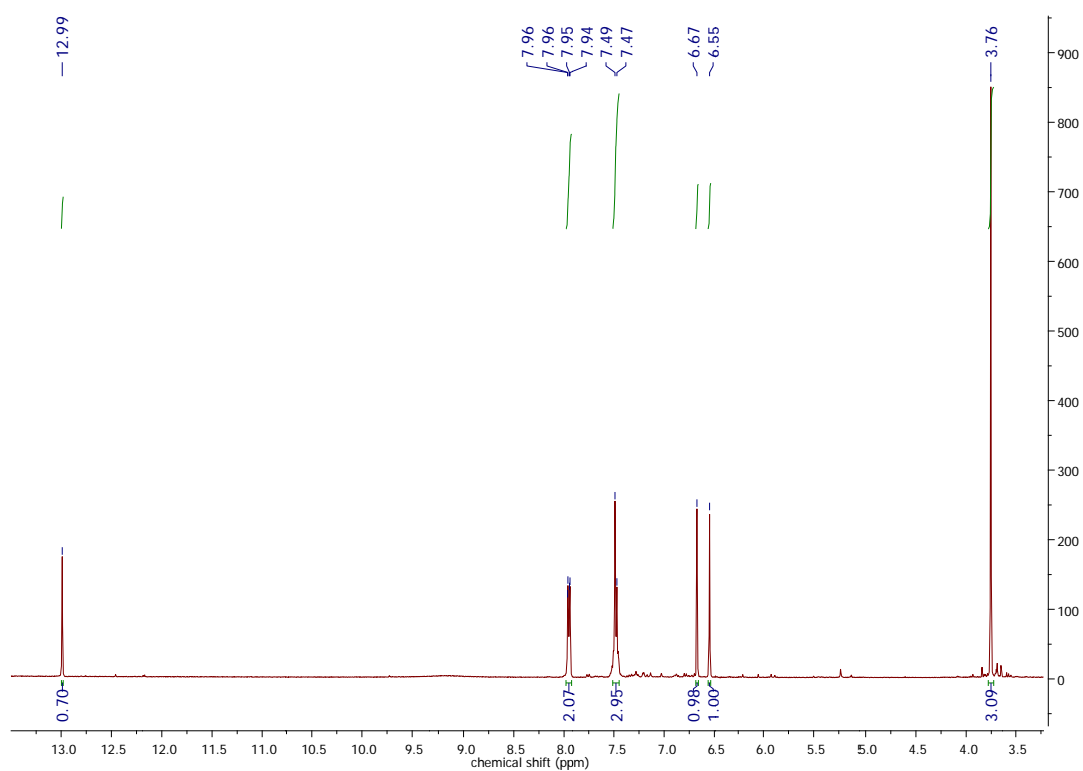


**Figure A-34** The <sup>1</sup>H-NMR spectrum of compound **7**

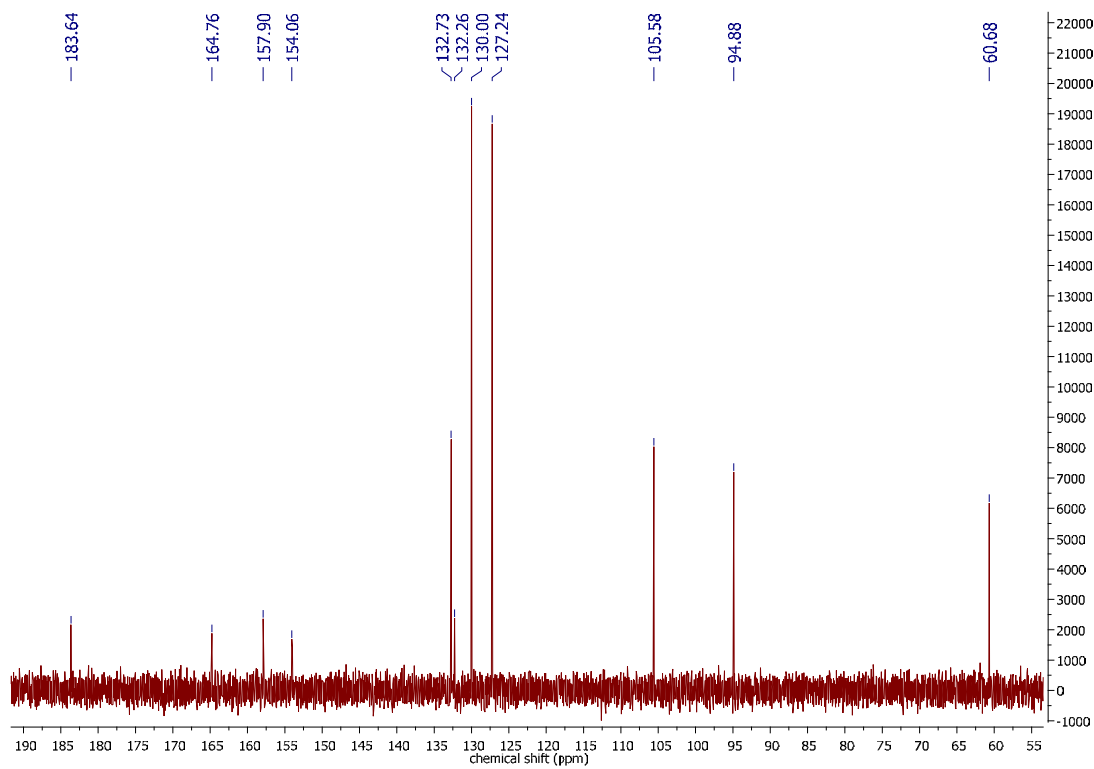


Figure A-35 The  $^{13}\text{C}$ -NMR spectrum of compound 7

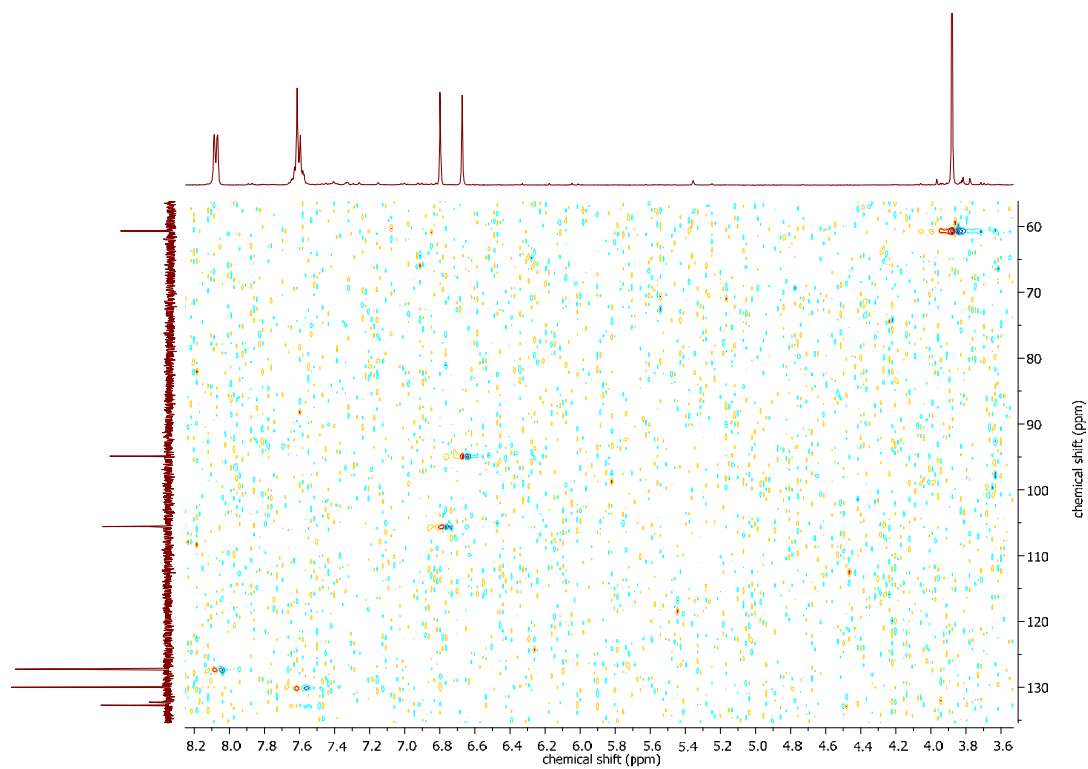
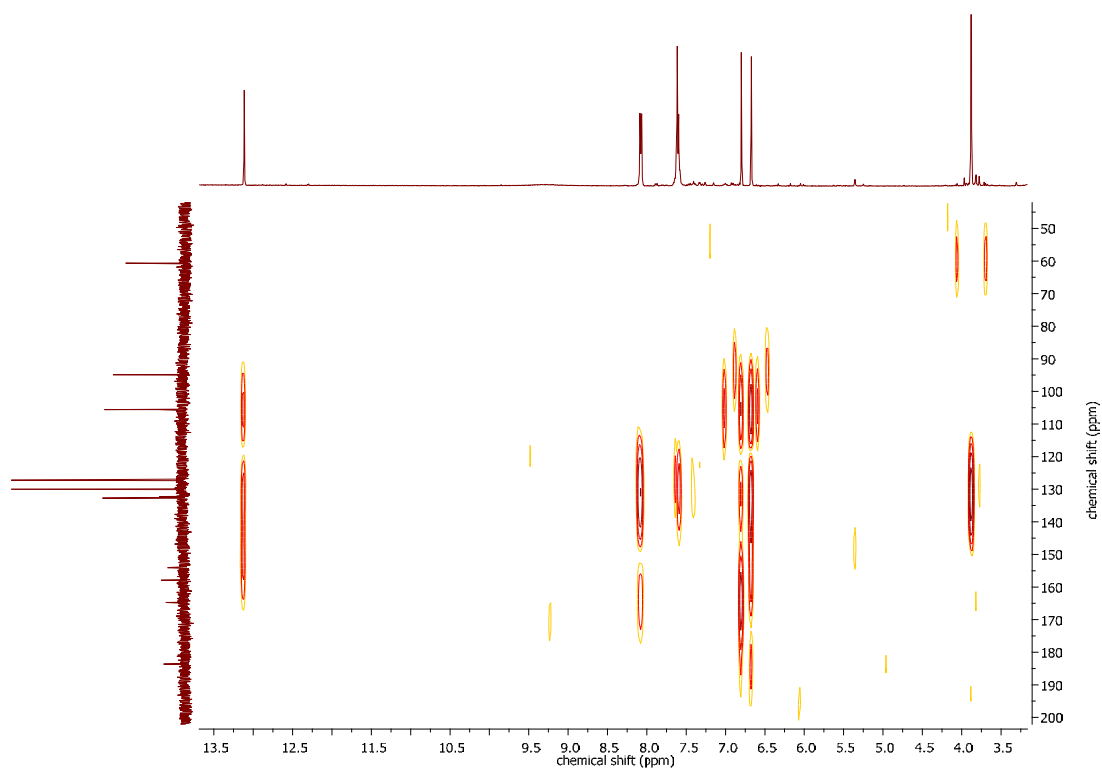
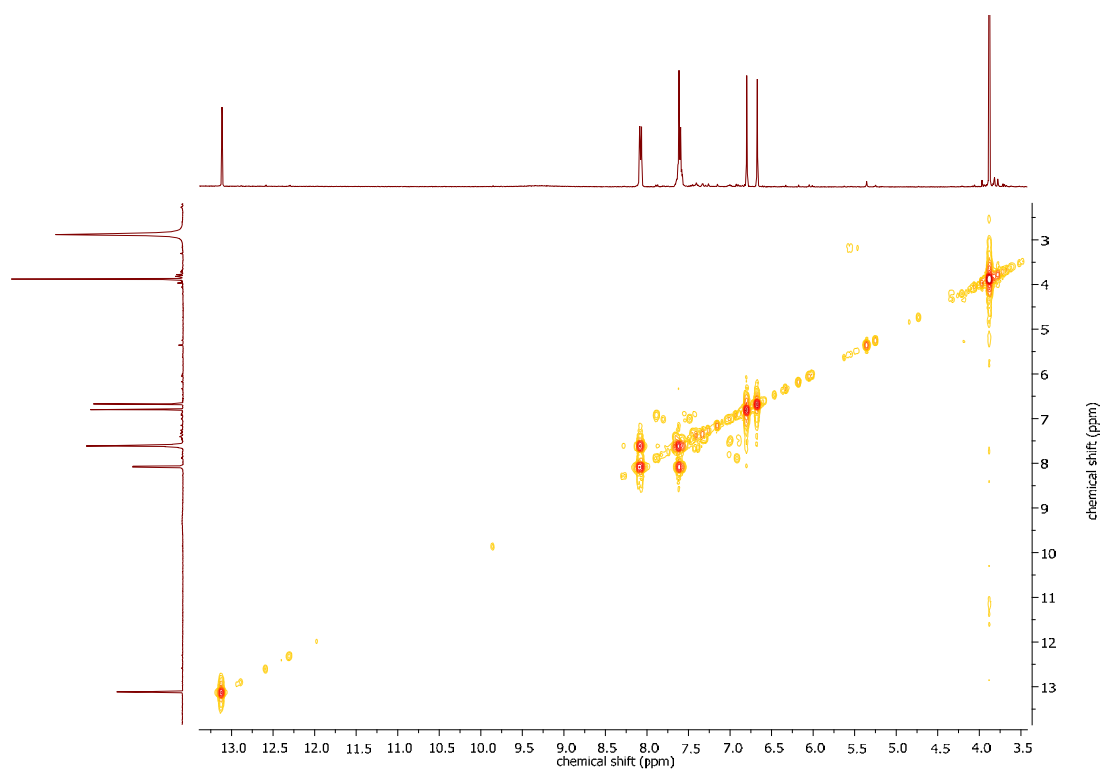


Figure A-36 The HSQC spectrum of compound 7



**Figure A-37** The HMBC spectrum of compound **7**



**Figure A-38** The COSY spectrum of compound **7**

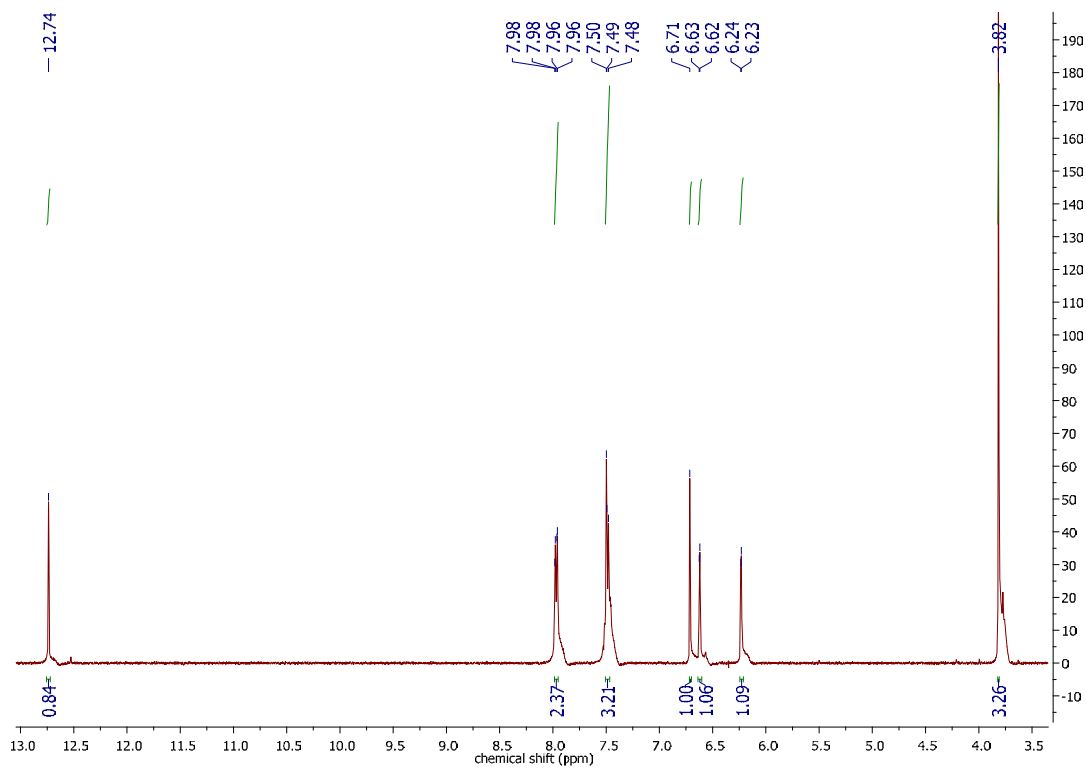


Figure A-39 The  $^1\text{H-NMR}$  spectrum of compound **8**

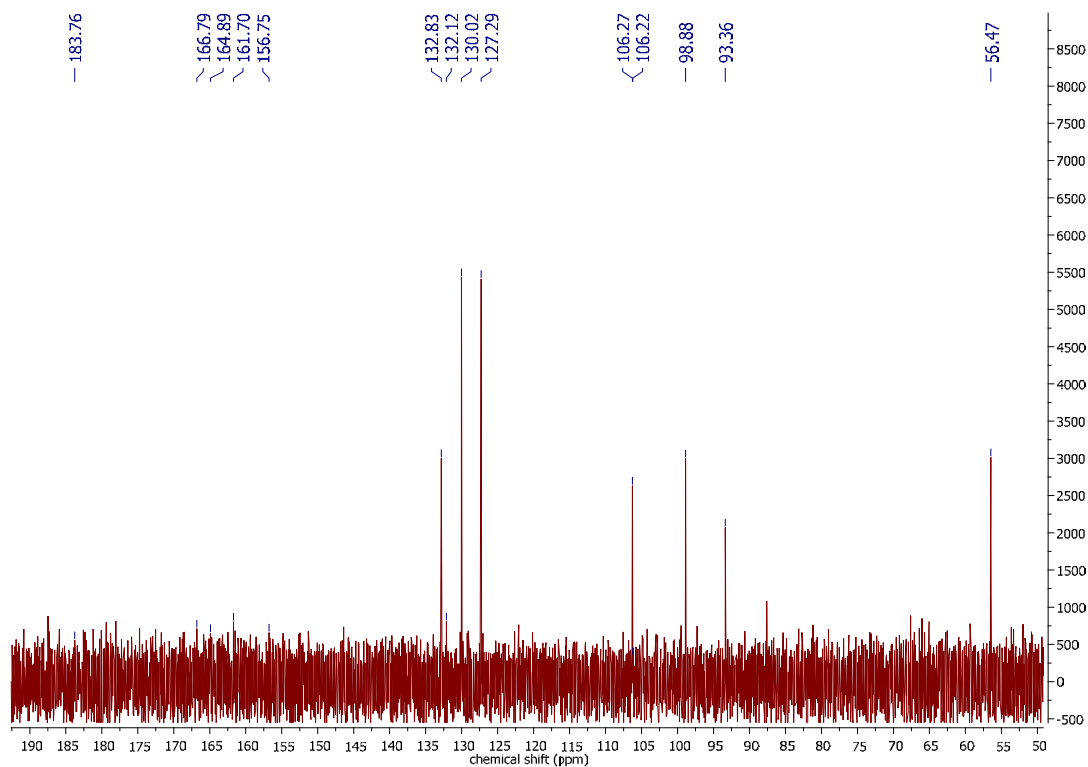
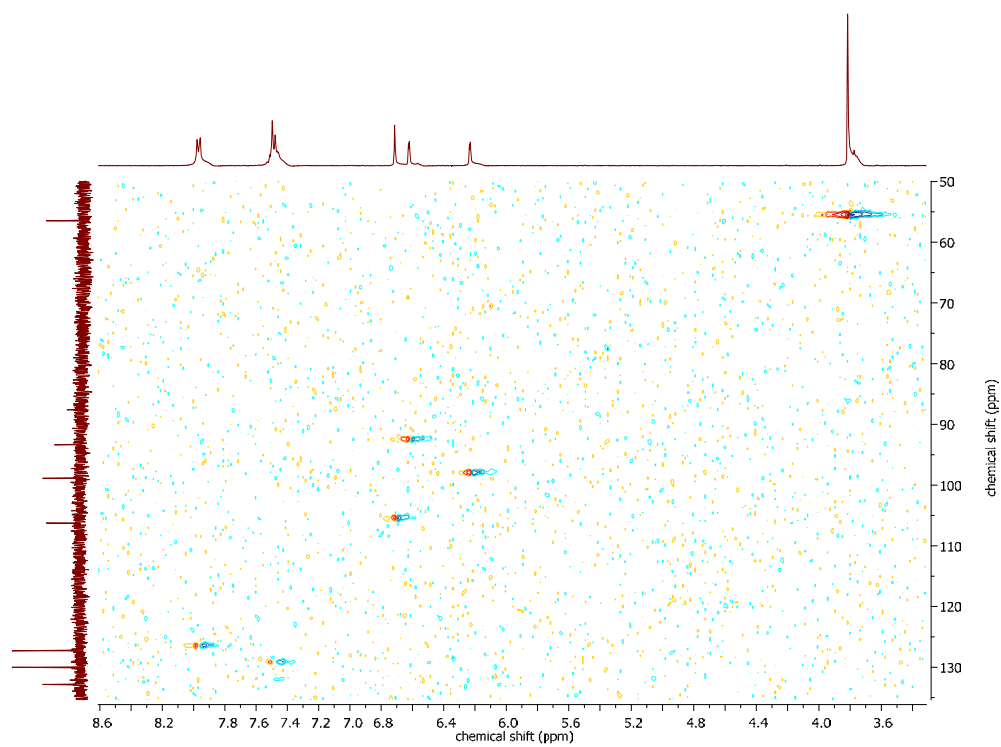
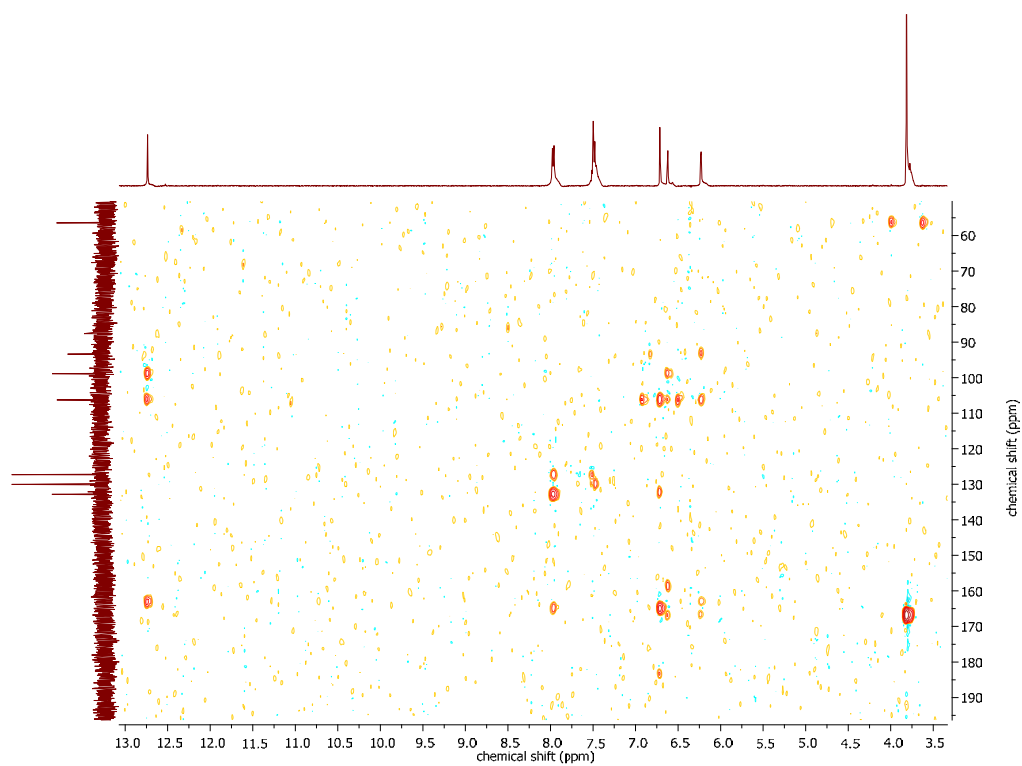


Figure A-40 The  $^{13}\text{C-NMR}$  spectrum of compound **8**





**Figure A-41** The HSQC spectrum of compound **8**



**Figure A-42** The HMBC spectrum of compound **8**

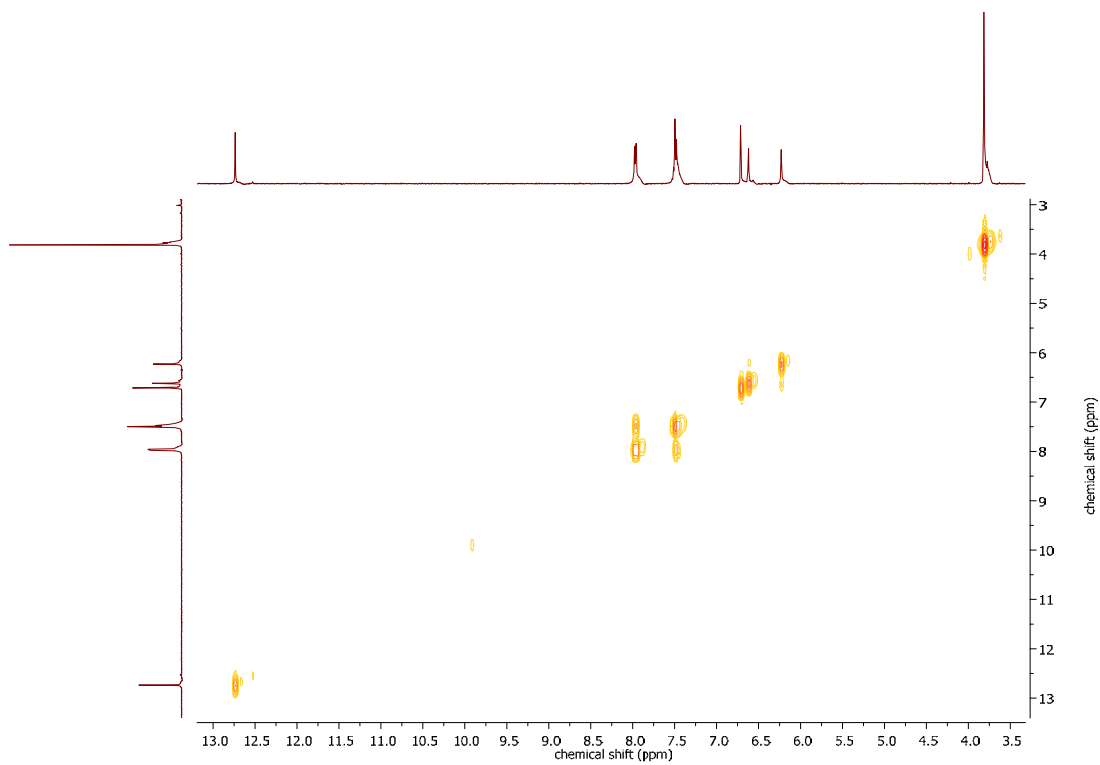


**Figure A-43** The COSY spectrum of compound **8**

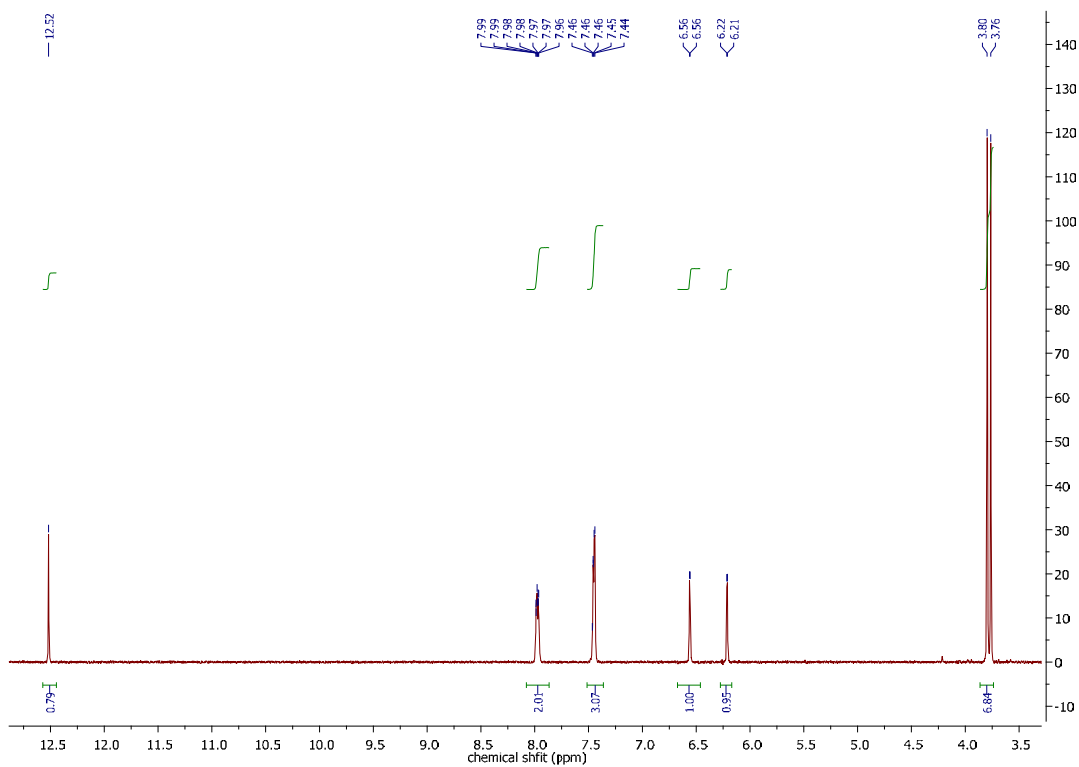


**Figure A-44** The <sup>1</sup>H-NMR spectrum of compound **9**

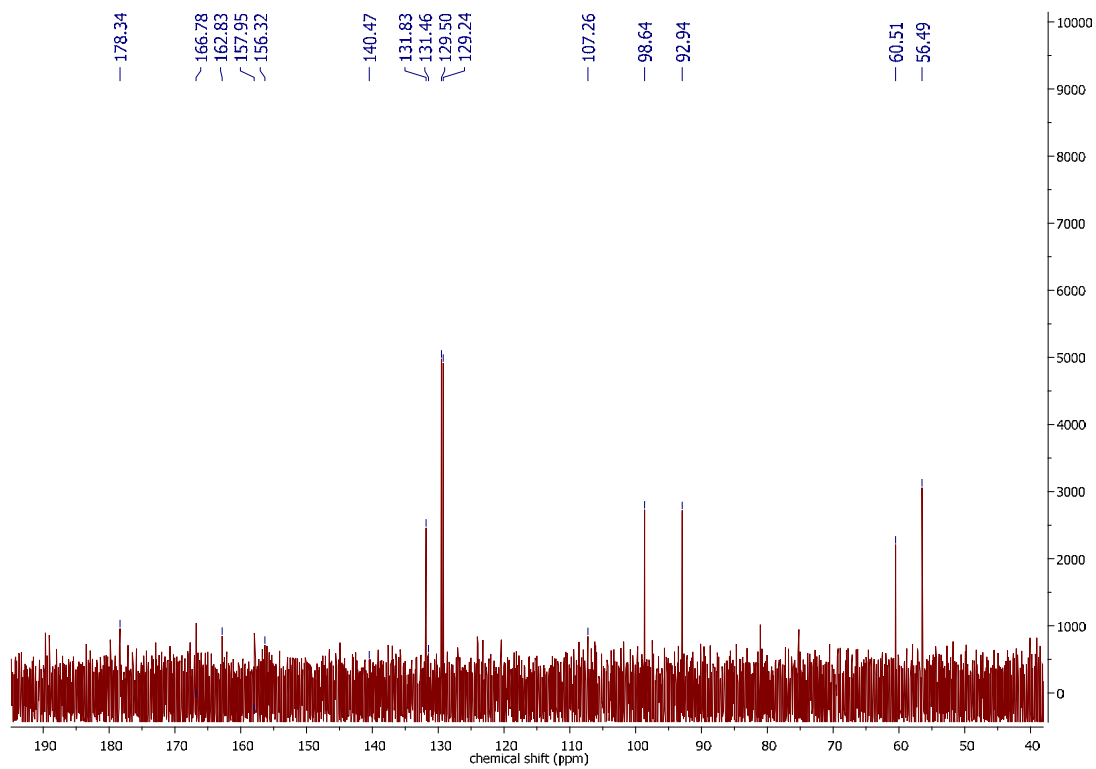


Figure A-45 The  $^{13}\text{C}$ -NMR spectrum of compound 9

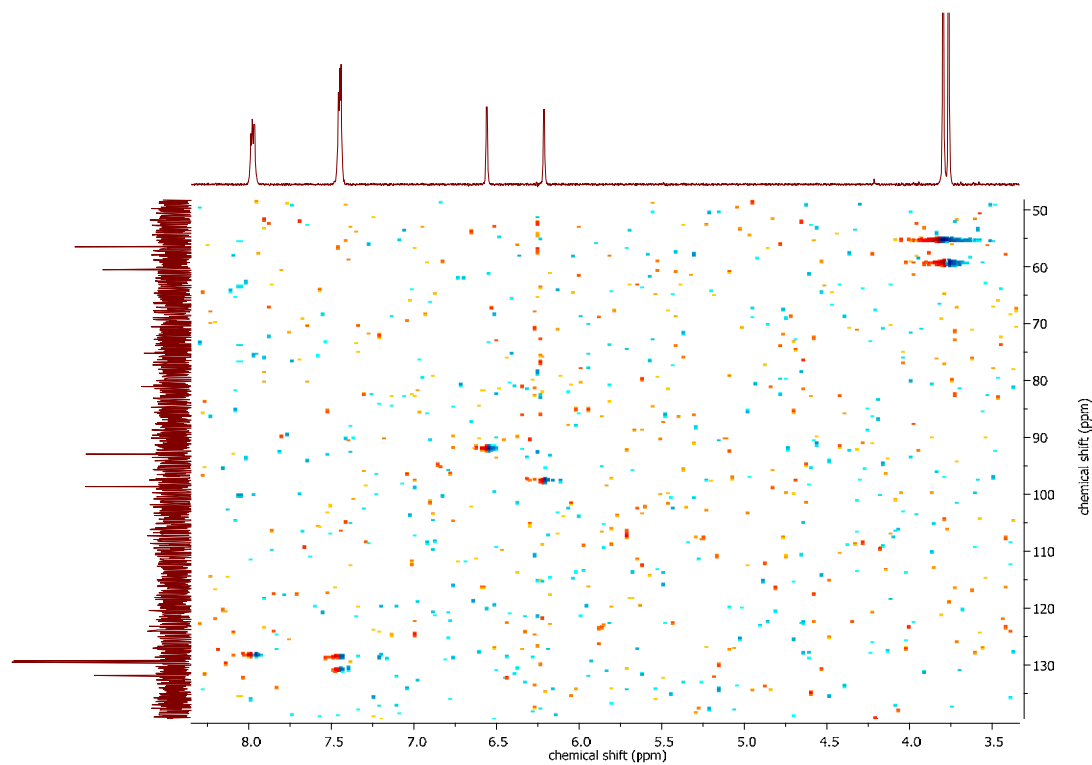
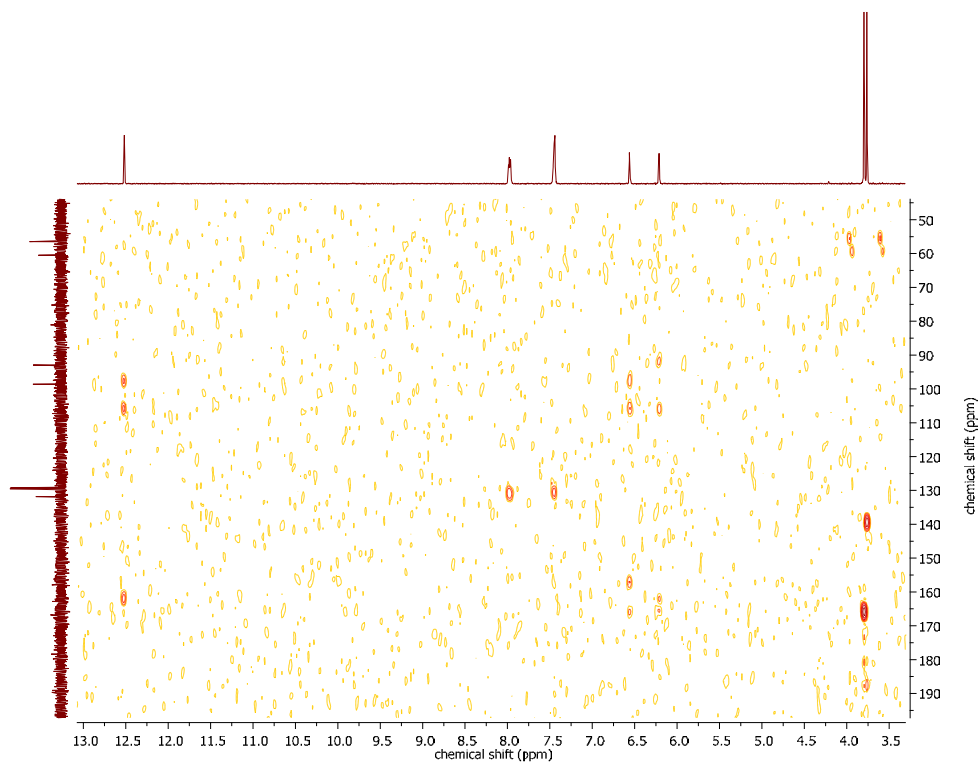
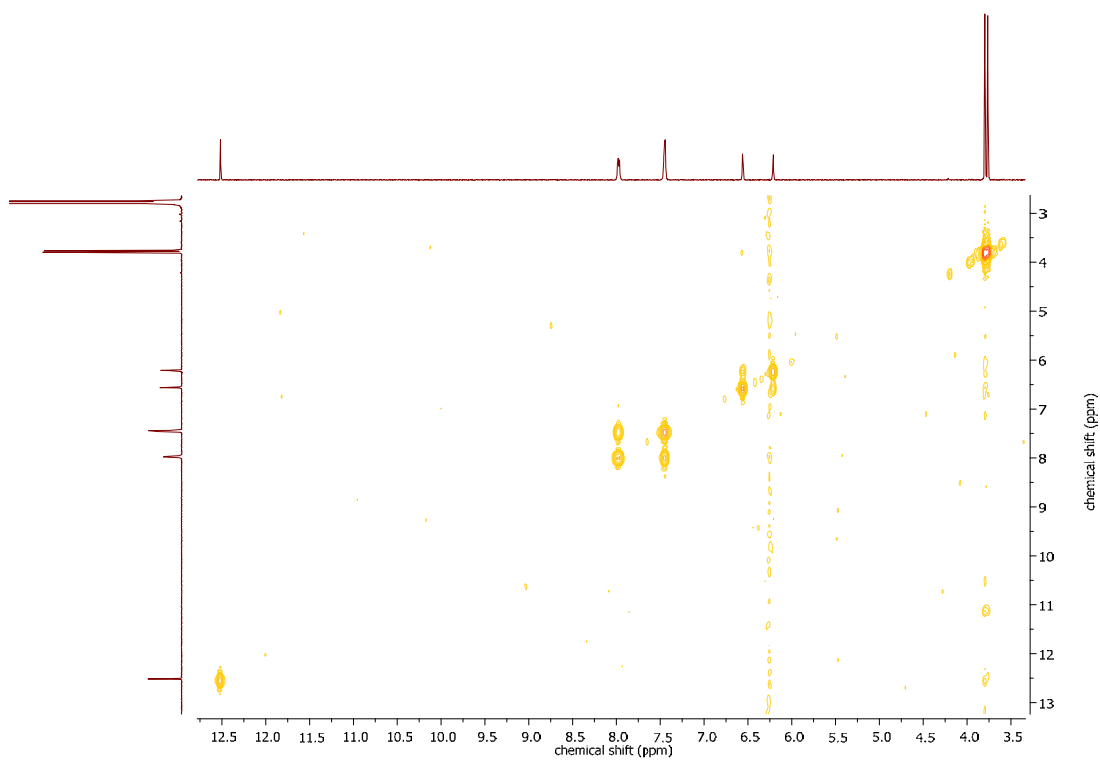


Figure A-46 The HSQC spectrum of compound 9



**Figure A-47** The HMBC spectrum of compound **9**



**Figure A-48** The COSY spectrum of compound **9**

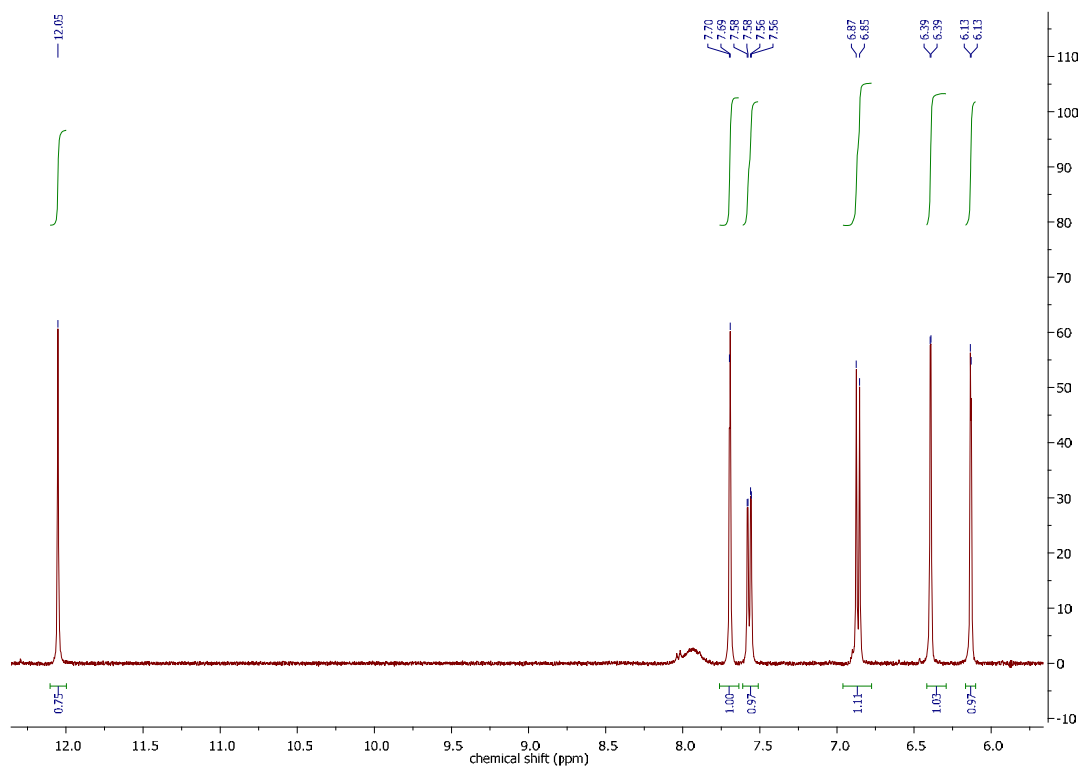


Figure A-49 The  $^1\text{H-NMR}$  spectrum of compound 10

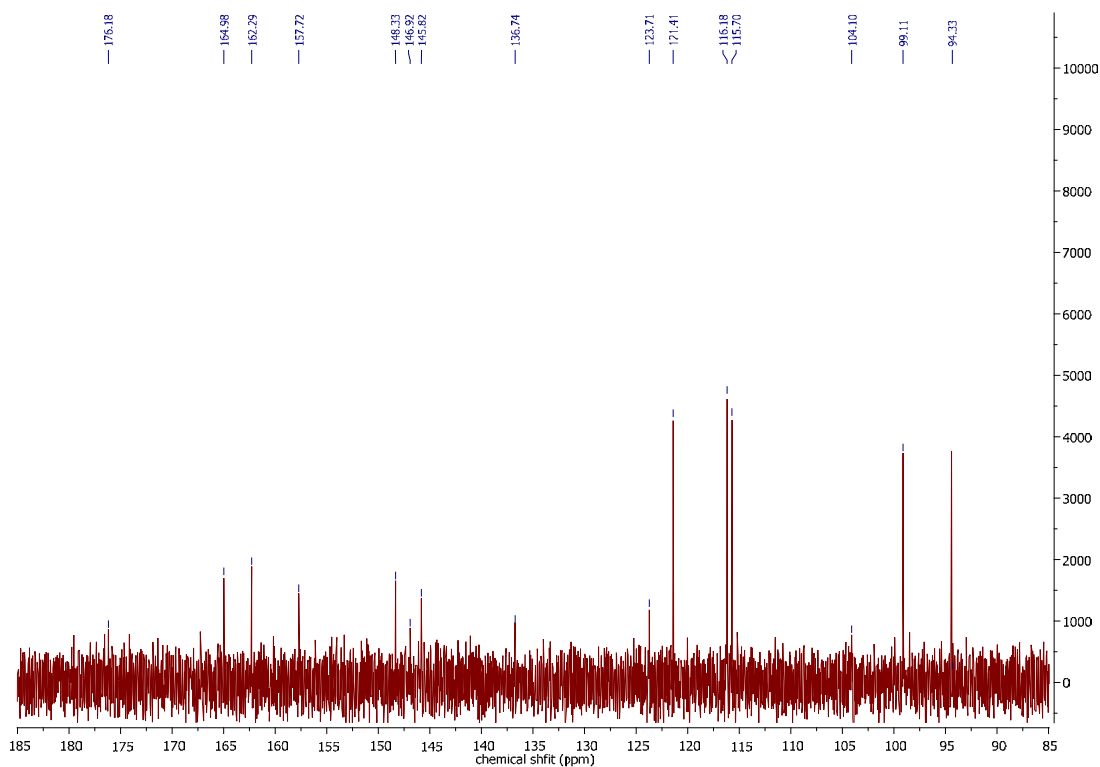
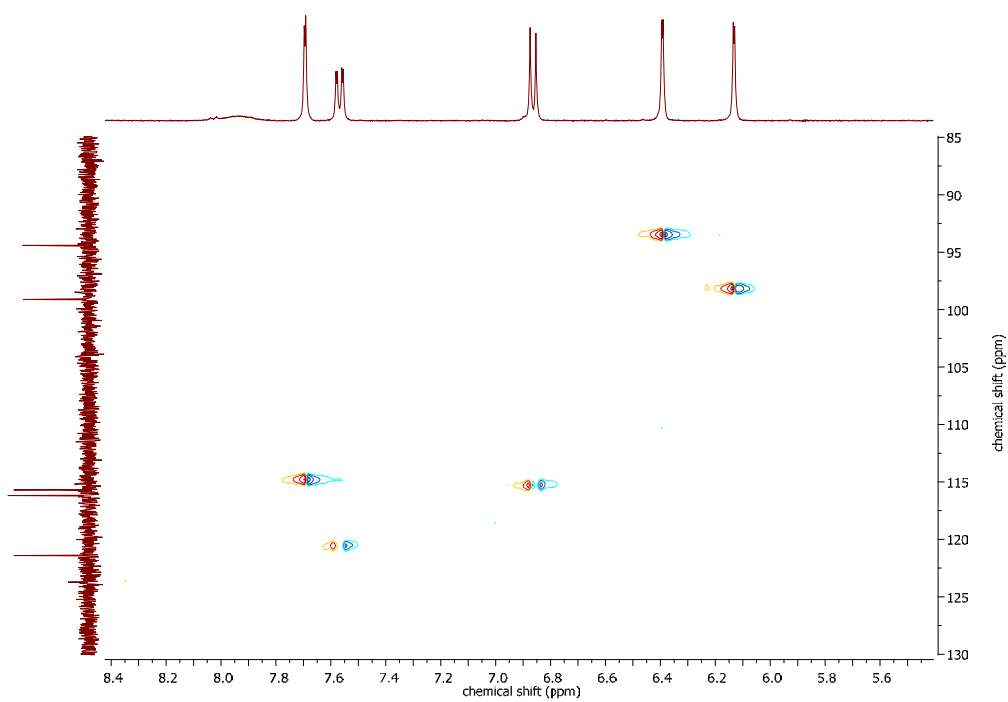
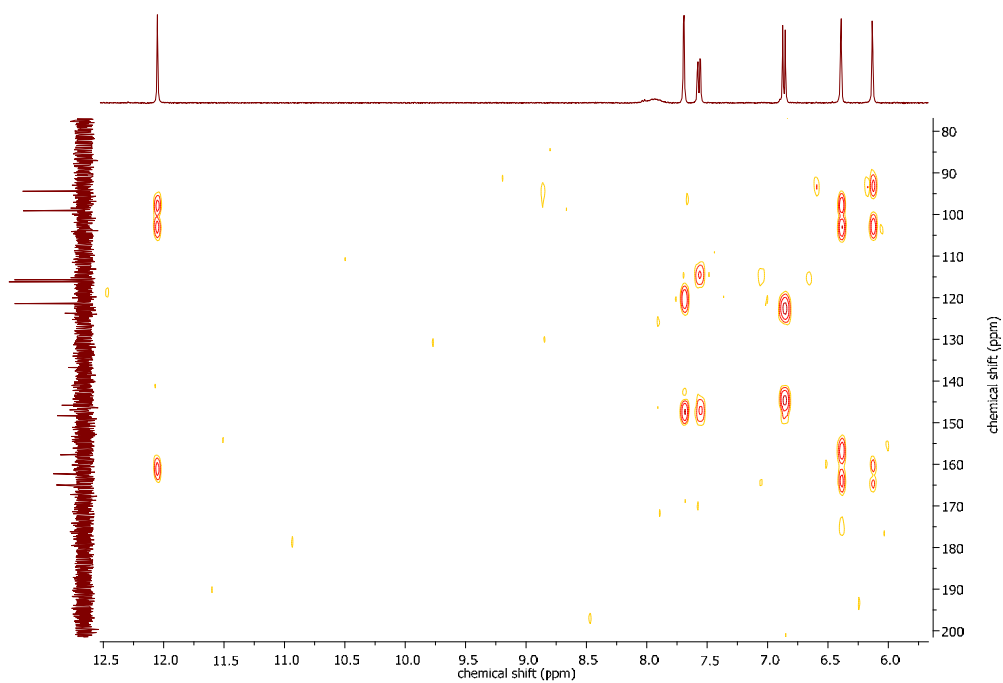


Figure A-50 The  $^{13}\text{C-NMR}$  spectrum of compound 10



**Figure A-51** The HSQC spectrum of compound **10**



**Figure A-52** The HMBC spectrum of compound **10**

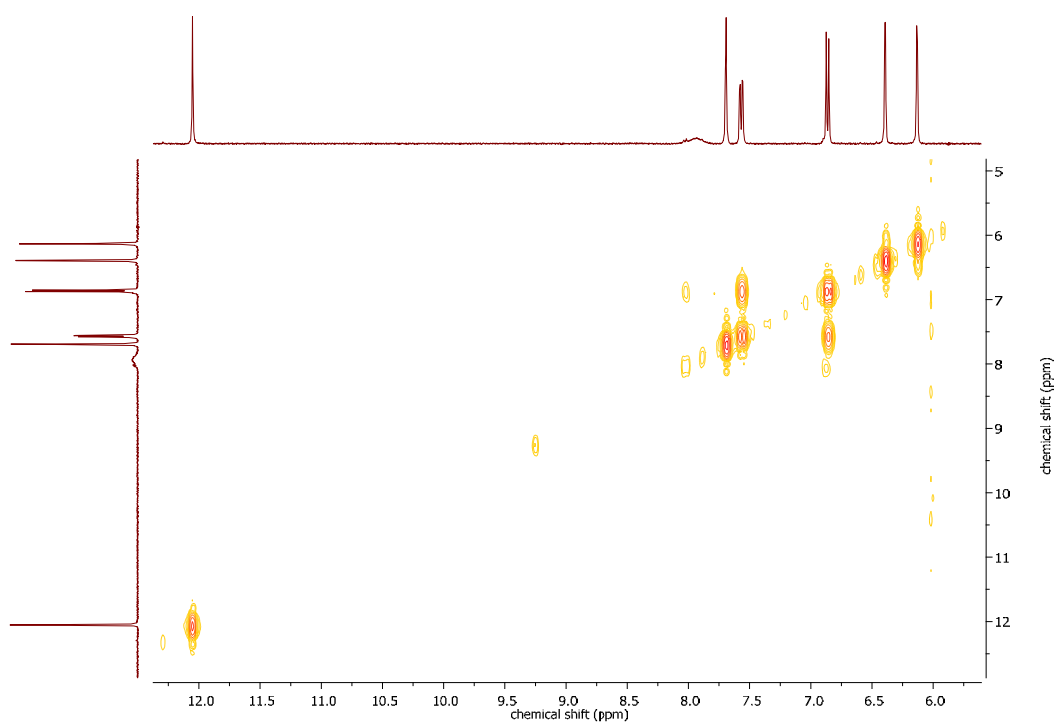


**Figure A-53** The COSY spectrum of compound **10**

## VITA

Mr. Thiendanai Sermboonpaisarn was born on May 3, 1987 in Bangkok, Thailand. He obtained a Bachelor Degree of Science, majoring in Chemistry and minoring in materials science (polymer and textile) from Chulalongkorn University, Bangkok, Thailand in 2008. Since 2009, He has been a graduate student studying Organic Chemistry at Department of Chemistry, Faculty of Science, Chulalongkorn University.

His present address is 479/96 Soi Sutthiporn, Prachasongkhro Road, Dindaeng district, Bangkok, Thailand 10400.